ISSN 2221-6413 (Print), ISSN 2223-2559 (Online)
Coden: PJSIB5 61(1) 1-58 (2018)

Pakistan Journal of Scientific and Industrial Research

Series A: Physical Sciences

Vol. 61, No.1, January-April, 2018

(for on-line access please visit web-site http://www.pjsir.org)

Published by
Scientific Information Centre
Pakistan Council of Scientific and Industrial Research
Karachi, Pakistan

Pakistan Journal of Scientific and Industrial Research

Series A: Physical Sciences

Pakistan Journal of Scientific and Industrial Research is published triannually into two series:

Series A: Physical Sciences [**ISSN 2221-6413 (Print); ISSN 2223-2559 (online)]** (appearing as issues of January-April, May-August and September-December) and
Series B: Biological Sciences [**ISSN 2221-6421 (Print); ISSN 2223-2567 (online)]** (appearing as issues of January-April, May-August and September-December).

This Journal is indexed/abstracted in Zoological Record, BIOSIS Preview, NCBI, Pub Med, Scimago, Research Gate, Clarivate Analytics.

Subscription rates (including handling and Air Mail postage): ***Local:*** Rs. 2500 per volume, single issue Rs. 425;
Foreign: US$ 450 per volume, single issue US$ 75.

Electronic format of this journal is available with: Bell & Howell Information and Learning, 300, North Zeeb Road, P.O. 1346, Ann Arbor, Michigan 48106, U.S.A; Fax.No.313-677-0108; http://www.proquest.com

Photocopies of back issues can be obtained through submission of complete reference to the Executive Editor against the payment of Rs. 25 per page per copy (by Registered Mail) and Rs. 115 per copy (by Courier Service), within Pakistan; US$ 10 per page per copy (by Registered Mail) and US$25 per page per copy (by Courier Service), for all other countries.

Printed and Published by: PCSIR Scientific Information Centre, PCSIR Laboratories Campus, Shahrah-e-Dr. Salimuzzaman Siddiqui, Karachi-75280, Pakistan.

Editorial Address

Executive Editor
Pakistan Journal of Scientific and Industrial Research, PCSIR Scientific Information Centre
PCSIR Laboratories Campus, Shahrah-e-Dr. Salimuzzaman Siddiqui, Karachi-75280, Pakistan
Tel: 92-21-99261914-99261916, 99261949, 99261917; Fax: 92-21-99261913; Web: http://www.pjsir.org, E-mail: info@pjsir.org

AIMS & SCOPE

Pakistan Journal of Scientific and Industrial Research (PJSIR) was started in 1958 to disseminate research results based on utilization of locally available raw materials leading to production of goods to cater to the national requirements and to promote S&T in the country. Over the past 60 years, the journal conveys high quality original research results in both basic and applied research in Pakistan. A great number of major achievements in Pakistan were first disseminated to the outside world through PJSIR.

It is a peer reviewed journal and published in both print and electronic form. Original research articles, review articles and short communications from varied key scientific disciplines are accepted however, papers of Pure Mathematics, Computer Sciences, Engineering and Medical Sciences are not entertained.

From 54th Volume in 2011, it has been bifurcated into Series A: Physical Sciences & Series B: Biological Sciences. Each series appeared three times in a year from 2011 to 2017.

From 61st Volume in 2018 both Series will be published Triannually with the following sequence:

Physical Sciences in April, August & December each year. It includes research related to Natural Sciences, Organic Chemistry, Inorganic Chemistry, Physical Chemistry, Environmental Sciences, Geology, Geography, Glass Technology, Material Sciences, Physics, Polymer Sciences and Technology.

Biological Sciences in April, August & December each year. Papers included in this series are from Agriculture, Agronomy, Botany, Biochemistry, Biotechnology, Food Sciences, Genetic Engineering, Pharmaceutical Sciences, Microbiology, Marine Sciences, Soil Sciences, Food Sciences, Tissue Culture, Natural Products, Toxicology, Ecology, Veterinary Sciences, Zoology and Technology.

Due to many global issues, we are encouraging contributions from scientists and researchers from all across the globe with the sole purpose of serving scientific community worldwide on the whole and particularly for our region and third world countries.

Pakistan Journal of Scientific and Industrial Research
Series A: Physical Sciences
Vol. 61, No. 1, January-April, 2018

Contents

Short Communication

Pak. j. sci. ind. res. Ser. A: phys. sci. 2018 **61A**(1) 1-7

Synthesis, Characterisation and Biological Activity of Schiff Base and its Cu(II), Pd(II), Pt(II) Complexes Derived from Tyrosine and Aromatic Aldehyde

Rukhsana Anjum[a]*,Bushra Khan[a] and Muhammad Javed[b]
[a]Department of Chemistry, Lahore College for Women University (LCWU), Lahore, Pakistan
[b]Gujranwala Institute of Nuclear Medicine (GINUM), Gujranwala, Pakistan

(received February 15, 2016; revised October 17, 2017; accepted October 18, 2017)

Abstract. Schiff base derived from the condensation of tyrosine and the salicylaldehyde has been synthesised and its Cu(II), Pd(II) and Pt(II) complexes have been prepared. The prepared Schiff base and its complexes were analysed and characterised by using different instrumental techniques, such as elemental analysis, FTIR, UV-Vis, ^{1}H NMR, thermal analysis and XRD. The analytical data revealed that the ligand L-1 can coordinate in tridentate manner via the phenolate-O, azomethine-N and tyrosine O-atoms, resulting in the formation of 1:1 [metal: ligand] complexes. Thermal analysis revealed the presence of water molecules in the complexes. In vitro antibacterial activity of the complexes was evaluated against different bacterial strains e.g., *Pseudomonas aeruginosa* and *Bacillus subtilis* by the well-diffusion method. The data showed that transition metal complexes have significant improved antibacterial activity than parent drug.

Keywords: Schiff base, amino acid, antibacterial activity, transition metal complexes

Introduction

Schiff bases and their bio-active complexes have been studied extensively over the past decade. Extensive investigations have been made on salicylidene-amino acid Schiff bases and their metal complexes (Sharma *et al.*, 1997). Metal chelates of the Schiff bases derived from salicylaldehyde and amino acids have been shown to an important class of compounds in elucidating the mechanism of transamination reaction in biological systems (Chohan *et al*., 1997). The special structure and ligand diversity are important factors to determine the chemical and biological importance of the Schiff bases. Hodnett prepared a series of Schiff base metal complexes and carried out antitumor experiments, which indicated that aldehyde substituent was superior to amine substituent in anticancer effect and salicylaldehyde Schiff bases were superior to other aldehyde Schiff bases (Hodnett and Dunn, 1972).

Various studies have shown that amino acid metal complexes of Schiff bases have antibacterial (Venkatesh, 2011; Mounika *et al*., 2010), anticancer (Miri *et al*., 2013; Ali *et al*., 2012) and antioxidant (Wei *et al*., 2000) activities. The antibacterial (Chohan *et al*.,1997) and antifungal (Łukaszuk *et al*., 2007) properties of a number of Cu(II) complexes have been evaluated against various pathogenic bacteria and fungi. Amino acid-palladium complexes have also revealed remarkable antibacterial activity against *Staphylococcus aureus* and *Escherichia coli* bacteria (Cristina *et al*., 2014). Schiff-bases of 1,1′ di-substituted ferrocene and their Pd(II) and Pt(IV) complexes were found to have valuable activity against the various bacterial strains Hegazy, 2012. In the present study, synthesis, characterisation and antibacterial evaluation of Schiff base and its complexes have been reported.

*Author for correspondence;
E-mail: rukhsanaanjum@yahoo.com

Materials and Methods

Tyrosine, salicylaldehyde, cupric acetate monohydrate, platinum chloride and palladium chloride were purchased from Sigma-Aldrich. KOH was obtained from Merk. All the solvents were of analytical grade and used as received without further purification.

The UV-spectra was recorded on UV-2800 spectrophotometer Hitachi, in the range of 200-800 nm. FTIR spectra were obtained by using Agilent-650 spectrophotometer in the region 4000-650 cm^{-1}. Elemental (CHN) analysis was performed by LECO (Truspec micro) apparatus at Forman Christian College, Lahore, Pakistan. The ^{1}H NMR spectra were obtained by the help of Bruker (Advance 400) spectrometer using ^{6}d-DMSO as a solvent at HEJ Research Institute of Chemistry, Karachi, Pakistan. Thermogravimetric analysis was performed using a simultaneous TGA-DSC analyzer (Instrument SDT Q600 V8.). The compounds were placed in

aluminium pan and heated in nitrogen atmosphere (100 mL/ min) up to 1000°C at a rate of 10 °C/ min.

Preparation of Schiff base ligand L-1. To a solution of (1.81g, 10 mmol) tyrosine in 10 mL of ethanol, KOH (0.5611g, 10 mmol) pellets were dissolved by continuous stirring in a 100 mL RB flask. Salicylaldehyde (1.06 mL, 10 mmol) in 10 mL of ethanol was added slowly to the RB flask and refluxed the reaction mixture for 3h at 50 °C to 60 °C. The resulting yellow precipitates were collected by vacuum filtration, washed successively, dried in vacuum and recrystallized with absolute ethanol (Fig. 1).

Preparation of L-1 Cu(II), Pd(II), Pt(II) complexes. To a solution of (1.81g, 10 mmol) tyrosine in 10 mL of ethanol, KOH (0.5611g, 10 mmol) pellets were dissolved by continuous stirring in a 100mL RB flask. Salicylaldehyde (1.06 mL, 10 mmol) in 10 mL of ethanol was added slowly to the RB flask and refluxed the reaction mixture for 3h at 50 to 60 °C. A solution of metal salt, copper acetate monohydrate (10 mmol) and palladium chloride, platinum chloride (5 mmol) in 10mL aqueous methanol was added drop wise to the ligand solution under reflux for further 3h at 50 to 60 °C. The precipitated complex was filtered off, washed several times with ethanol and dried in vacuum.

Antibacterial activity (*In vitro*). Antibacterial activities of the ligand and their complexes were checked *in vitro* against the bacterial species (*Pseudomonas aeruginosa, Bacillus subtilis*) by the well diffusion method. Nutrient broth E (LAB068) was dissolved in distilled water, autoclaved and inoculated with bacterial strains after cooling at 37 °C for 24h. In second day, nutrient agar (LAB008) was dissolved in distilled water and autoclaved. After cooling to 50 °C, 100 µL of the prepared bacterial culture added to the molten nutrient agar, and was poured into petri plates. Once the medium was solidified, wells were made with sterile borer (8 mm). A volume of 50 µL of the test sample (10,000 ppm) and positive control was poured into respective wells. The solvent in which sample was dissolved was used as negative control (Ihsan *et al*., 2012). These plates were incubated at 37 °C for 24h of incubation. The diameter of the clear zones showing no growth of bacteria around each well was measured.

Results and Discussion

The paper describes the synthesis of Schiff base ligands L-1 like salicylaldehyde-tyrosine and its complexes with Cu (II), Pd(II), and Pt(II) metal ions. The structure of the ligand L-1 and its complexes was established from FTIR, UV-Vis, CHN and thermal analysis. Proposed structure for schiff base L-1 was represented in Fig.1.

Physical characteristics and elemental analysis of Schiff base L-1. Synthesized compounds possessed solid physical state and were polar in nature hence, insoluble in non polar solvents. Molecular formula, molecular weight and elemental analysis data was depicted in Table 1. CHN analysis was performed at 950°C degrees with O_2 gas used in combustion furnace along with the attached IR detector for giving the required percentages. Data of elemental analysis was in good agreement with theoretical values (Table 1). Colour, yield, melting points and solubility of the compounds were mentioned in Table 2.

^{1}H NMR spectral analysis. ^{1}H NMR spectral analysis in ^{6}d-DMSO of the synthesized ligand L-1 was summarized in Table 1. In ^{1}H NMR spectra, the peak obtained at 14·34 ppm (s, 1H) was attributed to the phenolic –OH group and a broad singlet peak at 9.16 ppm may be for -OH_{tyr} group. The characteristic imino proton (H-C=N) was appeared at its expected value 8.021 ppm as singlet. The spectra exhibit the signals at 7.17 ppm (2m, 1H), 6.45 ppm (d, ^{1}H) and 6.56ppm (t, 1H) due to $(–CH)_{sali}$. Doublet signals at 6.90 ppm and at 6.67 ppm were attributed to $(–CH)_{tyr}$. Furthermore,

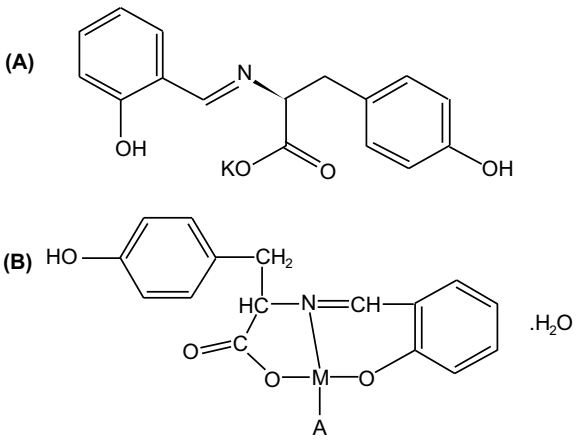

where M= Cu, Pt ions and A= CH_3 COO- for Cu-complex and A= Cl, for Pd and Pt complexes

Fig.1a. **(A)** Proposed structure for Schiff base L-1; **(B)** Proposed structure for Schiff base L-1 complexes

Table 1. Analytical data for Schiff base L-1

Schiff base	Mol. formula	Mol. weight	Elemental analysis found (calc.)%				^{1}H NMR spectral data (ppm)					
			C	N	H	S	-$OH_{salicy.}$	-$OH_{tyr.}$	-CH=N	Ar(-CH)	-CH	-CH_2
L-1	$C_{16}H_{14}KNO_4$	323.1	58.49 (59.42)	4.61 (4.32)	5.41 (4.36)	0 (0)	14.34 (s,1H,br)	9.16 (s,1H,br)	8.021 (s, 1H)	6.56-7.17 (m,1H)	3.13 (dd, 1H)	2.77 (dd,2H)

Table 2. Physical characterisation data of Schiff bases and their metal complexes

Compounds	Colour	Yield (%)	Melting point	Solubility
L-1	Pale yellow	54.32	222°C	Water, Methanol
L-1 Cu(II) complex	Green	41.46	140°C	Methanol
L-1 Pd(II) complex	Greyish brown	45.64	272°C	Ethanol
L-1 Pt(II) complex	Light brown	40.01	235°C	DMSO

the –CH and –CH_2 signals were found at 3.13 ppm and 2.77 ppm as doublet-doublet. The disappearance of aldehyde (δ = 9 10ppm) and amino (δ = 4-6 ppm) protons in the ligands spectra was the indication of its purity.

FTIR spectroscopy. The spectra were measured at room temperature (Table 3). The azomethine (C=N stretching) band at 1639 cm^{-1} in the FTIR spectrum of the ligand L-1 representing the formation of Schiff base. This bond in the Cu(II), Pd(II) and Pt(II) complexes shifted to 1641, 1609 and 1641 cm^{-1}, respectively suggesting the coordination of metal ion with azomethine nitrogen atom (Khander *et al*., 2005; Yusuff and Sreekala, 1991).

The bands in ligand L-1 at 1587 and 1372 cm^{-1} might be of $(COO^-)_{as}$ and $(COO^-)_s$, respectively. In the spectra of the complexes, the shift of carboxyl group bands [$(\nu)_{as}$ and $(\nu)_s$] means that the carboxyl group was in coordination with metal ion. In addition, the further evidence of this coordination was observed by the positive shift of the ν(phenolic C-O)band about (≈10 cm^{-1}) in the IR spectra of the Cu(II), Pd(II) and Pt(II) complexes, when compared to the IR spectrum of the free ligand with phenolic C-O band at 1248 cm^{-1} (Socrates, 2001; Hadi 2009). Accordingly, the ligand acts as a tridentate chelating agent, bonded to the metal ion via the phenolate-O, tyrosine-O and azomethine-N-atoms.

UV spectroscopy. The wavelengths of maximum absorbance (λ_{max}), of the ligand and its complexes were scanned and summarized in Table 3. The electronic absorption spectra of the Schiff base L-1 and its complexes showed π - π * (aromatic ring) and n -π * (HC=N) transitions.

The UV spectra of the ligand L -1 showed three bands. The absorption band appeared at 254 nm (L-1), may be attributed to the benzenoid π - π * transition. The absorption band at 226 nm (L-1) may be assigned to the azomethine n -π * transitions, while the band at 320 nm (L-1) may be due to the carbonyl group of the compounds.

The band corresponding to the azomethine group showed broadening and shifting to a longer wavelength on going from ligand to complex, indicating the coordination of ligand to metal through the azomethine moiety (Amundsen *et al*., 1977). Further, colour of the complexes was different from the ligands and salts which was also an important indication of coordination

Table 3. FTIR and UV data of Schiff base and its complex

Compounds	IR Frequencies (cm^{-1})				
	νC=N	$\upsilon(COO^-)_{asy.}$	$\upsilon(COO^-)_{sym.}$	υ(phenolic C-O).	λ max(nm).
L-1	1639	1587	1372	1248	226,254,320
L-1 Cu(II)complex	1641	1574	1404	1246	242,366,652
L-1 Pd(II)complex	1609	1587	1419	1246	224,276
L-1 Pt(II) complex	1641	1579	1410	1244	278,368

resulting in different absorption bands in their intensity and position (Al-Jeboori *et al*., 2014).

Complexes of L-1 showed a number of bands. The absorption bands appeared in two main wavelength zones, e.g., 224-278 nm (lower wavelength bands) and 276-368 nm (higher wavelength bans). The peaks appeared in the lower wavelength zones might be due to aromatic nature of Schiff base ligand and the peaks in the higher wavelength could be due to the presence of C=N or C=O or a combination of them.

The bands in the visible region at 652 nm (L-1 Cu(II) complex), also indicated that the imino nitrogen was involved in coordination to the metal ion which suggested the square planar geometry of the complexes (Byers *et al*., 1968).

Thermal analysis TGA and DSC were carried out to evaluate the thermal stability of the prepared Schiff base ligand L-1 and its Cu(II), Pd(II) and Pt(II) complexes (Table 4).

TGA & DSC analysis of L-1. The TGA scan of Schiff base L-1 showed the loss in weight in three stages. The initial loss was 10% in the temperature range of 60-260°C which may be due to water loss. Second loss 51.28% occurred at the temperature range of 260-769°C corresponding to the loss of 50.13% organic moiety ($C_9H_8NO_2$). Third loss about 23.12% was observed from 769-948°C corresponding to the calculated loss (24.14%) of benzene. The DSC curve of Schiff base L-1 showed two exothermic peaks at 455 °C, 592 °C and two endothermic peaks at 260 °C and at 819 °C. The endothermic peaks were probably attributed to phase transition and the exothermic peaks attributed to decomposition of compound.

TGA & DSC analysis of L-1 Cu(II) complex. The thermal decomposition of L-1 Cu(II) complex occurred in different stages . The initial loss of about 4.0% was noticed from 50-185°C temperature range. It may be due to the elimination of water molecule (calc. 4.25%). This range of temperature had two peaks at 98.27 °C (endo) and 165 °C (exo). The second stage of decomposition was occurred in 185-253°C temperature range, due to melting and partial decomposition of the ligand bringing the weight loss of about 27.0% (calc. 27.86%, for C_8H_8N moiety of the ligand) having a peak in DSC curve at 210 °C (endo). The decomposition of about 13.0% in the third temperature range 253-528 °C was in agreement with the calculated value 13.93%, CH_3COO^- loss. This temperature range had exothermic peak at 476°C. 35.0% loss in weight (calc. 35.93%) was noticed in the range of temperature 528-998 °C involving the formation of intermediates that may be C_7H_6O, COO^-. Fourth temperature range nearly 998-1000°C showed 18% weight loss which was in agreement with calculated weight 18% of CuO residue.

TGA & DSC analysis of L-1 Pd(II) complex. The thermal decomposition of L-1 Pd(II) complex was observed in number of stages. The first stage of 2.0%

Table 4. Thermogravimetric results of Schiff base metal complexes

Compounds	Temperature range (°C)	Loss in weight		DSC peak (°C)	Loss type
		Found	Calc.(%)		
L-1	60-260°C	10.00	10.52	260°C (endo)	2OH
	260-769°C	51.28	50.13	455°C(exo), 592°C(exo)	$C_9H_8NO_2$
	269-948°C	23.12	24.14	819°C (exo)	Residue of CH+K
L-1 Cu(II)complex	50-185°C	4.0	4.25	98.27°C(endo),165°C(exo)	H_2O
	185-253°C	27.0	27.86	210°C (endo)	C_8H_8N
	253-528°C	13.0	13.93	476°C(exo)	CH_3COO^-
	528-998°C	35.0	35.93	-	C_7H_6O,COO^-
	∼998–1000°C	18.0	18.0	-	CuO
L-1 Pd(II)complex	50-259°C	2.0	2.59	-	H_2O
	∼259–302°C	51.0	51.0	258°C	$H_{32}O_{22}NO_3$
	302-840°C	27.0	27.0	305°C	$C_9H_6NO_4$
	∼840-1000°C	17.0	17.67	764°C(endo),779°C(exo)	PdO
L-1 Pt(II) complex	∼50-250°C	3.0	3.38	-	H_2O
	250-300°C	20.0	20.13	290°C(exo),291°C(endo)	C_7H_7O
	300-700°C	36.0	36.78	-	$C_9H_6NO_2Cl$
	∼700-1000°C	39.0	39.6	-	PtO

mass loss was in agreement with calculated 2.59% loss of H_2O molecule in 50-259 °C temperature range with an exothermic peak at 258 °C. The second stage of decomposition occured in the temperature range of nearly 259-302 °C, due to melting and partial decomposition of the ligand showing one endothermic peak at 305°C, involing the weight loss of about 51.0% which was same to the calculated value 51.0%, corresponding to the loss of $C_{32}H_{22}NO_3$ molecule. The decomposition temperature range from 302-833 °C was involved 27.0% weight loss in third stage which was close to the calculated value 27.7%. This may be due to the removal of $C_9H_6NO_4$ moiety involving two peaks at 764 °C (endo) and 779 °C(exo). In temperature range ~833-964 °C, 17 % lose was observed that was near to the calculated 17.67 % mass loss. This may be attributed to Pd oxide residue.

TGA & DSC analysis of L-1 Pt(II) complex. The thermal decomposition of L-1 Pt(II) complex was observed in three stages. The first stage of degradation was 3.0% (Calc.3.38%) in the temperature range nearly 50-250 °C. It may be due attributed to the elimination of water molecule. In the second stage of decomposition about 20.0 % was occurred in 250-300 °C temperature range, with one exothermic peak at 255 °C and one endothermic peak at 291°C, due to further decomposition and removal of C_7H_7O moiety of the ligand (cal.20.13%). The decomposition range (300-700 °C) is third stage showing 36.0% weight loss which was in agreement (calculated 36.78%) of $C_9H_6NO_2Cl$ loss from the complex. The final remnant mass 39.0% loss may be of metallic oxide in the temperature range nearly 700-1000 °C.

X-ray powder diffraction studies. The X-ray diffraction study was performed on Panalytical automated X-ray powdered diffractometer. The following experimental conditions in reading the pattern were employed. The operating target voltage was 40-45 kV. Copper was employed as anode and 1.54060Å wavelength for K-Alpha1 [Å] and K-Alpha2 [Å] was used. The powdered XRD analysis was carried out to determine the crystalline or amorphous nature of the compounds. The complex formation was confirmed by the appearance of strong and broad peak. In the diffractograms of ligand L-1 and its complexes namely L-1 Cu(II), L-1 Pd(II) and L-1 Pt(II), sharp peaks were obtained that confirmed there crystalline nature.

The average particles size for ligand L-1 and its L-1 Cu(II), L-1 Pd(II) and L-1 Pt(II) complexes, were

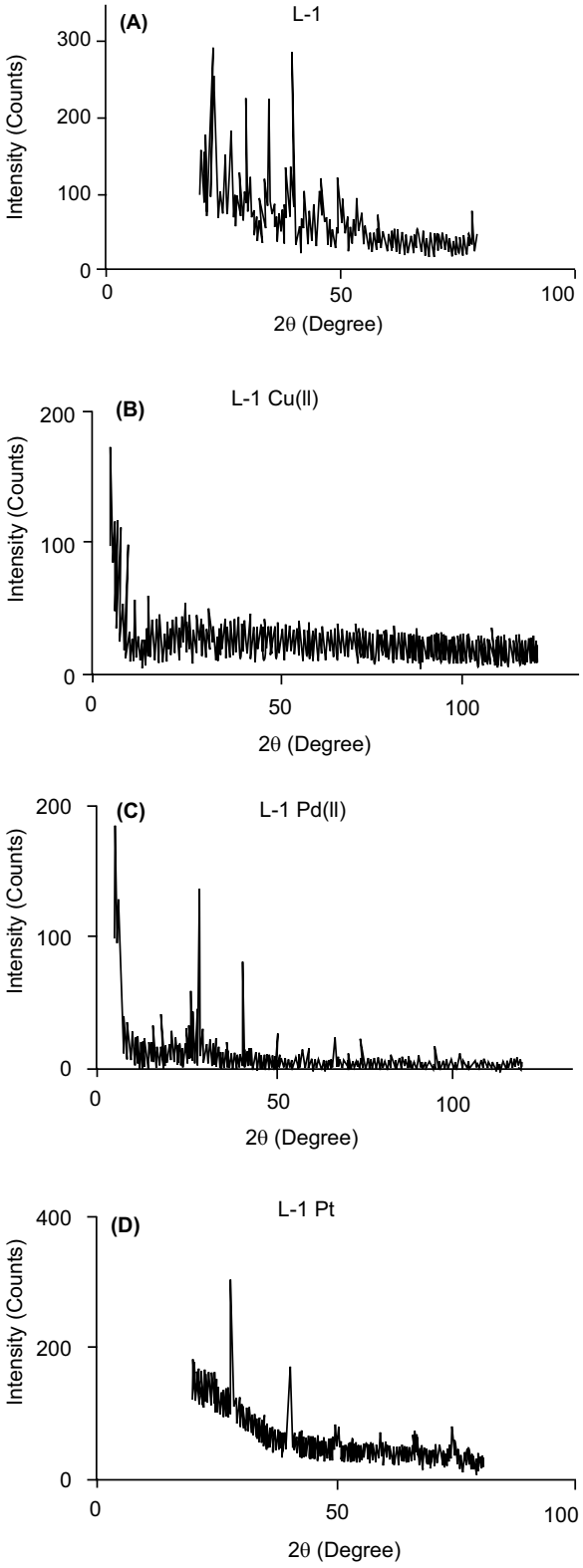

Fig. 2. XRD Diffractogram of **(A)** ligand L-1, **(B)** L-1 Cu(II) Complex, **(C)** L-1 Pd(II) Complex and **(D)** L1-Pt Complex

calculated to be about 67.51, 84.56, 108.85 and 36.23 nm, respectively by applying full width at half maximum (FWHM) and the value of 2θ of characteristic peak using the Debye-Scherer equation.

$$D = k\lambda / \beta \cos \theta$$

Where:

D was the average size,K was a constant(ca. 0.9), λ was the wavelength of Cu Kα, β was the full width at half maximum (FWHM) of the diffraction peak and θ was the Bragg's angle.The diffractogram of compounds were shown in Fig. 2 (A-D).

Antibacterial activity (*In vitro*). All the synthesized Schiff base ligand L-1 and its metal complexes were screened (*in vitro)* for their antibacterial activity against bacteria such as *Pseudomonas aeruginosa* and *Bacillus subtilis* by well diffusion method. The zone of inhibition values were measured in mm. The antibacterial activity results were depicted in Fig 3.

The compound L-1 showed antibacterial activity against *P. aeruginosa* and no activity against *B. subtilis,* while the complexes of L-1 Schiff base exhibited highest activity against *B. subtilis* bacteria and least in *P. aeruginosa* bacteria. When compared to the Schiff base ligand L-1, all the complexes exhibited higher zone of inhibition against both the bacterial strains due to the differences in their structures.

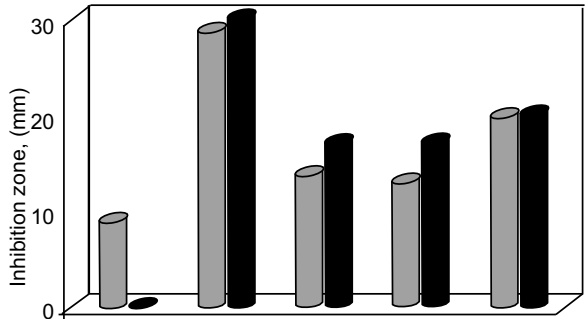

Bacterial strains	L-1	L1-Cu(II)	L1-PD(II)	L1-Pt(II)	Std.Drug (100ppm)
P.aeruginosa	9	29	14	13	20
B. subitilis	0	30	17	17	20

Fig. 3. Effect of ligand L-1 and its Cu(II), Pd(II) and Pt(II) complexes toward *Pseudomonas aeruginosa* and *Bacillus subtilis* at 10,000 ppm concentration.

The higher antibacterial of metal complexes than those of the free ligand can be explained on the basis of Chelation theory. On chelation, the metal ion polarity will be reduced to a greater extent due to the overlap of the ligand orbital and partial sharing of the positive charge of the metal ion with donor groups. Further, it increases the delocalization of pi-electrons over the whole chelating ring and increases the complexes penetration into lipid membranes and blocking of the metal binding sites in the enzymes of micoorganisms. (Singh *et al*., 2008; Iqbal *et al*., 2006).

Conclusion

In the present research study, mononuclear transition metal complexes of Cu(II), Pd(II) and Pt(II) with a newly synthesised ligand derived from salicylaldehyde and tyrosine were prepared. The synthesised compounds were characterised by various physicochemical and spectral analyses. The results exhibited that the ligand L-1 was bonded to the metal (Cu(II), Pd(II) and Pt(II)) ion in a tridentate manner *via* the phenolate-O, tyrosine O-and azomethine-N atoms. The antibacterial data showed that the metal complexes have more biological activity compared to that of free ligand. The copper complexes have remarked antibacterial activities towards bacterial strains, *Pseudomonas aeruginosa* and *Bacillus subtilis*. The L-1 Cu(II) complex showed excellent antibacterial activity against *Bacillus subtilis* strain relative to the Pd (II) and Pt(II) complexes. L-1 Cu(II) complex also showed more antibacterial potency then the control drug. The promising antimicrobial results of ligand and complexes are encouraging further research for application against infections caused by microbial pathogens. Further investigations may prove some of these complexes as suitable agents for future antibiotic drugs especially for the treatment of infections caused by any of these particular bacterial strains.

Acknowledgement

Authors are grateful to the HEC-Islamabad for financial assistance and to the Department of Chemistry, LCWU, Lahore, for providing the facilities for this research project.

References

Ali, S.M.M., Azad, M.A.K., Jesmin, M. 2012. *In vivo* anticancer activity of vanillin semicarbazone *Asian*

Pacific Journal of Tropical Biomedicine, **2:** 438-442.

Al-Jeboori, F. H., Al-Shimiesawi, T. A. M., Abd Oun, M. A., Abd ul-Ridha, A., Abdulla, A. Y. 2014. Synthesis and characterization of amino acid (phenylalanine) Schiff bases and their metal complexes. *Journal of Chemical and Pharmaceutical Research*, **6:** 44-53.

Amundsen, A.R., Whelan, J., Bosnich, B. 1977. Biological analogues. On the nature of the binding sites of copper containing proteins. *Journal of American Chemical Society*, **99:** 6730-6739.

Byers, W., Lever, A.B.P., Parish, R.V. 1968. Stereochemistry of amine oxide metal complexes Stereochemistry of amine oxide metal complexes. *Inorganic Chemistry*, **7:** 1835-1840.

Cimerman, Z., Miljanic, S., Galic, N. 2000. Schiff bases derived from aminopyridines as spectrofluorimetric analytical reagents. *Croatia Chemical Acta*, **73:** 81-95.

Chohan, Z.H., Praveen, M., Ghaffar, A. 1997. Structural and biological behaviour of Co(II), Cu(II) and Ni(II) metal complexes of some amino acid derived schiff-bases. *Metal Based Drugs,* **4:** 267-72.

Cristina, R., Ramona, D., Aurel, P. 2014. Schiff bases have a variety of applications in chemical, biological and pharmeceutical fields. *Chemical and Pharmaceutical Bulletin*, **62:** 12-15.

Hadi, M.A. 2009. Preparation and characterization of some transition metal complexes with schiff base ligand 325 (DBAB). *Journal of Kerbala University,* **7:** 52-57.

Hodnett, E.M., Dunn, W.J. 3rd. 1972. Cobalt derivatives of schiff bases of aliphatic amines as antitumor agents. *Journal of Medicinal Chemistry*, **15:** 339.

Hegazy, W.H. 2012. Synthesis of organometallic-based biologically active compounds: in vitro antibacterial and antifungal of asymmetric. International Journal of Pure and Applied Chemistry, **2:** 170-182.

Ihsan-Ul-Haq, Mannan. A., Ahmed. I., Hussain. I., Jamil. M., Mirza B. 2012. Antibacterial activity and brine shrimp toxicity of *Artemisia dubia* extract. *Pakistan Journal of Botany*, **44:** 1487-1490.

Iqbal, J., Tirmizi, S.A., Wattoo, F.H., Imran, M. 2006. Biological properties of chloro-salicylidene aniline and its complexes with Co(II) and Cu(II). *Turkish Journal of Biology,* **30:**1-4.

Khandar, A., Nijati, K., Rezvani, Z. 2005. Synthesis, characterization and study of the use of cobalt (II) schiff- base complexes as catalysts for the oxidation of styrene by molecular oxygen. *Molecules*, **10:** 302-311.

Łukaszuk, C., Krajewska-Kułak, E., Niewiadomy, A., Stachowicz, J., Głaszcz, U., Oksiejczuk, E. 2007. In vitro antifungal activity of 2,5 disubstituted amino-oksometyloso-arylo-thiadiazole derivatives. *Journal of Advance Medical Science,* **52:** 26-29.

Mounika, K., Anupama, B., Pragathi, J., Gyanakumari, 2010. Synthesis, characterization, antifeeding and insect growth-regulating activities of Cr(III), Mn(II), Fe(III), Co(II), Ni(II) and Cu(II) complexes with N- acetylacetonyl-3-aminocoumarin. *Journal of Scientific Research*, **2:** 513-524.

Miri, R., Razzaghi-asl, N., Mohammadi, M.K. 2013. QM study and conformational analysis of an isatin Schiff base as a potential cytotoxic agent. *Journal of Molecular Modeling,* **19:** 727-735.

Sharma, P. K., Sen, A.K., Singh, K., Dubey, S.N. 1997. Divalent copper and zinc-complex of N-salicylidene amino acids. *Journal of the Indian Chemical Society,* **74:** 446-447

Singh, V.P., Katiyar, A., Singh, S. 2008 Synthesis, characterization of some transition metal(II) complexes of acetone p-amino acetophenone salicyloyl hydrazone and their antimicrobial activity. *Biometals*, **21:** 491- 501.

Socrates, G. 2001, *Infrared and Raman Characteristic Group Frequencies: Tables and Charts*, 3rd edition, Wiley Chichester, pp. 173.

Venkatesh, P. 2011. Synthesis, characterisation and antimicrobial Activity of various schiff- base complexes of zinc (II) and copper (II) ions. *Asian Journal of Pharmaceutical and Health Science,* **1:** 8-11.

Wei, D. Y., Lu, G., Yao, K. M. 2000. Synthesis, properties and catalytic activity of rare earth complexes with noncyclic polyether-phenylalanine schiff-base. *Acta Chimical Sinica (in Chinese)*, **58:** 1398-1402.

Yusuff, K. K. M., Sreekala, R. S. 1991. New complexes of iron(III), cobalt(II) nickel(II) and copper(II) with the schiff-base derived from quinoxaline-2-carboxaldehyde and glycine. *Synthesis and Reactivity in Inorganic*, *Metal Organic and Nano-Metal Chemistry*, **21:** 553-565.

Pak. j. sci. ind. res. Ser. A: phys. sci. 2018 **61A**(1) 8-14

Thermodynamics and Kinetics of Reduction of Fe(III) Acetohydroxamic Acid Complex by Ascorbic Acid

Muhammad Perviaz[a]*, Shazia Nisar[a], Syed Arif Kazmi[a] and Saima Imad[b]
[a]Department of Chemistry, University of Karachi, Karachi-75270, Pakistan
[b]Chemical Metrology Division, National Physical and Standards Laboratory (NPSL), PCSIR, Plot # 16, Sector-H/9, Islamabad, Pakistan

(received December 19, 2016; revised January 4, 2018; accepted January 5, 2018)

Abstract. Kinetic and thermodynamic studies of reduction of Fe(III) acetohydroxamic acid ([Fe(III)-AHA]) complex by ascorbic acid (AA) was performed at pH values ranging from 3.00-4.50 ± 0.1 (ionic strength 0.2) and temperature 05.0 - 25.0 ± 0.5 °C. The redox reactions were studied, spectrophotometrically, under pseudo first order conditions of [AA] over the [Fe(III)-AHA] under the experimental conditions. The redox reaction was found to be highly pH dependent. The values of 2nd order rate constants (k_2), at 25 °C and pH 3.0, 3.5, 4.0 and 4.5 were found out to be 2.3920, 2.1550, 2.0122, 1.7596 $M^{-1}s^{-1}$, respectively. At 20 °C the values were 1.7290, 1.4000, 1.3400, 1.2650 $M^{-1}s^{-1}$ at pH 3.0, 3.5, 4.0 and 4.5, respectively. The results at 15 °C and pH 3.0, 3.5, 4.0 and 4.5 were 1.1410, 0.9459, 1.0390, 0.9126 $M^{-1}s^{-1}$, respectively. While, the values of rate constants at 10 °C were 0.7847, 0.7697, 0.6810, 0.7096 $M^{-1}s^{-1}$ and at 5 °C were 0.6167, 0.5106, 0.4775, 0.4833 $M^{-1}s^{-1}$, respectively. In addition to that, the following rate law was evaluated. Rate = $dp/dt = k_2$ [Fe(III)-AHA] [AA]. Moreover, the thermodynamic activation parameters of the reaction were also determined. The values of $\Delta Ea^{\#}$ at pH 3.0, 3.5, 4.0 and 4.5 were found out to be 22.4058, 16.3243, 19.9636, 14.6050 J/mol, respectively. While, the values of $\Delta H^{\#}$ were 58.5056, 42.6258, 52.1288, 38.1363 J/mol, respectively at pH 3.0 to 0 4.5. Values of $\Delta S^{\#}$ were also evaluated as -23.0297, -68.7567, -37.8287, -84.1377 J/mol/K at pH 3.0, 3.5, 4.0 and 4.5, respectively.

Keywords: acetohydroxamic acid, ascorbic acid, hydroxamate, siderophore, thermodynamics

Introduction

Siderophores are low molecular weight organic molecules that are produced by microorganisms under iron-stress conditions. Siderophores have been the core interest for many years, amongst the biological scientists due to the fact that they help boost the uptake of iron to the microbial cells. These siderophores, with respect to their three main classes i.e., hydroxamate, catecholate and carboxylate share extensive areas of research. Under aerobic environment, the Fe(III) form of iron is insoluble, due to its low ksp and hence is inaccessible at physiological pH (7.40). Under such conditions, microorganisms synthesise siderophores that have high affinity for Fe(III). They chelate Fe(III) and these complexes are then transported to cytosol, where ferric iron is reduced to ferrous iron and becomes available to microorganism. In recent years, siderophores have attracted much attention due to its potential roles in different fields (Saha *et al*., 2016). Three different siderophores mycobactins (Francis *et al*., 1949), ferrichrome (Neilands, 1952) and coprogen (Hesseltine *et al*., 1952) were isolated as growth factors during 1949 to 1952. By the end of the 1960s, several hydroxamate siderophores were recognized. So, there are three main classes of siderophores like catecholate, hydroxamate and hydroxycarboxylate that have high affinity for iron(III) (Xiao *et al*., 1992).

Iron is the most important and abundantly available element but its extremely low solubility in the form of $Fe(OH)_3$ ($Ksp=10^{-39}$) (Neilands, 1952; Francis *et al*., 1949) is very challenging for its bioavailability. The total soluble form of Fe(III) containing hydroxyl species is 10^{-10} M (Hesseltine *et al*., 1952). Iron is very valuable for all living organisms (Crichton, 2001; Xiao *et al*., 1992) as it performs variety of functions in biology. To cope up this low solubility problem, microorganisms are very efficient to synthesize the iron carrier compounds known as siderophores. These microorganisms capture, store and transfer the iron (Sandy and Butler, 2009; Dhungana and Crumbliss, 2005; Raymond *et al*., 2003; Pierre *et al*., 2002; Stintzi *et al*., 2000; Albrecht-Gary and Crumbliss, 1998). Very high Fe(III) complex formation constants (logβ =30-50) (Andrews *et al*., 2003; Pierre *et al*., 2002; Howard, 1999; Guerinot, 1994) for these complexes reveal the reduction

*Author for correspondence; E-mail: pervaizhej@gmail.com

mechanism pathways from Fe(III) to Fe(II) (Harrington and Crumbliss, 2009; Boukhalfa *et al*., 2000; Kwak, and Rhee, 1992; Cooper *et al*., 1978) proceeded by some biological reductants (Matzanke *et al*., 2004; Hallé and Meyer, 1992; Monzyk and Crumbliss, 1979; Neilands, 1952).

On biological grounds, ascorbic acid has immense values in performing many key functions in the body (Packer and Fuchs, 1997). Its tremendous role as a biological redutant exhibits to protect different components of the cell from oxidative damage. In this regard, it scavenges different radicals and damaging oxygen involving requisitions (Arrigoni and Tulio, 2002; Tolbert *et al*., 1975).

Desferrioxamine B, a hydroxamate siderophore, has long been used for the treatment of iron overload conditions in β-thalassemia (Raymond *et al*., 1982). Acetohydroxamic acid (Fig. 1a), a model, synthetic monohydroxamic acid, can be used as a ligand to investigate the chemistry of Fe(III) with hydroxamate siderophores. This study was conducted by Alvin Crumbliss and his students (Monzyk and Crumbliss, 1979). The complexes of iron(III) with AHA have high stability constants and hence are very stable as compared to iron(II) complexes. So, the reduction (Bezkorovainy, 1980) of iron(III) in [Fe(III)-AHA] complex can provide a suitable pathway for release of iron from this complex (Crosa, 1989). A comparison of stability constants of Fe^{+2} and Fe^{+3} siderophore complexes is given in Table 1.

Acetohydroxamic has long been used as a drug to treat UTI (urinary tract infections). Keeping in view the strong complexation between Fe(III) and AHA, biological significance of AA and AHA, a study of reduction of [Fe(III)-AHA] complex by ascorbic acid (AA) is reported here. This study is aimed at the removal and

Table 1. Stability constants for some iron siderophore complexes (Boukhalfa and Crumbliss, 2002)

Siderophores	Log[(β Fe(III))]	Log[(β Fe(II))]
Enterobactin	49.0000	23.9100
Pyoverdin	30.8000	9.7800
Ferrichrome A	32.0000	9.9100
Ferrichrome E	32.5000	11.1600
Ferrichrome B	30.6000	10.2900
Aerobactin	22.5000	4.8600
Acetohydroxamic acid	28.2900	11.2000

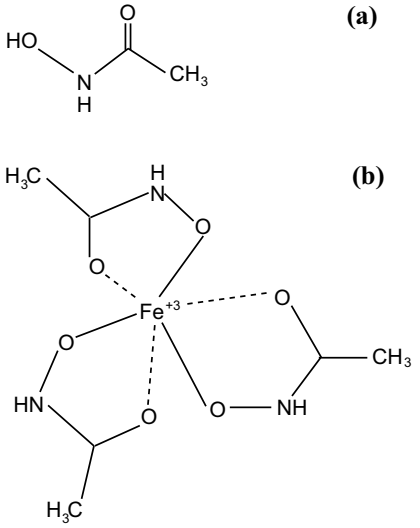

Fig. 1. (a) Acetohydroxamic acid (b) Iron(III) acetohydroxamic complex.

subsequent recovery of Fe(III) from this complex and was carried out through visible spectrophotometry.

For the present study, [Fe(III)-AHA] complex (Fig. 1b) was synthesized in solution under varying conditions of pH and temperature, and its subsequent reduction by ascorbic acid (AA) was studied.

Materials and Methods

In the present study the complexes of Fe(III) with AHA were prepared and reduced further by AA at different pH of the solution. Figure 2 shows the absorption spectra of these complexes at different pH. The colour change from intense to colourless exhibits the extent of the reduction.

Analytical grade chemicals were used throughout the experiments. For the preparation of solutions, each time distilled de-ionized water was used. This de-ionized water was also boiled, degassed and cooled in air tight containers.

Preparation of solutions. ***Preparation of stock solution of $Fe(NO_3)_3.9H_2O$ and standardisation.*** An approximately 1.01×10^{-2} M stock solution of Fe(III) was prepared by dissolving 1.01 g of $Fe(NO_3)_3.9H_2O$ (Riedel de Haen) in 250 mL volumetric flask.

i- The solution was acidified with 1.5 mL of 0.05 M HNO_3 before making it up to the mark.

ii- This solution was standardised by Fe-opt method (Ford-Smith and Sutin, 1961; Bandemer

and Schaible, 1944; Fortune and Mellon, 1938; Saywell and Cunningham, 1937).

The actual concentration was found to be 1.00×10^{-2} M with 5% impurities. This solution was used as a stock solution for preparation of complex solutions at desired pH.

Acetohydroxamic acid solution. This solution was prepared as per requirement by dissolving the calculated and accurately weighed amount of AHA (Wako) in the buffer solutions of respective pH i.e., 3.0, 3.5, 4.0, and 4.5.

Ascorbic acid solution (Wako). Ascorbic acid was prepared freshly in the buffer solutions of desired pH, before each use. This solution was degassed and purged with N_2 for 10-15 min, especially, to remove oxygen gas.

Buffer solutions. Formate buffer solutions of pH 3.0, 3.5, 4.0 and acetate buffer of pH 4.5 were prepared in deionized water. The ionic strength of buffer solutions was 0.2 M which was maintained by NaCl and KCl.

Preparation of formate buffers. Format buffers of pH 3.0, 3.5, and 4.0 were prepared by taking 100.0 mL of standardized 1.6 M NaOH (Merck). Formic acid (TEDIA) was added drop wise to this solution till the pH values 3.0, 3.5 and 4.0 were obtained. To make the ionic strength equal to 0.2 M, 4.68 g of NaCl (Merck) were added to the same volumetric flask before making up the volume up to 2000.0 mL, using de-ionized water.

Preparation of acetate buffer. Acetate buffer of pH 4.5 was prepared in the same way except that acetic acid (Merck) was used instead of formic acid. In this case the ionic strength was maintained using 5.96 g of KCl (Avonchem).

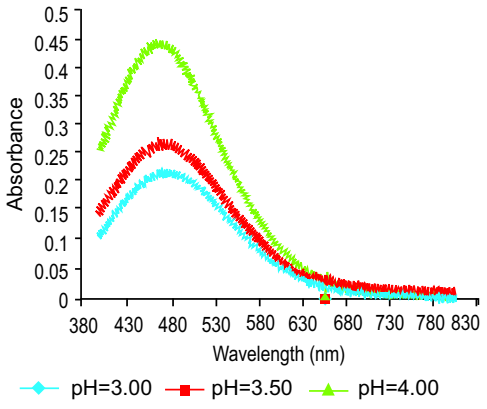

Fig. 2. Sample absroption spectrum of [Fe(III)-AHA] at different pH. [Fe(III)-AHA] = 2.0×10^{-4} M, μ = 0.2 M.

Formation of [Fe(III)-AHA] complex. [Fe(III)-AHA] complex was prepared by mixing Fe(III) solution and AHA solution of known concentrations. The concentration of AHA solution was kept 5 times over the concentration of Fe(III) to ensure the complete complexation in form of 1:3 (M:L). Molar extinction coefficients (ε) of [Fe(III)-AHA] complex were calculated at different pH and temperature as shown in Table 2.

Instrumentations. Diode array spectrometer model HP 8452A, logger pro 3.2 and stopped flow model RX-2000 were used to follow the reaction and record the absorbance and changes in absorbance during the kinetic experiments. Analytical balance model TE214S Sartorius was used for weighing in the entire research work. The re-circulating water chiller model 470 was used for the maintenance of temperature. It allows the effective re-circulating water chilling system with a temperature display. The temperature control is the most important part of the chiller and can be set manually as per requirement of the experiment.

Kinetic experiments. The kinetics of reduction of Fe(III)-hydroxamic acid complexes by ascorbic acid, under the pseudo first order conditions was studied spectrophotometrically. These reactions were monitored at λ_{max} of the complexes through diode array spectrophotometer in a compatibility of stopped flow. The other conventional spectrophotometer is not effective for such kind of measurements because the reaction between Fe(III)-AHA and AA was found to be too fast to be observed by manual mixing.

The drive syringes with equal volumes of both the reagents were filled or loaded and then stayed for 15-20 min to maintain the temperature through water circulating bath. The cuvette of the stopped flow was set into the cuvette holder of photodiode array spectrophotometer. Thus both syringes are operated simultaneously as it reaches to the trigger block. Different sets of reactions were observed under different conditions till 4-5 half lives.

The rate of reduction of Fe(III)-acetohydroxamic acid complexes by ascorbic acid was observed in a range of concentration from 1.5×10^{-3} to 2×10^{-2} M at a particular temperature 05.0 to 25.0 ± 0.5 °C, pH 3.00 - 4.50 ± 0.1 with ionic strength 0.2 M and at the λ_{max} of complex at respective pH.

Results and Discussion

Stoichiometry of the [Fe(III)-AHA] complex. The complex formation reaction between Fe^{+3} and AHA has already been studied extensively by Kazmi and McArdle (1981). Those studies have shown a linear dependence of k_{obs} on AHA. Moreover, the formation of $[Fe(AHA)_2]$ was discussed that supports the formation of $[Fe(AHA)]^{+2}$. The studies show that the stoichiometry of complex depends upon the pH of the solution. At lower pH (Nisar and Kazmi, 2006) such as 3.00 and 3.50, $[Fe(III)\text{-}(AHA)_2]$ species may exist whereas $[Fe(III)\text{-}(AHA)_3]$ may exist at higher pH, such as, 4.00 and 4.50. So, the pH will be a key parameter in deciding the stoichiometry of the [Fe(III)-AHA] complex.

The reduction of [Fe(III)-AHA] complex by ascorbic acid was investigated spectrophotometrically under pseudo 1st order conditions, over a range of pH 3.00 to 4.50. The preparation of the complex solution was carried out in the buffers of respective pH. The values of λ_{max} for [Fe(III)-AHA] complex at pH 3.0, 3.5, 4.0 and 4.5 are given in Table 2.

$$Fe(III) + n(CH_3CONHOH) \underset{+H^+}{\overset{-H^+}{\rightleftharpoons}}$$

$$CH_3CONHO^- \longrightarrow [(CH_3CONHO)_nFe] \text{ ..... } 1$$

It was previously observed that as the pH values are increased, λ_{max} increases (Kazmi and McArdle, 1981) significantly.

$$Fe(III)\,(CH_3CONHO)^{+(3-n)_n} + H^+ \underset{k_{-1}}{\overset{k_1}{\rightleftharpoons}}$$

$$[(CH_3CONHO)_{n-1}(F(III)] + CH_3CONHO$$

$$[(CH_3CONHO)_{n-1}(F(III)] + HAsc^- \xrightarrow{k_2} Fe(II) + Asc\cdot + (n\text{-}l)CH_3CONHOH$$

In the above equation 1, n is representing the number of moles of AHA; 1, 2 or 3 depending on the pH. The maximum possibility for the complexation i.e. 1:3 increases as we keep on increasing the value of pH. The k_{obs} values were determined through the linear regression analysis of the raw data. The slopes of the plots of $\ln(A_t\text{-}A_\alpha)/(A_o\text{-}A_\alpha)$ vs t correspond to the values of the pseudo first order rate constant (k_{obs}) according to equation 2.

$$\ln(A_t\text{-}A_\alpha)/(A_o\text{-}A_\alpha) = k_{obs} \cdot t \text{ ..... } 2$$

We obtained a straight line by plotting $\ln(A_t\text{-}A_\alpha)/(A_o\text{-}A_\alpha)$ versus time for many half lives and out of these sample plots one plot of kinetic runs is given in Fig. 3. For the reactions at pH 3, k_{obs} values are tabulated in Table 3. The values of k_{obs} were plotted against the [AA] and gave a straight line suggesting that the reaction is first order with respect to the concentration of ascorbic acid. These plots of k_{obs} verses concentration of ascorbic acid for each corresponding pH are shown in Fig. 4.

The plots of k_{obs} *vs* [AA] were found to be linear, indicating a simple 1st order pathway for reduction of Fe^{+3} to Fe^{+2} in the complex. The values of rate constants are given in Table 4.

Table 2. Molar absorptivity of Fe(III) acetohydroxamic complex at different pH

pH	λ_{max}	ε (M/cm)
3.00	480	1046.5000
3.50	470	1196.0000
4.00	472	1410.5000
4.50	468	1635.0000

Table 3. Values of k_{obs} (s^{-1}) for the reduction of Fe(III)-AHA by AA at pH = 3.00

[AA] M	k_{obs} (s^{-1})				
	25 °C	20 °C	15 °C	10 °C	05 °C
0.02	4.2768	3.2500	2.2928	1.4630	1.2000
0.015	3.5300	2.7500	1.9190	1.2060	1.0300
0.01	2.9092	2.2500	1.4928	1.0525	0.8800
0.005	2.5647	1.6850	1.2018	0.8237	0.7661
0.0025	2.0122	1.2650	0.9126	0.7096	0.6167
0.0015	1.7392	1.0250	0.6495	-	0.5695

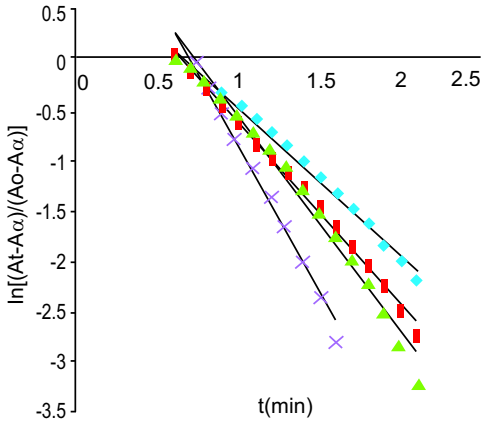

Fig. 3. Sample plot for $\ln(At\text{-}A\alpha)/A_0\text{-}A\alpha$ versus t.

It has already been reported that at lower pH 3.00 and 3.50, the formation of bis (acetohydroxamato)-Fe(III) complex is more feasible (Nisar and Kazmi, 2006; Kazmi and McArdle, 1981). In the presence of suitable reducing agent, [Fe(III)-$(AHA)_2$] complex undergoes reduction to [Fe(II)-$(AHA)_2$] complex easily.

Table 4. Values of rate constants at different pH and temperatures

T (°C)	pH	k_2 (M/s)	k_o
5	3.00	32.72	0.5492
	3.50	64.65	0.352
	4.00	58.89	0.357
	4.50	59.20	0.294
10	3.00	41.91	0.610
	3.50	92.77	0.480
	4.00	108.3	0.392
	4.50	96.24	0.507
15	3.00	82.99	0.664
	3.50	88.7	0.926
	4.00	167.6	0.492
	4.50	130.9	0.722
20	3.00	116.8	0.985
	3.50	178.5	0.976
	4.00	192.9	0.942
	4.50	150.1	1.408
25	3.00	127.0	1.690
	3.50	185.3	1.285
	4.00	235.1	1.890
	4.50	164.5	1.665

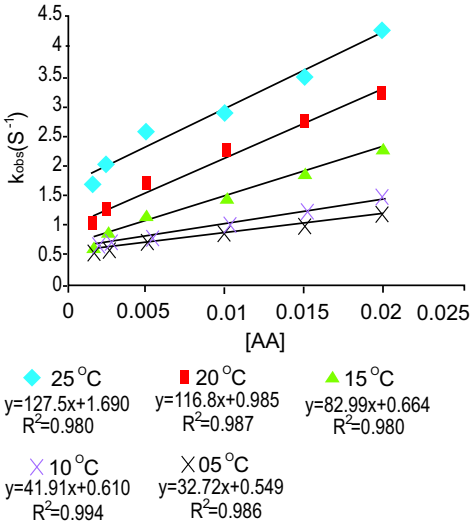

Fig. 4. Sample plot between k_{obs} (s^{-1}) and [AA] at pH 3.00 and different temperature [Fe(III)-AHA] = 2.0×10^{-4} M; λ_{max} = 480 nm; pH = 3.00; μ = 0.2 M; T = 5.0 - 25.0 ± 0.5 °C.

At higher pH, 4.00 and 4.50, the reduction process becomes more challenging because of the change in stoichiometry from1:1 to 1:3, through 1:2 hence, the value of k_2 must decrease. But in the present study, the trends in the values are in reverse order that is, instead of decreasing, the values of rate constants are increasing as shown in Table 4.

The two competing factors are very important and responsible for these trends in k_2 values at different pH. One factor is the stoichiometry of the complex and the second, is the redox potential of the reducing agent at different pH. At low pH, 1:1 & 1:2 complexation dominates over 1:3 species, which are easier to be reduced. On the basis of equation 1, as the pH is raised n goes from 1 to 3 making its reduction a challenging task for the reducing agents. While, the E° value of AA is also highly pH dependent (Daniel *et al*., 1985). Values of formal potential are available (Daniel *et al*., 1985) and show an increased reducing power with the rise of pH. Trends in the values of k_2 from Table 4 indicate that the increased redox potential of AA with pH is the dominant factor in this case.

k_o is insignificant as $k_o <<< k_2$
Hence, $k_{obs} = k_o + k_2$ [AA]

Here k_2 depends upon the concentration of ascorbic acid but k_o is independent. Under the conditions $k_o <<< k_2$

$k_{obs} = k_2$[AA]
Rate = k_{obs} [Fe(III)-AHA]
Rate = k_2 [Fe(III)-AHA] [AA]

On the basis of all above observations, our suggested mechanism for the given reaction is as:

$$AAH \rightleftharpoons AA^- + H^+$$

$$AA^- \longrightarrow AA^{\cdot} + e^-$$

$$2AA^{\cdot} \longrightarrow 2AA$$

$$AAH + [Fe(III)\text{-}(AHA]_n \xrightarrow{RDS} AA^{\cdot} + [Fe(II)\text{-}AHA]_n$$

$$2AA^{\cdot} \xrightarrow{Fast} AAAA$$

Here, AA = Ascorbic acid
Rate = -d[Fe(III)-$(AHA)_n$]/ dt = k [AA] [Fe(III)-$(AHA)_n$]
Rate = k_{obs} [Fe(III)-$(AHA)_n$]
So, $k_{obs} = k_2$ [AA]

Thermodynamic studies. Thermodynamic parameters (ΔEa, $\Delta H^{\#}$ and $\Delta S^{\#}$) of the reaction were determined through Arhenius (equation 3) and Eyring (equation 4) plots and the values are tabulated in Table 5.

$$-\ln k = \ln A + (-Ea/RT) \quad \ldots\ldots\ldots\ldots\ldots\ldots\ldots 3$$

Equation 3 is the equation of a straight line whose slope is $-Ea/R$. This helps in determining the activation energy from values of rate constant at different temperatures, by plotting ln*k* as a function of 1/*T*.

$$\ln k/T = -\Delta H^{\#}R/T + \ln kB/h + \Delta S^{\#}/R \quad \ldots\ldots\ldots\ldots 4$$

where:

k is the rate constant
kB is the Boltzmann's constant (1.381×10^{-23} J/K),
T is the absolute temperature in Kelvin (K) and
h is Planck's constant (6.626×10^{-34} Js).

The values for $\Delta H^{\#}$ and $\Delta S^{\#}$ can be determined from kinetic data obtained from a plot of lnk/T vs. 1/T. The equation is a straight line with negative slope, $-\Delta H^{\#}/R$, and a y-intercept, $\Delta S^{\#}/R + \ln k_B/h$. $\Delta H^{\#}$ is changing from +58.5056 kJ/mol to +38.1363 by changing the pH from 3.00 to 4.50 but $\Delta S^{\#}$ goes from -23.0297 to -84.1376 as shown in Table 5. Here the negative sign of $\Delta S^{\#}$ supports an associative mechanism for the redox reaction. Negative values for $\Delta S^{\#}$ indicate that entropy decreases on forming the transition state, which often indicates an associative mechanism in which two reaction partners form a single activated complex (Johnstone and Nolan, 2015).

Table 5. Activation parameters $\Delta Ea^{\#}$, $\Delta S^{\#}$ and $\Delta H^{\#}$ at different pH

pH	$\Delta Ea^{\#}$	$\Delta H^{\#}$ J/mol	$\Delta S^{\#}$ J/mol/K
3.00	22.4058	58.5056	-23.0297
3.50	16.3243	42.6258	-68.7568
4.00	19.9636	52.1288	-37.8287
4.50	14.6050	38.1363	-84.1377

Conclusion

The results of this study have shown that increasing the pH of the medium also increases the reduction of the said complex. Moreover, the trends in the values of rate constants with increasing pH show that the physiological pH could enhance the reduction of [Fe(III)-AHA] complex. If acetohydroxamic acid administered during UTI, chelates iron stores present in the body, a proper dose of vitamin C might be helpful in reducing this complex and maintaining iron stores of the body. So, it is recommended that vitamin C should be given to the patients taking acetohydroxamic acid (lithostate) drug to treat urinary tract infections.

References

Albrecht-Gary, A.M., Crumbliss, A. 1998. *Metal Ions in Biological Systems*, A. Sigel and H. Sigel (eds.), vol. **35,** pp. 239, Marcel Dekker, New York, USA.

Andrews, S.C., Robinson, A.K., Rodríguez-Quiñones, F. 2003. Bacterial iron homeostasis. *FEMS Microbiology Reviews*, **27:** 215-237.

Arrigoni, O., De Tulio, M.C. 2002. Ascorbic acid much more than just an antioxidant. *Biochimica Biophysica Acta*, **1569:** 1-9.

Bandemer, S.L., Schaible, P.J. 1944. Determination of iron. A study of the *o*-phenanthroline method. *Industrial & Engineering Chemistry Analytical Edition*, **16,** pp. 317-319.

Bezkorovainy, A. 1980. *Biochemistry of Nonheme Iron*, pp. 395-419, Plenum Press. New York and London, UK.

Boukhalfa, H., Crumbliss, A.L. 2002. Chemical aspects of siderophore mediated iron transport. *Bio-Metals*, **15:** 325-339.

Boukhalfa, H., Brickman, T.J., Armstrong, S.K., Crumbliss, A.L. 2000. Kinetics and mechanism of iron(III) dissociation from the dihydroxamate siderophores alcaligin and rhodotorulic acid. *Inorganic Chemistry*, **39:** 5591-5602.

Cooper, S.R., McArdle, J.V., Raymond, K.N. 1978. Siderophore electrochemistry: relation to intracellular iron release mechanism. *Proceedings of the National Academy of Sciences of the United States of America*, **75:** 3551-3554.

Crichton, R. 2001. *Inorganic Biochemistry of Iron Metabolism: From Molecular Mechanisms to Clinical Consequences*, **133,** pp. xvi-xvii, 2nd edition, John Wiley, Chichester, UK.

Crosa, J.H. 1989. Genetics and molecular biology of siderophore-mediated iron transport in bacteria. *Microbiological Reviews*, **53:** 517-530.

Dhungana, S., Crumbliss, A.L. 2005. Coordination chemistry and Redox processes in siderophore mediated iron transport. *Geomicrobiology Journal*, **22:** 87-98.

Fontecave, M., Pierre, J.L. 1993. Iron, metabolism, toxicity and therapy. *Biochimie*, **75:** 767-773.

Ford-Smith, M., Sutin, N. 1961. The kinetics of the reactions of substituted 1, 10-phenanthroline, 2, 2'-dipyridine and 2, 2', 2 ″-tripyridine complexes of

iron(III) with iron(II) ions. *Journal of the American Chemical Society*, **83:** 1830-1834.

Fortune, W.B., Mellon, M. 1938. Determination of iron with O-phenanthroline, a spectrophotometric study. *Industrial & Engineering Chemistry Analytical Edition*, **10:** 60-64.

Francis, J., Madinaveitia, J., Macturk, H.M., Snow, G. 1949. Isolation from acid-fast bacteria of a growth-factor for *Mycobacterium johnei* and of a precursor of phthiocol. *Nature*, **163:** 365.

Guerinot, M.L. 1994. Microbial iron transport. *Annual Reviews in Microbiology*, **48:** 743-772.

Hallé, F., Meyer, J.M. 1992. Iron release from ferriside-rophores. *European Journal of Biochemistry*, **209:** 621-627.

Harrington, J.M., Crumbliss, A.L. 2009. The redox hypothesis in siderophore-mediated iron uptake. *Bio-Metals*, **22:** 679-689.

Harris, D.C., Rinehart, A.L., Hereld, D., Schwartz, R.W., Burke, F.P., Salvador, A.P. 1985. Reduction potential of iron in transferrin. *Biochimica et Biophysica Acta*, **838:** 295-301.

Hesseltine, C.W., Pidacks, C., Whitehill, A.R., Bohonos, N., Hutchings, B.L., Williams, J.H. 1952. Coprogen, A new growth factor for Coprophilic fungi. *Journal of the American Chemical Society*, **74:** 1362-1363.

Howard, D.H. 1999. Acquisition, transport, and storage of iron by pathogenic fungi. *Clinical microbiology Reviews*, **12:** 394-404.

Johnstone, T.C., Nolan, E.M. 2015. Beyond iron: non-classical biological functions of bacterial siderophores. *Dalton Transactions*, **44:** 6320-6339.

Kazmi, S.A., McArdle, J.V. 1981. Kinetics of formation of bis- and tris(acetohydroxamato)Fe(III). *Journal of Inorganic Nuclear Chemistry*, **43:** 3031-3034.

Kwak, M.Y., Rhee, J.S. 1992. Cultivation characteristics of immobilized *Aspergillus oryzae* for kojic acid production. *Biotechnology and Bioengineering*, **39:** 903-906.

Matzanke, B.F., Anemüller, S., Schünemann, V., Trautwein, A.X., Hantke, K. 2004. FhuF, part of a siderophore-reductase system. *Biochemistry*, **43:** 1386-1392.

Monzyk, B., Crumbliss, A.L. 1979. Mechanism of ligand substitution on high-spin iron(III) by hydroxamic acid chelators. Thermodynamic and kinetic studies on the formation and dissociation of a series of monohydroxamatoiron(III) complexes. *Journal of the American Chemical Society*, **101:** 6203-6213.

Neilands, J.B. 1952. A crystalline organo-iron pigment from a rust fungus (*Ustilago sphaerogena*). *Journal of the American Chemical Society*, **74:** 4846-4847.

Nisar, S., Kazmi, S.A. 2006. Kinetics of the reduction of Fe(III)-Acetohydroxamic acid complex by L-cysteine. *Journal of Applied and Emerging Sciences*, **1:** 58-63.

Packer, L., Fuchs, J. 1997. *Vitamin C in Health and Disease*, pp. 425-455, Marcel Dekker, Inc., New York, USA.

Pierre, J., Fontecave, M., Crichton, R. 2002. Chemistry for an essential biological process: the reduction of ferric iron. *BioMetals*, **15:** 341-346.

Raymond, K.N., Dertz, E.A., Kim, S.S. 2003. Entero-bactin: An archetype for microbial iron transport. *Proceedings of the National Academy of Sciences of the United States of America*, **100:** 3584.

Raymond, K.N., Chung, T.D.Y., Pecoraro, V. L., Carrano, C.J. 1982. In: *The Biochemistry and Physiology of Iron*, P. Saltman and L. Sieker (eds.), 649 pp., Elsevier Biochemical Amsterdam, The Netherland.

Saha, M., Sarkar, S., Sarkar, B., Sharma, B.K., Bhattacharjee, S., Tribedi, P. 2016. Microbial siderophores and their potential applications: a review. *Environmental Science and Pollution Research International*, **23:** 3984-3999.

Sandy, M., Butler, A. 2009. Microbial iron acquisition: Marine and terrestrial siderophores. *Chemical Reviews* (Washington, DC, United States), **109:** 4580-4595.

Saywell, L., Cunningham, B. 1937. Determination of iron: colorimetric *O*-phenanthroline method. *Industrial & Engineering Chemistry Analytical Edition*, **9:** 67-69.

Stintzi, A., Barnes, C., Xu, J., Raymond, K.N. 2000. Microbial iron transport via a siderophore shuttle: A membrane ion transport paradigm. In: *Proceedings of the National Academy of Sciences of the United States of America*, **97:** 10691-10696.

Tolbert, B.M., Downing, M., Carlson, R.W. 1975. Chemistry and metabolism of ascorbic acid and ascorbate sulfate. *Annals of the New York Academy of Sciences*, **258:** 48-69.

Xiao, G., van derHelm, D., Hider, R.C., Dobbin, P.S. 1992. Structure stability relationships of 3-hydroxypyridin-4-one complexes. *Journal of the Chemical Society, Dalton Transactions*, Issue **22:** 3265-3271.

Pak. j. sci. ind. res. Ser. A: phys. sci. 2018 **61A**(1) 15-18

Antibacterial Potential Assessment of Schiff Bases Derived from 1-Aminoanthracene-9, 10-Dione

Ghulam Fareed[a]*, Fouzia Khan[b], Nazia Fareed[c] and Shahana Urooj Kazmi[b]
[a]Pharmaceutical Research Centre, PCSIR Laboratories Complex, Karachi-75280, Pakistan
[b]Department of Microbiology, University of Karachi, Karachi-75270, Pakistan
[c]Department of Chemistry, Federal Urdu University of Arts, Science and Technology, Karachi, Pakistan

(received June 4, 2017; revised June 20, 2017; accepted June 22, 2017)

Abstract. A variety of Schiff bases **1-17** of 1-aminoanthracene-9, 10-dione were synthesized using a reported catalytic method and evaluated for their antibacterial potential against *Staphylococcus aureus* multidrug resistant (MDR), *Escherichia coli* (MDR), *Klebsiella* species (MDR), *Salmonella typhimurium* (MDR), *Pseudomonas aeruginosa* (MDR), *Escherichia coli* ATCC-8739, *Staphylococcus aureus* ATCC-25923, *Staphylococcus aureus, Escherichia coli, Klebsiella* species and *Pseudomonas aeruginosa.* Compounds **2**, **3, 4, 13** and **14** were found to be potent against (MDR) bacterial strains when compared with the cefotaxime standard, however compound **8** exhibited good activities against *S. aureus* and *Klebsiella* species. Compounds **2** and **15** were found to be good to moderately active against *P. aeruginosa* and compounds **4** and **15** demonstrated moderate activity against *S. aureus*. All the remaining compounds except **11** and **17** showed weak antimicrobial activity against non-MDR strains of bacterial isolates.

Keywords: Schiff base, 1-aminoanthracenedione, antibacterial activity, multidrug resistant

Introduction

The fast growing resistance of bacteria towards available antibiotics is a foremost medical issue. Increasing resistance against known antibiotics that causes severe infections is directly linked with the dramatic increase in mortality rate (daSilva *et al*., 2011). The bacterial resistance against multiple available antibiotics is due to their toxicity and different modes of action. In order to cope with the growing human pathogen resistance, there is an urgent medical need to discover some additional antibacterial drugs that have no adverse effects due to their unusual mode of action (Alekshun and Levy, 2017; Rice, 2006).

Schiff bases or imines are the compounds bearing azomethine (-C=N-) functionality (Fareed *et al*., 2013) with numerous biological applications including antibacterial, antifungal, antiviral, antioxidant, anti-tuberculosis, analgesic and anti-inflammatory activities (Kajal *et al*., 2013; daSilva *et al*., 2011; Piotr *et al*., 2009). Several natural and non-natural compounds with imine group are biologically active. The presence of imine functionality in such compounds is responsible for their significant biological potential (Guo *et al*., 2007; Souza *et al*., 2007; Bringmann *et al*., 2004).

*Author for correspondence; E-mail: fareedchm@yahoo.com

Derivatives of anthracene-9, 10-dione have attracted the attention of medicinal chemists due to a wide spectrum of significant pharmacological activities such as anti-tumour (Ashnagar *et al*., 2010; Ge and Russell, 1997), anti-inflammatory (Yadav *et al*., 2010), anti-malarial (Osman *et al*., 2010; Yadav *et al*., 2010), antioxidants, antimicrobial (Yadav *et al*., 2010; Xiang *et al*., 2008), antifungal (Rath *et al*., 1995), antileukemic (Chang and Lee, 1984), antiviral and anti-HIV properties (Alves *et al*., 2004; Schinazi *et al*., 1990). It has also been reported that derivatives of aminoanthracene-9, 10-dione show considerably increased antitumor activities (Nor *et al*., 2013). In view of the wide interest of medicinal chemists towards imines and anthracenedione, synthesis and antibacterial activities of the Schiff bases have been reported here.

Materials and Methods

The melting points were recorded in a glass capillary using Gallenkamp MF-370 melting point apparatus and are uncorrected. ^{1}H-NMR (300MHz) and ^{13}C-NMR (75MHz) spectra were recorded on Bruker AV-300 NMR Spectrometer in DMSO-d_6 with trimethyl silane (TMS) as an internal standard. IR spectra were recorded on Nicolet Avatar 300 DTGS. Mass spectra were recorded on a Finnigan LCQ Advantage Max. Elemental

analysis were conducted on a Carlo Erba Strumentazion-Mod-1106 instrument.

General method for the synthesis of Schiff bases 1-17. A mixture of 1-aminoanthracene-9,10-dione (1 mmol), variety of aromatic carbonyl compounds (1 mmol) and *dodeca*-tungstosilicic acid/P_2O_5 (0.2 g, 1 mol% of 1-aminoanthraquinone/P_2O_5) as a catalyst was ground in mortar with a pestle under solvent free conditions at room temperature for 1-3 min (Scheme 1). The reaction mixture turned to paste like material which indicated the completion of the reaction. Crushed ice was added to afford precipitates of the Schiff bases. In order to remove catalyst, the product was washed several times with ice cooled water. The solid products were obtained in excellent yield (Fareed *et al*., 2013).

***In vitro* antibacterial assay.** *In vitro* antimicrobial activity was performed by determining MIC of compounds by broth micro dilution method (Wayn, 2012) against multidrug resistant (MDR) and normal strains *viz*., methicillin resistant *Staphylococcus aureus*

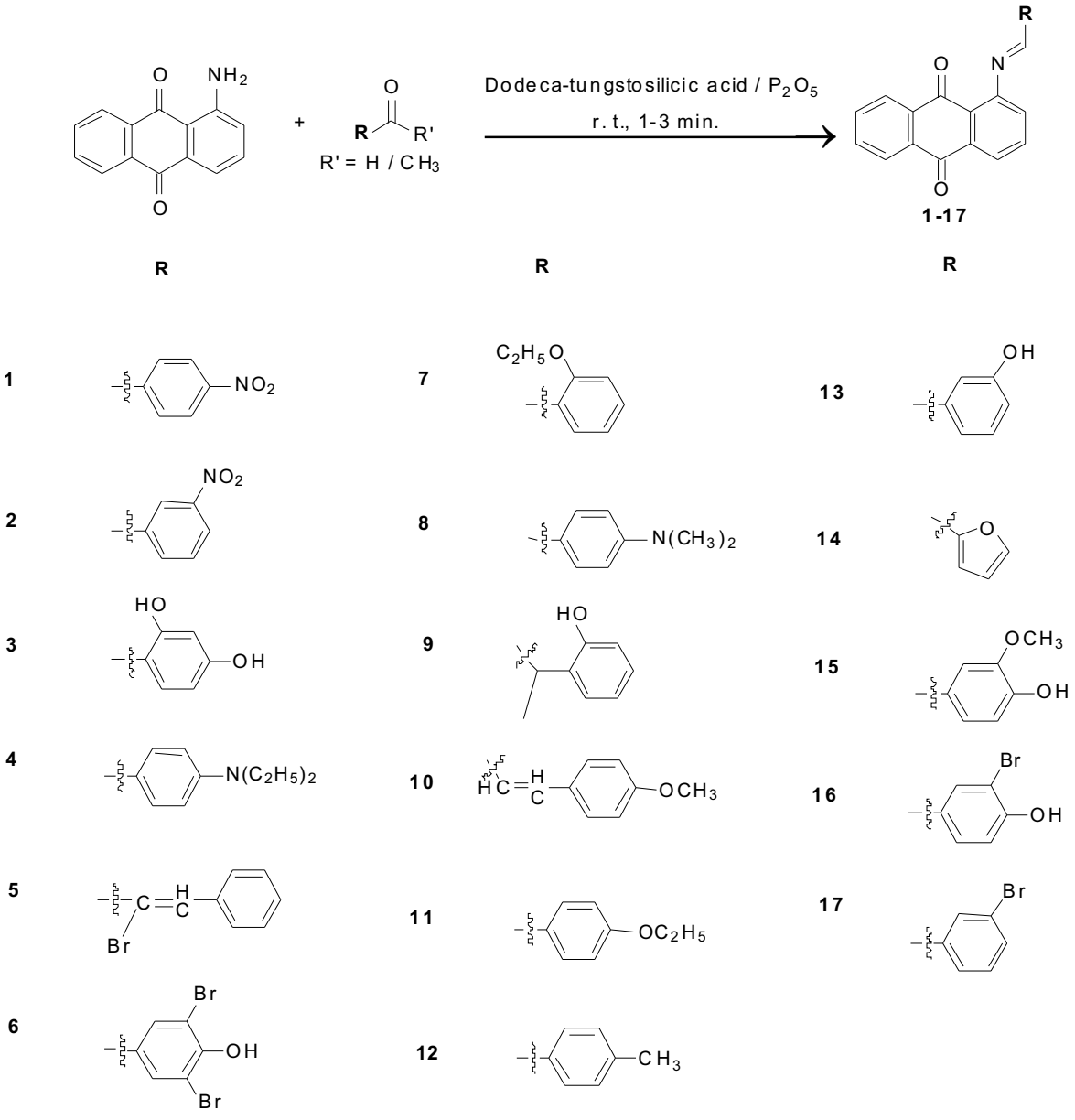

Scheme 1. Structures of synthesized Schiff bases **1-17**

(MRSA), *Escherichia coli* (MDR), *Klebsiella* species (MDR), *Salmonella typhimurium* (MDR), *Pseudomonas aeruginosa* (MDR), *E. coli* ATCC 8739*, Staphylococcus aureus* ATCC 25923*, Staphylococcus aureus, Escherichia coli, Klebsiella* species, and *Pseudomonas aeruginosa.* Stock solution was prepared by dissolving 5 mg of compounds in 1ml of sterile DMSO. 100 µL from the stock solution of each compound was taken in first rows of well then serially half dilution were made by taking Mueller Hinton broth. The bacterial suspensions were adjusted with sterile saline to a concentration of 1.0×10^5 CFU/mL then 10 µL inocula were taken and added in each well. Micro titer plates were incubated for 24 h at 37 °C to check the results. Well showed no visible growth was taken as MIC of compound. Each experiment was performed in triplicate to authenticate the results.

Results and Discussion

Antibacterial activity. Schiff bases **1-17** were synthesized by condensation of 1-aminoanthracene-9,10-dione with variety of aromatic and aliphatic carbonyl compounds using reported catalytic method (Fareed *et al*., 2013).

The antibacterial tests of the compounds **1-17** were carried out to determine MIC (Minimum Inhibitory Concentration) against multidrug resistant (MDR) strains *viz*., *S. aureus*, *E. coli* , *Klebsiella* species , *S. typhimurium*, *P. aeruginosa*, *E. coli* ATCC 8739, *S. aureus* ATCC-25923, and non-MDR strains of *S. aureus, E. coli, Klebsiella* species, and *P. aeruginosa.* The antibacterial studies were performed by broth micro dilution method by means of CLSI (Clinical and Standards Institute, 2012) formerly NCCLS (National Committee for Clinical Laboratory Standards) guidelines. All the isolates were isolated from various clinical samples (pus, urine, ear swabs, wound swabs, blood, fluid) of patients attending various hospitals in Karachi. The results were compared with Cefotaxime, which was used as standard drug. The results are depicted in Table 1.

Compounds **2**, **3, 4, 13** and **14** were found to be potent against multidrug resistant (MDR) bacterial strains when compared with the Cefotaxime standard, however compound **8** exhibited good activities against *S. aureus* and *Klebsiella* species. Compounds **2** and **4** exhibited lower MIC (250 µg/mL) against MDR *S. typhinurium*. Compound **14** showed MIC (250 µg/mL) against MDR *S. typhinurium*, *E. coli* and *P. aeruginosa*. Compounds **2** and **5** were found to have MIC (31.25 µg/mL) against

Table 1. Antibacterial activity of synthesized schiff bases **1-17**

Name of bacteria/compound no.	**1**	**2**	**3**	**4**	**5**	**6**	**7**	**8**	**9**	**10**	**11**	**12**	**13**	**14**	**15**	**16**	**17**	Cefotaxime
Staphylococcus aureus (MDR)	-	250	500	250	-	-	-	1000	-	-	-	-	1000	750	-	-	-	>800
Escherichia coli (MDR)	-	500	750	500	-	-	-	1000	-	-	-	-	750	250	-	-	-	>800
Klebsiella species (MDR)	-	1000	500	500	-	-	-	750	-	-	-	-	500	500	-	-	-	>800
Salmonella typhimurium (MDR)	-	250	500	250	-	-	-	750	-	-	-	-	500	250	-	-	-	>800
Pseudomonas aeruginosa (MDR)	-	500	500	1000	-	-	-	1500	-	-	-	-	500	250	-	-	-	>800
Escherichia coli ATCC-8739	500	250	500	750	250	500	62.5	1000	250	125	-	500	500	125	500	1000	-	3
Staphylococcus aureus ATCC-25923	250	250	125	125	125	250	125	750	250	250	-	250	750	125	250	500	-	3
Staphylococcus aureus	250	500	125	62.5	31.25	-	250	1000	125	250	-	500	500	750	62.5	500	-	6
Escherichia coli	-	250	500	1000	125	500	750	250	250	125	-	500	750	62.5	500	750	-	5
Klebsiella species	250	62.5	500	250	31.25	500	1000	500	500	750	-	750	1000	125	500	1000	-	6
Pseudomonas aeruginosa	250	31.25	1500	125	500	250	500	250	750	500	-	1000	1500	125	62.5	500	-	6

Results are presented as MIC value; MIC (µg/mL) = minimum inhibitory concentration; No. of isolates = 11.

non-MDR *P. aeruginosa* and *S. aureus* and *Klebsiella* species, respectively. Compounds **2** and **15** were found to be good to moderately active against *P. aeruginosa* with MIC values 31.25 µg/mL and 62.5 µg/mL, respectively and compounds **4** and **15** showed moderate activity against *S. aureus* with MIC 62.5 µg/mL. All the remaining compounds except **11** and **17** showed weak antimicrobial activity against non-MDR strains of bacterial isolates. Therefore, pharmacodynamic studies would be required to make them useful as potential antimicrobial agents.

References

Alekshun, M.N., Levy, S.B. 2007. Molecular mechanisms of antibacterial multidrug resistance. *Cell*, **128:** 1037-1050.

Alves, D.S., Pérez-Fons, L., Estepa, A., Micol, V. 2004. Membrane-related effects underlying the biological activity of the anthraquinones emodin and barbaloin. *Biochemical Pharmacology*, **68:** 549-561.

Ashnagar, A., Bruce, J.M., Dutton, P.L., Prince, R.C. 1984. One- and two-electron reduction of hydroxy-1,4-naphthoquinones and hydroxy-9,10-anthraquinones. *Biochimica et Biophysica Acta (BBA) - General Subjects*, **801:** 351-359.

Bringmann, G., Dreyer, M., Faber, J.H., Dalsgaard, P.W., Jaroszewski, J.W., Ndangalasi, H., Mbago, F., Brun, R., Christensen, S.B. 2004. Ancistrotanzanine C and related 5,1′- and 7,3′-coupled naphthylisoquinoline alkaloids from *Ancistrocladus tanzaniensis*. *Journal of Natural Products*, **67:** 743-748.

Chang, P., Lee, K.H. 1984. Cytotoxic antileukemic anthraquinones from *Morinda parvifolia*. *Phytochemistry*, **23:** 1733-1736.

daSilva, C.M., daSilva, D.L., Modolo, L.V., Alves, R.B., deResende, M.A., Martins, C.V.B., deFátima, Â. 2011. Schiff bases: A short review of their antimicrobial activities. *Journal of Advanced Research*, **2:** 1-8.

Fareed, G., Versiani, M.A., Afza, N., Fareed, N., Ali, M.I., Kalhoro, M.A. 2013. An efficient synthesis and spectroscopic characterization of Schiff bases containing the 9,10-anthracenedione moiety. *Journal of the Serbian Chemical Society*, **78:** 477-482.

Ge, P., Russell, R.A. 1997. The synthesis of anthraquinone derivatives as potential anticancer agents. *Tetrahedron*, **53:** 17469-17476.

Guo, Z., Xing, R., Liu, S., Zhong, Z., Ji, X., Wang, L., Li, P. 2007. Antifungal properties of Schiff bases of chitosan, N-substituted chitosan and quaternized chitosan. *Carbohydrate Research*, **342:** 1329-1332.

Kajal, A., Bala, S., Kamboj, S., Sharma, N., Saini, V. 2013. Schiff bases: A versatile pharmacophore. *Journal of Catalysts*, **2013:** 14.

Nor, S., Sukari, M., Azziz, S., Fah, W., Alimon, H., Juhan, S. 2013. Synthesis of new cytotoxic aminoanthraquinone derivatives via nucleophilic substitution reactions. *Molecules*, **18:** 8046.

Osman, C.P., Ismail, N.H., Ahmad, R., Ahmat, N., Awang, K., Jaafar, F.M. 2010. Anthraquinones with antiplasmodial activity from the roots of *Rennellia elliptica* Korth. (Rubiaceae). *Molecules*, **15:** 7218.

Piotr, P., Adam, H., Krystian, P., Bogumil, B., Franz, B. 2009. Biological properties of Schiff bases and azo derivatives of phenols. *Current Organic Chemistry*, **13:** 124-148.

Rath, G., Ndonzao, M., Hostettmann, K. 1995. Antifungal anthraquinones from *Morinda lucida*. *International Journal of Pharmacognosy*, **33:** 107-114.

Rice, L.B. 2006. Unmet medical needs in antibacterial therapy. *Biochemical Pharmacology*, **71:** 991-995.

Schinazi, R.F., Chu, C.K., Ramesh Babu, J., Oswald, B.J., Saalmann, V., Cannon, D.L., Eriksson, B.F.H., Nasr, M. 1990. Anthraquinones as a new class of antiviral agents against human immunodeficiency virus. *Antiviral Research*, **13:** 265-272.

Souza, A.O.D., Galetti, F.C.S., Silva, C.L., Bicalho, B., Parma, M.M., Fonseca, S.F., Marsaioli, A.J., Trindade, A.C.L.B., Gil, R.P.F., Bezerra, F.S., Andrade-Neto, M., Oliveira, M.C.F.D. 2007. Antimycobacterial and cytotoxicity activity of synthetic and natural compounds. *Quimica Nova*, **30:** 1563-1566.

Xiang, W., Song, Q.S., Zhang, H.J., Guo, S.P. 2008. Antimicrobial anthraquinones from *Morinda angustifolia*. *Fitoterapia*, **79:** 501-504.

Yadav, J.P., Arya, V., Yadav, S., Panghal, M., Kumar, S., Dhankhar, S. 2010. *Cassia occidentalis* L.: A review on its ethnobotany, phytochemical and pharmacological profile. *Fitoterapia*, **81:** 223-230.

Pak. j. sci. ind. res. Ser. A: phys. sci. 2018 **61A**(1) 19-27

Structural, Electrical and Thermal Properties of Lead Borate Glass Doped by V_2O_5 Content

Rahma Hamed Marhoom[a], Mohamed Said Dawelbeit[a], Essam Elsayed Assem[bc]* and Adel Ashour Mohamed[bd]

[a]Department of Electronics Engineering, Faculty of Engineering and Technology, University of Gezira, Sudan
[b]Physics Department, Faculty of Science, Islamic University, Kingdom of Saudi Arabia
[c]Physics Department, Faculty of Science, Kafrelsheikh University, Egypt
[d]Physics Department, Faculty of Science, Minia University, Egypt

(received March 13, 2017; revised November 11, 2017; accepted February 6, 2018)

Abstract. Glass samples of compositions xV_2O_5 +y Pb+ [100-(x+y)] B_2O_3 with the number of moles x varying from 0 to 2.5% and y varying from 0.2 to 0.195% are prepared by the technique of melting and quenching. The structural analysis of glass is achieved by studying the density and the molar volume. The glass density is increased from 1.8748 to 1.9347 g/cm according to the increase of the vanadium pentoxide contents. Also, the structural analysis of these glasses points out the conversion of structural units of BO_3 into BO_4, which leads to increased density and molar volume. However, the transition temperature, the crystallization temperature, and the glass stability are decreased. The VO_4 and VO_5 structural units of vanadium are formed in the structural network. The electronic conduction of borate glass can be explained using Polaron hopping between V^{+4} and V^{+5}. On the other hand, ionic conduction takes place by the Pb ion movement in all of the studied samples.

Keywords: glasses, density, molar volume, thermal properties, conductivity

Introduction

The shielding behavior of gamma radiation, optical properties of lead borate containing vanadium and structural properties of vanadium lead glasses show that vanadium plays a rule of a modifier (Rada *et al*., 2015; Abdelghany *et al*., 2012; Ghoneim *et al*., 2011). The effect of transition element on AC conductivity of borate glasses, vanadium borate glasses as rechargeable ionic batteries, elastic and structural properties of alkali borosilicate glasses containing vanadium, the structure and some physical properties of both borophosphate and borosilicate glasses containing vanadium have been studied (Ibrahim *et al*., 2017; Choi and Ryu, 2015; Laopaiboon and Bootjomchai, 2015; Afyon *et al*., 2014; Petru, 2010; Kashif *et al*., 2009; Marzouk *et al*., 2006; Assem, 2005; Khattak *et al*., 2003). Thermal properties of manganese bismo-borate glasses containing vanadium and semiconducting behavior of vanadium borate glasses have also been studied (Dahiya *et al*., 2016; Yousef *et al*., 2010). This paper details the preparation of a certain borate glass and highlights some of its structural, electrical and thermal properties using different experimental techniques. Six samples of borate glass were prepared and their densities were measured as a function of composition. The molar volume was then calculated from the density measurement results. Moreover, a thermal analyzer has been used to assess the thermal parameters such as glass transition temperature and crystallization temperature. Consequently, the stability of glasses and their network structure have been determined (Vijayalakshmi and Vasantharani, 2011).

The electrical conductivity of the glass system has been measured in the temperature range from 300 to 600 K. The results show a semiconducting behavior, which is in agreement with earlier studies (Ashwajeet *et al*., 2016; Bhavani *et al*., 2013; Mansour *et al*., 2001). The semiconducting behavior might be attributed to the presence of more hopping centers like V^{+4} ions and V^{+5} ions in the glass network. The vanadium ions may also exist in the glass network in the unstable ionic state V^{+2} and V^{+3}, which may also play a rule of hopping centers (Bhavani *et al*., 2013; Costigan *et al*., 2001; Chambers and Holliday, 1975). Furthermore, it is also important to mention that the study of electrical conductivity of this glass system shows an ionic conduction type produced by Pb ions and B^{+3} ions at a specific concentration of V_2O_5. Additionally, this kind of borate glass has the ability to accept vanadium ions in the network both as

*Author for correspondence;
E-mail: e_assem_2000@sci.kfs.edu.eg

a former or modifier (Pranesh *et al*., 2015). The aim of this work is to study the effect of V_2O_5 and Pb doping on the thermal, electrical and structural properties of borate glass. This work is part of a more general project to investigate the thermal, electrical, structural, dielectric constant and forier transformer infrared (FTIR) of latter borate glass system. To our knowledge such an investigation has not been presented in literature.

Materials and Methods

Samples preparations. The composition of each glass sample is prepared according to the percentage formula:

[100- (x+y)] moles of B_2O_3 + x moles of V_2O_5 +y moles of Pb ..... (1)

where:

x = 0.0, 0.5, 1.0, 1.5, 2.0, and 2.5 mole %, y = 0.2, 0.199, 0.198, 0.197, 0.196 and 0.195 mole % for the samples numbered 1, 2, 3, 4, 5 and 6, respectively.

Boron trioxide is introduced in terms of crystalline boric acid (H_3BO_3) in powder form with chemical purity grade 99.117% and containing impurities of sulphate (SO_4) (not more than 0.04%) and water (H_2O) (not more than 0.458%). While, vanadium pentoxide (V_2O_5) is added with chemical purity grade 99.5% as oxide containing 0.5% of other vanadium oxides.

For each of the above-mentioned samples, a homogeneous mixture of boron trioxide and vanadium pentoxide are made by putting the mixture in a vessel which is moderately shaking horizontally and vertically. Afterward, each mixture is poured in a porcelain crucible and melted in an electrically heated furnace at 800 °C for two hours and then quenched in air.

Measurements. ***Density measurement.*** The glass density is measured using the standard Archimedes method with ethanol (of density = 0. 78 g/cm^3) as the immersion liquid (Fig. 1). The masses, in this method, are measured by using a sensitive balance of range 0.0001 –160.0000 g. The density of each sample is calculated from the formula (Khasa *et al*., 2013):

$$D_G = (D_L M_G)/\Delta M \quad (2)$$

where:

D_G and D_L are the glass and liquid densities, respectively. M_G is the mass of the sample in air and ΔM is the equivalent loss of the mass in the liquid.

Molar volume calculations. The molar volume, V_m, for each sample is calculated from the formula (Khasa *et al*., 2012):

$$V_m = \Sigma\, n_i M_i/D_G \quad (3)$$

where:

M_i is the molar mass of the component which enters with the ratio n_i.

Electrical conductivity. The resistance, R, of each sample at different temperatures in the range 310-600 K is measured as follows: the sample is held by a copper holder and is heated up to 600 K by an electrical furnace. The heating is then stopped and the sample is left to cool freely down to 310 K.

The resistance of the sample is measured in the above-mentioned range of temperature in steps of 10 K decreasingly, using a digital multimeter (DT9205A+) ranged from 200 Ω -20 MΩ. From the results of the resistance measurements, the electrical conductivity is calculated for each sample in the desired temperature range. A plot for each sample, Fig. 2, is made for the natural logarithm of the conductivity, Ln(σ), versus the reciprocal of the absolute temperature (1/T). From the plots the activation energy, E_a of the electrical conductivity is calculated as a function of temperature using Arrhenius relation (Atkins and Julio, 2010; Wallwork *et al*., 1977; James and Prichard, 1974):

$$\sigma = \sigma_o \exp(-E_a/k_BT) \quad (4)$$

where:

σ_o is a constant and k_B is the Boltzmann's constant. Fig. 3 gives the activation energy of the electrical conductivity of the studied glass as a function of composition.

Differential scanning calorimetry. The differential scanning calorimetry (DSC) of the studied samples has been performed using the TA instrument (Inc.159 Lukens, New Castle, DE19720) programmed heating rates 10 K/min, 20 K/min, 30 K/min, 40 K/min at 300-1000 K temperature range. The glass crystallization temperature ,T_c, of these glasses has been determined from differential scanning calorimetry thermograms (Fig. 5 with sample 2 as a selected sample). The crystallization temperature at different heating rates (α) have been plotted as a function of vanadium pentoxide (V_2O_5) concentration (Fig. 6). Finally, as can be seen in Fig. 7, the activation energy of the crystallization

temperature is deduced using Kissinger's equation (Faeghinia *et al*., 2016; Yadav *et al*., 2012):

$$\text{Ln}\,(\alpha/T_c^2) = -\,(E_c/RT_c) + \text{constant} \quad \ldots\ldots\ldots\ldots\ldots\ldots\ (5)$$

where:

α is the heating rate and R is the universal gas constant. It is seen from equation (5) that the plot of Ln (α/T_c^2) versus $1/T_c$ is a straight line, from which the activation energy of crystallization temperature, E_c, is calculated. A plot of activation energy of crystallization as a function of V_2O_5 concentration is then made.

Results and Discussion

Density and molar volume. The density measurement is an important tool to detect the structural changes in the glass network (Soliman, 2008; Mansour *et al*., 2001). The density is supposed to change when the structure of the glass changes (Singh *et al*., 2011) while the molar volume changes according to the oxygen spatial distribution (Ashwajeet *et al*., 2016).

It can be seen from the Fig. 1, that the density of glass increases from 1.8748 to 1.9347 g/cm^3 with increasing vanadium pentoxide content from 0 mole% to 2.5 mole%. The increase of density may be attributed to: (Kashif *et al*., 2010; Doweidar *et al*., 2005):

(i) Replacement of low density ions of boron (2.46 g/cm^3) by higher density ions of vanadium density (6.11 g/cm^3).
(ii) Structural changes that cause conversion of BO_3 to BO_4.

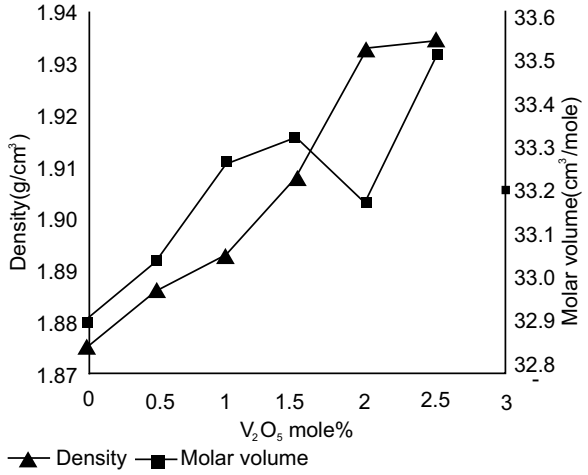

Fig. 1. Effect of doping V_2O_5 on density and molar volume of borate glass.

Regarding the second reason, the BO_4 is a denser structural unit than any BO_3 species (Singh *et al*., 2011; Assem and Elmehasseb, 2011; Gohar *et al*., 1993). The random configuration of the B_2O_3 glass network is relatively open; it contains large voids filled by V_2O_5 content. Hence, the mass increases while the volume expands slightly, and this causes the density to increase. The molar volume also increases as shown in Fig. 1. The gradual change appeared in the molar volume can be explained as follows: the excess of nonbridging oxygen atoms supplied to the glass structure by the addition of the V_2O_5 contents could be the cause of the conversion of triangular BO_3 units into tetrahedral BO_4 units, which led to an expansion in the glass network structure. Moreover, the increase of molar volume of the glass system is attributed to the modifier behavior of the doping oxides, which produces nonbridging oxygen and expands the lattice (Assem and Elmehasseb, 2011).

The changes in density and molar volume indicate that V_2O_5 acts as a glass modifier. The vanadium pentoxide introduced in the glass network exist in the form of two ions, V^{5+} (which acts as a glass former) and V^{4+} (which acts as a glass modifier), by occupying the empty spaces in the formerly open glass network. In our glass system, it seems that the modifier behavior is predominant, so that the glass network is disrupted and expanded, which in turn increases the molar volume (Gautam *et al*., 2012; Assem and Elmehasseb, 2011; Kashif *et al*., 2010).

Electrical conductivity. The electrical conductivity of glasses varies with composition and rises with increasing temperature. Studies of the electrical conduction mechanism in several glass systems showed that the thermal activation energy plays a dominant role in electrical conduction (Panchal, 2014; Dhote, 2014). It was also observed, by the latter authors, that the activation energy is influenced by the changes of the molar ratio of glass modifiers. The conductivity of glasses might be electronic, ionic or a mixture of both. The mobility of ions depends on both glass temperature and composition (Gawande *et al*., 2015; Meikhail, 2005). At high temperatures, most semiconductors tend to show rising movement of ions (Vijayalakshmi and Vasantharani, 2011; Kanchan and Panchal, 1998).

The glasses with a basic structure composed of B_2O_3 are insulating in nature and insensitive to the ionic migration, due to the high total energy required to produce B^{3+} ions, which is far more than would be

compensated by the lattice energies of ionic compounds or by hydration of such ions in solution. However, the addition of transition metal ions and alkaline earth ions to these glasses can produce mixed types of electrical conductivity (electronic and ionic) and thereby their electrical properties would be improved (Kundu *et al*., 2010; Kanchan and Panchal, 1998; Ahmed *et al*., 1984).

Figure 2 shows the temperature dependence of the conductivity of the studied glass samples. It has been observed that the conductivity of all samples increases as the temperature increases. The ionic conduction takes place by the mobility of Pb ions in all samples. In samples with vanadium content the electronic conduction increased due to the increase of the conversion of V^{4+} ions into V^{5+} ions as the vanadium pentoxide content is increased. As seen from molar volume results, the presence of nonbridging oxygen causes expansion in the glass structure, which facilitates the mobility of the lead ions and increases the ionic conductivity. The vanadium pentoxide ions contribute gradually to (electronic) conduction according to their amount in the samples. The increase in V_2O_5 content increases the electronic hopping between V^{4+} ions and V^{5+} ions (Khasa *et al*., 2014; Bhavani *et al*., 2013; Maloney, 1968). It has been observed that although samples 3 and 4 has less vanadium content than samples 5 and 6 the increase in their conductivity is higher. The reason for this is the appearance of ionic conduction carried by B^{3+} and Pb ions. However, the B^{3+} and Pb ionic conduction is less in samples 5 and 6 compared to samples 3 and 4 because the introduction of V_2O_5 into the glass network causes the conversion of BO_3 units into BO_4 units. Thus addition of more V_2O_5 produces a larger amount of nonbridging oxygen. The increase in the nonbridging oxygen ions, in samples 5 and 6, may cause blocking to the movement of the B^{3+} and Pb ions, as compared to samples 3 and 4. This blocking decreases the B^{+3} and Pb ionic conduction as can be seen in Fig. 2 (Pranesh *et al*., 2015; Nagaraja *et al*., 2014; Mansour *et al*., 2001). Another reason is that an increase in the nonbridging oxygen ions increases the distance between vanadium ions, this decreases the electron hopping between V^{5+} and V^{4+} which, in turn, decreases the conductivity (Al-Hajry *et al*., 2005).

The variations of both electrical conductivity and its activation energy with the composition at constant temperature are shown in Fig. 3-4, respectively, Fig. 4 shows that a long side the increase of the vanadium pentoxide content the conductivity is also slightly increased. This is in agreement with previous studies

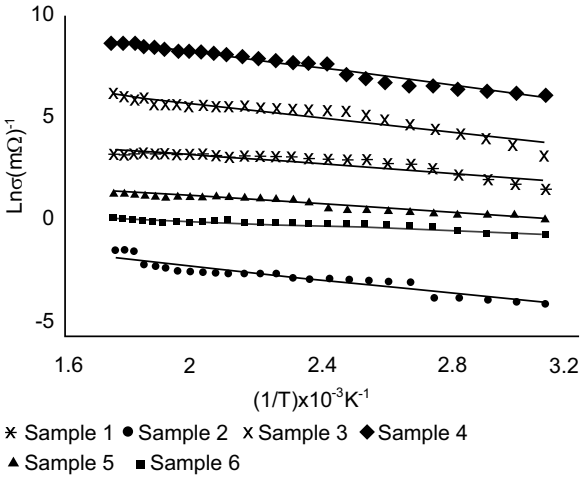

Fig. 2. Temperature dependence of electrical conductivity.

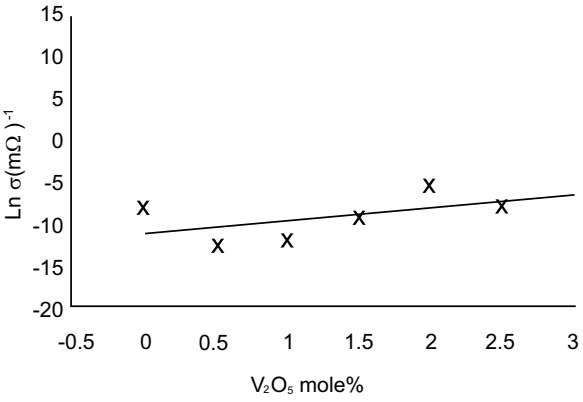

Fig. 3. Composition dependence of electrical conductivity at 313 K.

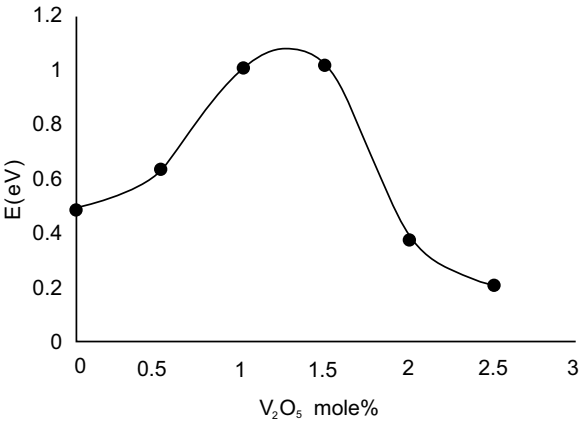

Fig. 4. Activation energy (E) for different V_2O_5 concentrations.

(Bhavani *et al*., 2013; Mansour *et al*., 2001; Shimakawa and Miyake, 1989).

Differential scanning calorimetry. The thermogram of the Fig. 5 represents a differential scanning calorimetry for the selected representative sample (sample 2) at four different heating rates. It can be seen that all of the samples have similar differential thermal calorimetry behavior. The curves show deep broaden endothermic peaks in the range 442 - 472 K due to water dehydration because these glasses are unstable against atmospheric moisture (Bhavani *et al*., 2013; Fatih *et al*., 2006). They show a broad halo, which is a characteristic of amorphous nature of the system and an absence of crystalline phase (Grega *et al*., 2010). All the thermograms show that there are no clear sharp peaks representing the characteristic temperature, such as glass transition temperature and crystallization temperature as well as absence of melting temperatures. Thus the thermograms indicate high resistance to crystallization (Thombre, 2016).

Figure 5 shows the increasing of transition temperature with increasing heating rate. This indicates the lack of tendency to crystallization of the investigated glass system (Assem *et al*., 2006). The transition temperatures of the studied samples become relatively low as the concentration of V_2O_5 is increased compared to other glasses not containing V_2O_5. This might be attributed to the replacement of strong B-O bonds by weak V-O bonds (Dahiya *et al*., 2015; Pranesh *et al*., 2015; Kashif *et al*., 2010).

Figures 6-7 show a decrease in both transition temperature, T_g and crystallization temperature, T_c with increasing V_2O_5 content at a fixed heating rate. Both T_g and T_c depend on the nonbridging oxygen density of the glass network, which is a measure of the tightness of packing factor. The oxygen density of the glass structure increases according to the degree of the replacement of B_2O_3 by V_2O_5 (Dahiya *et al*., 2015; Silva *et al*., 2014). Another reason for the decrease of the two temperatures T_g and T_c is due to the replacement of the weaker O-V-O bonds by stronger B-O-B and B-O-V bonds. The boron atoms, which have small radii and strong field's strength, are replaced by the vanadium atoms, which have large radii and small field's strength. These two reasons lead to a decrease in the packing and the two temperatures T_g and T_c (Al-Hajry *et al*., 2005; Mansour *et al*., 2001).

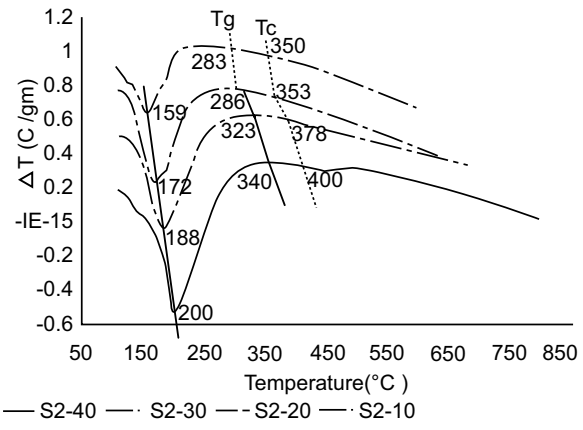

Fig. 5. DSC pattern of sample 2 at different heating rates (10 - 40) K /min.

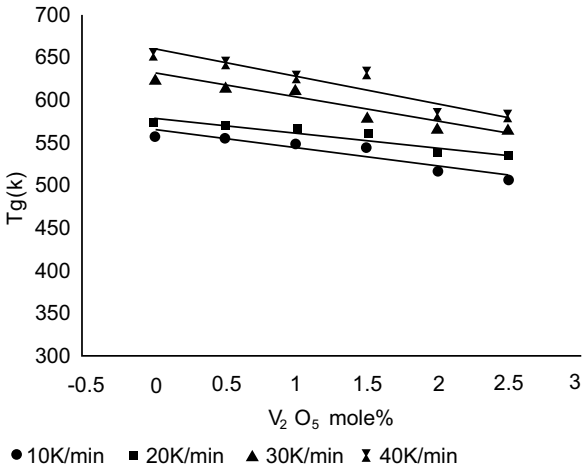

Fig. 6. Variation of glass transition temperature, T_g, with composition.

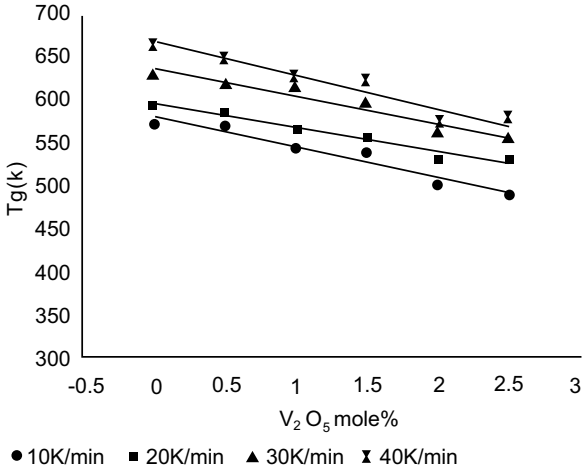

Fig. 7. Variation of crystallization temperature, T_c, with composition.

Figure 8 shows a decrease in the degree of the glass stability with increasing concentration of V_2O_5, although it is still large as compared to other glass systems. This is due to the increase in nonbridging oxygen and molar volume (Asha, 2014; Thombre and Thombre, 2014; Desirena *et al*., 2009). The decrease of the glass transition temperature and the high stability of the glass system with increasing concentration of V_2O_5 makes this glass system useful for low T_g applications (Khasa *et al*., 2014; Khan *et al*., 2014).

From Fig. 9, it can be seen that the activation energy of the crystallization is constant with increasing V_2O_5 concentration. This is due to the resistance of crystallization of the glass system.

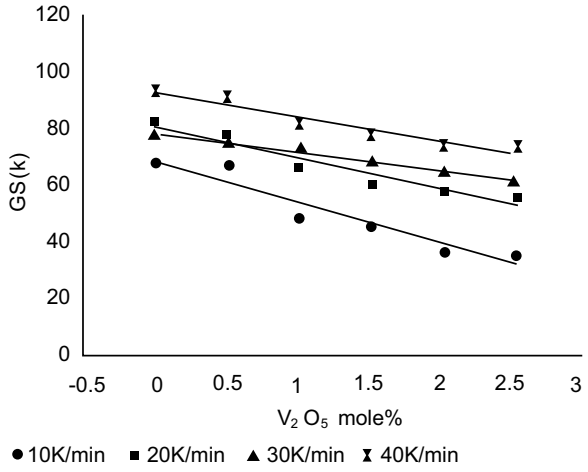

Fig. 8. Variation of glass stability (GS) with composition.

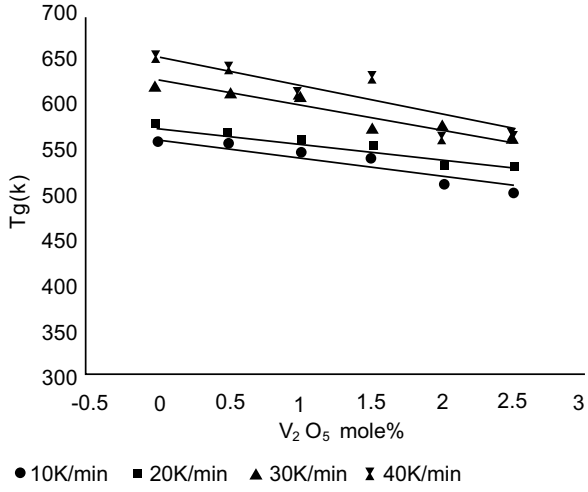

Fig. 9. Composition dependence of the activation energy of crystallization.

Conclusion

The density of the borate glass with vanadium content increases with the replacement of B_2O_3 with V_2O_5 and Pb, due to the fact that they have higher molar mass. The molar volume increases with increasing V_2O_5 and Pb due to increasing nonbridging oxygen and expanding of lattice.

The electrical conduction of the above mentioned glass system is partly ionic and partly electronic. The ionic conduction reaches its maximum value at 1.5 mole % of V_2O_5 and 0.197 mole % of Pb concentration above which it decreases due to blocking effect. The thermal parameters decrease with increasing V_2O_5 content and decreasing Pb content, due to the nonbridging oxygen density of the glass network. The activation energy of crystallization is constant with respect to doped vanadium oxide. This behavior may be attributed to the high resistance of crystallization of this glass system.

References

Abdelghany, A.M., ElBatal, H.A., Marei, L.K. 2012. Optical and shielding behavior studies of vanadium-doped lead borate glasses. *Radiation Effects and Defects in Solids*, **167:** 49-58.

Afyon, S., Krumeich, F., Mensing, C., Borgschulte, A., Nesper, R. 2014. New high capacity cathode materials for rechargeable Li-ion batteries: vanadate-borate glasses. *Scientific Reports*, **4:** doi10:1038/srep 07113.

Ahmed, M.M., Hogarth, C.A., Ghaghara, M.A. 1984. X-ray diffraction, density and electrical conductivity studies of some zinc borate glasses. *Journal of Material Science Letters*, **3:** 341-344.

Al-Hajry, A., Soliman, A.A., El-Desoky, M.M. 2005. Electrical and thermal properties of semiconducting Fe_2O_5-Bi_2O_5-$Na_2B_4O_7$ glasses. *Thermochimica Acta-Elsevier*, **427:** 181-186.

Asha, R. 2014. Physical, Thermal, Transport and Optical Studies on Borate and Phosphate Glasses Synthesized by Microwave Method. *Ph.D. Thesis*. Jain University, Bangalore, India.

Ashwajeet, J.S., Sankarappa, T., Rammana, R., Sujatha, T. 2016. Study of polaron transport mechanisms in two transition metal ions doped borophosphate glasses. *Glass Physics and Chemistry*, **42:** 27-32.

Assem, E.E., Elmehasseb, I. 2011. Structure, magnetic and electrical studies on vanadium phosphate glasses containing different oxides. *Journal Material*

Science, **46:** 2071-2073.

Assem, E.E., Mahmoud, K.R., Sharshar, T., Siligardi, C.J. 2006. Structure, magnetic and positron lifetime studies on CaO–ZrO_2–SiO_2 glass system doped with vanadium oxides. *Journal of Physics D: Applied Physics*, **39:** 734-739.

Assem, E.E. 2005. Effect of iron oxide on the structure, electrical and magnetic properties of (70% mole V_2O_5- (15-x)% mole P_2O_5-15% mole B_2O_3) semi conducting glass system. *Key Engineering Materials*, **280:** 327-332.

Atkins, P., Julio, De P. 2010. Physical Chemistry 9th edition, pp. 835-859, Oxford University Press, New Delhi, India.

Bhavani, P., Nagalakshmi, V., Iqbal, A.W., Emmanuel, K.L. 2013. Structrural study of PbO-PbF_2-B_2O_3 glass system doped withV_2O_5 through spectroscopic and magnetic properties. *Chemistry Journal*, **3:** 75-80.

Chambers, C., Holliday, A.K. 1975. *Modern Inorganic Chemistry*, pp. 359-369, 1st edition, Butterworth & Co., UK.

Choi, Su-Y., Ryu, B.K. 2015. Nanocrystallization of vanadium borophosphate glass for improving the electrical and catalytic properties. *Journal of Nanomaterials*, doi.org/10.1155/2015/201597.

Costigan, M., Gary, R., Dopson, S. 2001. Vanadium pentoxide and other inorganic vanadium compounds. Concise International Chemical Assessment Document 29, UK.

Dahiya, M.S., Khasa, S., Agarwal, A. 2016. Thermal characterization of novel magnesium oxyhalide bismo-borate glass doped with VO_2+ ions. *Journal of Thermal Analysis and Calorimetry*, **123:** 457-465.

Dahiya, M.S., Khasa, S., Agarwal, A. 2015. Physical thermal, structural and optical absorption study of vanadyl doped magnesium ox-chloride bismo-borate glasses. *Journal of Asian Ceramic Societies*, **3:** 206-211.

Desirena, H., Schulzgen, A., Sabet, S., Ramos-Ortiz, G., De la Rosa, E., Peyghambarian, N. 2009. Effect of alkali metal oxides R_2O(R=Li, Na, K, Rb, and Cs) and network intermediate MO (M=Zn, Mg, Ba and Pb in tellurite glasses. *Optical Materials*, **31:** 784-789.

Dhote, D.S. 2014. Transport properties of vanadium borate glasses. *International Research Journal of Science and Engineering*, **2:** 161-166.

Doweidar, H., Eldamroui, G.M., Moustafa, Y., Ramadan, R.M. 2005. Density of mixed alkali borate glasses: A structural analysis. *Physica B: Physics of Condensed Matter*, **362:** 123-132.

Faeghinia, A., Nemati, R., Sheighani, M. 2016. The crystallization kinetic of Te-Li glass. *Journal of Material, Mechanics, and Manufacturing*, **5:** 24-27.

Fatih, S., Fatih, D., Murat, B., Hüseyin, O. 2006. Kinetic analysis of (thermal) transition decomposition of boric acid thermogravimetric data. *Korean Journal of Chemical Engineering*, **23:** 736-740.

Gautam, C., Yadav, A.K., Singh, A.K. 2012. A review on infra-red spectroscopy of borate glasses with effect of different additives. *International Scholarly Research Network (ISRN) Ceramics*, **2012:** 1-17.

Gawande, W.J., Yawale, S.S., Yawale, S.P. 2015. Hopping conduction mechanism in amorphous CuO-Bi_2O_3 semiconducting pellets. *International Journal of Innovative Science, Engineering and Technology*, **2:** 209-213.

Ghoneim, N.A., ElBatal, H.A., Abdelghany, A.M., Ali, I.S. 2011. Shielding behavior of V_2O_5 doped lead borate glasses towards gamma irradiation. *Journal of Alloys and Compounds*, **509:** 6913-6919.

Gohar, I.A., Megahed, A.A., Assem, E.E. 1993. Halogen form in the calcium borate glasses containing iron. *Journal of Crystal Research Technology*, **28:** 217-224.

Grega, K., Jozef, M., Permoz, M. 2010. Differential thermal analysis and differential scanning calorimetry as a method of material investigation. *Material and Geoenvironmental*, **1:** 127-142.

Ibrahim, S., Marzouk, M.A., El-Komy, G.M. 2017. Structural characteristics and electrical conductivity of vanadium-doped lithium ultraphosphate glasses. *Silicon*, **9:** 403-410.

James, A.M., Prichard, F.E. 1974. *Practical Physical Chemistry*, 3rd edition, Prentice Hall Press, ISBN 978-0582442597.

Kanchan, D.K., Panchal, H.R. 1998. Infrared absorption study of potassium –boro-vanadate-iron glasses. *Turkish Journal of Physics*, **22:** 989-996.

Kashif, I., Abd-Elghany, A., Abd-Elmaboud, A., Elshirbeny, M.A., Sanad, A.M. 2010. IR, density, and DTA studies the effect of replacing Pb_3O_4 by CuO in Pseudo-binary $Li_2B_4O_7$-Pb_3O_4 glass

system. *Journal of Alloys and Compound*, **503:** 384-388.

Kashif, I., Rahman, S.A., Soliman, A.A., Ibrahim, E.M., Abdel-Khalek, E.K., Mostafa, A.G., Sanad, A.M., Physica, B. 2009. Effect of alkali content on AC conductivity of borate glasses containing two transition metals. *Physica B: Physics of Condensed Matter*, **404:** 3842-3849.

Khan, M.S., Shahzadi, P., Alam, S., Javed, K., Shaheen, F., Naqvi, J., Shahnaz, A. 2014. Developement of heat resistant of borosilicate glass doped with sodium silico fluoride compound. *Journal of Chemistry and Materials Research*, **4:** 13-18.

Khasa, S., Dahiya, S., Agarwal, A. 2014. Effect of alkali edition on DC conductivity & thermal properties of vanadium-bismo- borate glasses. *AIP Conference Proceedings*, **1591:** 796-798.

Khasa, S., Dahiya, M.S., Agarwal, A. 2013. Structural investigations of some lithium vanadoxide bismo-borate glasses. *Journal of Integrated Science and Technology*, **1:** 44-47.

Khasa, S., Manjeet, A.A. 2012. Synthesis and characterization of vanadyl ion doped alkaline halide borate glasses. *International Journal of Physics & Mathematical Science*, **2:** 104-108.

Khattak, G.D., Tabet, N., Salim, M.A. 2003. X-ray photoelectron spectroscopic studies of vanadium-strontium-borate [(V_2O_5) x (SrO) 0.2(B_2O_3) 0.8-x]oxide glasses. *Journal of Electron Spectroscopy and Related Phenomena*, **133:** 103-111.

Kundu, V., Dhiman, R.L., Maan, A.S., Goyal, D.R., Arora, S. 2010. Characterization and electrical conductivity of vanadium doped strontium bismuth borate glasses. *Journal of Optoelectronics and Advanced Materials*, **12:** 2373-2379.

Laopaiboon, R., Bootjomchai, C. 2015. Characterization of elastic and structural properties of alkali-borosilicate glasses doped with vanadium oxide. *Glass Physics and Chemistry*, **41:** 352-358.

Maloney, F.J.T. 1968. *Glass in the Modern World: A study in Materials Development*, Published by Aldus Books Ltd., ISBN 10:0490001068.

Mansour, E., Eldamrawi, G.M., Moustafa, Y.M., Abd-Elmaksoud, S., Doweidar, H. 2001. Polaronic conduction in barium borate glasses containing iron oxide. *Physica B*, **293:** 268-275.

Marzouk, S.Y., Elalaily, N.A., Ezz-Eldin, F.M., W.M. 2006. Optical absorption of gamma-irradiated lithium-borate glasses doped with different transition metal oxides, *Physica B: Condensed Matter*, **382:** 340-351.

Meikhail, M.S. 2005. Conduction modelling in mixed alkali borate glasses. *Journal of Pure & Applied Physics*, **1:** 191-197.

Nagaraja, N., Sankarappa, T., Sujatha, T.D.C. 2014. Dielectric relaxation studies in CuO doped borate glasses. *International Journal of Engineering Science and Innovative Technology*, **3:** 284-289.

Panchal, H.R. 2014. Structural, physical and electrical properties of boro-vanadate-iron glasses doped with K_2O alkali. *Turkish Journal of Physics*, **38:** 136-144.

Petru, P. 2010. Structural investigations of some bismuth–borate–vanadate glasses doped with gadolinium ions. *Journal of Materials Science: Materials in Electronics*, **21:** 338-342.

Pranesh, S., Krishna, D.K., Rumu, H., Ajithkumar T.G., Abraham, G., Mishra, R.K., Kaushik, C.P., Dey, G.K., Pinckney, L. 2015. Vanadium in borosilicate glass. *Journal of the American Ceramic Society*, **98:** 88-96.

Rada, M., Rus, L., Rada, S., Pascuta, P., Stan, S., Dura, N., Rusu, T., Culea, E. 2015. Role of vanadium ions on structural, optical and electrochemical properties of the vanadate-lead glasses. *Journal of Non-Crystalline Solids*, **414:** 59-65.

Shimakawa, K., Miyake, K. 1989. Hopping transport of localized electron in amorphous carbon films. *American Physics Society*, **39:** 7578-7584.

Silva, V.A., Nascimento, M.I.F., Morais, P.C., Datas, N.O. 2014. The structure role of Ti in a thermally –treated Li_2O-B_2O_3-AL_2O_3 glass system. *Journal of Non-Crystalline Solids*, **404:** 104-108

Singh, G., Singh, P., Kaur, P., Kaur, S., Singh, D.P. 2011. Role of V_2O_5 in structural properties of V_2O_5-MnO_2-PbO-B_2O_3 Glasses. *Materials Physics and Mechanics*, **12:** 58-63.

Soliman, A.A. 2008. Electrical and thermal properties of semiconducting Fe_2O_5-Bi_2O_5-$Na_2B_4O_7$ glasses. *Armenian Journal of Physics*, **1:** 188-197.

Thombre, D.B. 2016. Estimation of glass-forming ability and glass stability of lithium-borosilicate glasses. *International Journal of Innovative Research in Science, Engineering and Technology*, **5:** 124-132.

Thombre, D.B., Thombre, M.D. 2014. Study of physical properties of lithium borosilicate glasses. *International Journal of Engineering Research and*

Development, **10:** 9-19.

Vijayalakshmi, M., Vasantharani, P. 2011. Characterization of (50-x)Pb.xTiO_2 Glass system by spectroscopic and thermal analysis. *International Journal of Recent Scientific Research*, **2:** 10-13.

Wallwork, S.C., Phil, M.A.D., Inst, P.F., Grant, D.J.W. 1977. Physical Chemistry for Student of Pharmacy and Biology, pp. 164-171, 3rd edition, Longman, London and NewYork, USA.

Yadav, A.K., Gautam, C., Singh, P. 2012. Crystallization kinematic and dielectric behaviour of (Ba,Sr) TiO_3 borosilicate glass ceramics. *New Journal of Glass and Ceramics*, **2:** 126-131.

Yousef, El-Sayed, Shaaban, E.R., Hawary, M., Al-Salami, A.E., Al-Assiri, M.S. 2010. Crystallization kinetics of semiconducting vanadium borate glass using DSC. *Physica Scripta*, doi.org/10.1088/0031-8949/82/04/045603.

Pak. j. sci. ind. res. Ser. A: phys. sci. 2018 **61A**(1) 28-34

Influence of Chemical Surface Modifications on Mechanical Properties of *Combretum dolichopetalum* Fibre - High Density Polyethylene (HDPE) Composites

Azeez Taofik Oladimeji[a]*, Onukwuli Okechukwu Dominic[b], Walter Peter Echeng[b] and Menkiti Mathew Chukwudi[b]

[a]Biomedical Technology Department, Federal University of Technology, P. M. B. 1526, Owerri, Imo State, Nigeria

[b]Chemical Engineering Department, Nnamdi Azikiwe University, P. M. B. 5025, Awka, Anambra State, Nigeria

(received February 11, 2016; revised December 22, 2017; accepted January 8, 2018)

Abstract. Maximizing the use of natural fibres as ecofriendly materials in polymer composite applications reduces its threat posed to human through increased biomass in the environment. In this study, the effect of chemical surface modifications using acetic anhydride and sodium hydroxide solution on the mechanical properties of *Combretum dolichopetalum* fibre-HDPE composites was aimed to be investigated. Fibres were treated with 6 % acetic anhydride and 12 % NaOH solutions for 30 minutes at room temperature based on optimum treatment conditions after water retting extraction process, then, the composites were prepared. The mechanical properties (tensile strength, tensile modulus, flexural strength, flexural modulus, hardness and impact strength) of the *C. dolichopetalum* fibre reinforced HDPE matrix composites and scanning electron microscope analysis were studied. *C. dolichopetalum* fibre was not only effective as reinforcement of HDPE matrix but mercerization and acetylation of C. *dolichopetalum* fibre ultimately enhanced the mechanical properties of HDPE composites. Scanning electron microscope analysis revealed that HDPE matrix possess better adhesive interaction with acetylated and mercerized *C. dolichopetalum* fibre compared with untreated *C. dolichopetalum* fibre at ultimate tensile strength.

Keywords: *Combretum dolichopetalum,* fibre, mechanical properties, HDPE matrix, mercerization, acetylation

Introduction

Combretum dolichopetalum plant is commonly known as *sun birds wine* plant which belongs to the genus *Combretum* that comprises of about 20 genera and 600 species distributed in Africa and Asia. The extract of *C. dolichopetalum* species are extensively applied in traditional medicine in southern part of Nigeria. After extraction of the active ingredients, the crystalline fibre of *C. dolichopetalum* usually disposed to the environment, thus increasing biomass in the environment. The gradual depletion of petroleum resources worldwide and the enactment of new rules and regulations on environmental preservation and management have triggered the demand for new materials that are ecofriendly (Hashim *et al*., 2012; Srinivasa and Bharat, 2011; Sinha and Rout, 2009). Products made from synthetic fibre reinforced composites are non-recyclable and constitute a threat to the environment at the end of their useful life, since they cannot be conveniently disposed (Saira *et al*., 2007). Therefore, the use of natural cellulosic fibres as reinforcement for polymeric matrix has become an attractive venture. For three thousand years now, natural fibres have been used to reinforce materials (Ashik and Sharma, 2015; Sakthivei and Romesh, 2013). Currently, natural fibre have been employed in combination with plastics. Composites made by reinforcing natural fibres are less dense, ecofriendly, and improved electrical resistance, high strength to weight ratio and corrosion resistance (Azeez and Onukwuli, 2017; Thompson, 2013; Ishak *et al.*, 2009). These composites reduce wear of processing equipment and devoid of health implication during processing, application and upon disposal. However, the inclusion of lignocellulosic fibres into thermoplastic or thermosetting polymer is often associated with poor fibre dispersion due to the large differences in polarity between the fibre and polymer, strong intermolecular and hydrogen bond between the fibres and matrix (Sanjay *et al*., 2016; Shah *et al*., 2010 Siregar *et al*., 2010). These bottlenecks have been overcome by suitable physical, chemical and enzymatic treatments (Osorio *et al*., 2012). The chemical treatment

*Author for correspondence;
E-mail: taofikoladimeji@gmail.com

may be used to improve hydrophilic in nature of natural fibre, interfacial bonding between matrix and fibre, surface roughness, wettability and decreased moisture absorption, thermal and electrical properties (Beckermann and Pickering, 2008; Noranizan and Ahmad, 2012; Raj *et al*., 2011). Many researchers have applied mercerization and acetic anhydride treatment with remarkable improvement in the mechanical properties of both treated fibres and/or composites at optimum conditions (Hossain *et al*., 2014; Punyamurthy *et al*., 2014; Singha and Thakur, 2014; Tlijania *et al*., 2014; Noorunnisa *et al*., 2011; Zhong *et al*., 2010). Higher concentration of alkali solution may also lead to excess delignification of fibre which weakens and damages the fibre (Li *et al*., 2007). Sampathkumar *et al.* (2012) and Arsene *et al.* (2005) reported decline in properties after alkali treatment of areca fibre, sugar cane bagasse and banana tree trunk fibres respectively. However, the investigation was not only pioneer the use of *C. dolichopetalum* fibre as reinforcement of HDPE matrix which will reduce the threat posed by biomass of *C. dolichopetalum* fibre but influence of chemical surface modifications to improve the mechanical properties of *C. dolichopetalum* fibre-HDPE composites was aimed to be investigated.

Materials and Methods

Combretum dolichopetalum plant was obtained from Bayaoje in Surulere Local Government Area of Oyo state, Nigeria. HDPE matrix obtained from Eleme Petrochemical Company, Port Harcourt in River State, Nigeria was used with tensile strength, tensile modulus, flexural strength, flexural modulus, hardness and impact strength of 24.619 MPa, 836.25 MPa, 27.114 MPa, 1390.7 MPa, 21 HR and 859.3 kPa, respectively. Sodium hydroxide and acetic anhydride used for fibre modifications were collected from Rovert Scientific Limited (RC-627785), Benin City in Edo State, Nigeria.

Fibre extraction. The *C. dolichopetalum* fibres were extracted from the plant stem using water retting extraction process in accordance with the method described by Nguyen *et al.* (2012). 30kg of plant stem was retted in deionized water for 21 days, washed at 3 days interval until fibre was produced, then sun dried for 7 days and later dried at a temperature of 60 °C for 2 h.

Mercerization and acetylation of *C. dolichopetalum* fibre. Strands of *C. dolichopetalum* fibres (average length of 150 mm was cut into 10 mm) mercerized with 12% NaOH solution (mCDF) and acetylated with 6% acetic anhydride (aCDF) having tensile strength of 71.267 and 99.282 MPa, respectively, at room temperature for 30 min as optimum treatment conditions reported by Walter *et al*. (2016), then washed severally with deionized water to ensure neutral pH. The fibres were finally dried in an air oven at 60 °C for 2 h.

Composite preparation. The untreated and treated *C. dolichopetalum* fibres of 10 mm length were mixed with high density polyethylene pellets (HDPE) in different proportions (0:100, 2.5:97.5, 3.75:96.25, 5:95, 6.25: 93.75 and 7.5:92.5). The fibre - HDPE mixtures were processed by injection moulding method. Rectangular test specimens having dimensions of 150 x 25 x 3 mm^3 were cut from the composites according to ASTM 638-90 standard.

Characterization of composites. ***Tensile testing.*** Tensile test using tenstometer machine (Model: M500-25KN, OL11 1NR, England) was carried out at Foundary Department, Federal Institute of Industrial Research, Osodi, Lagos in accordance with BS EN ISO 903: 1998 on a rectangular shape of CDF - HDPE laminates having dimensions of 80 mm (span) × 25 mm (width) × 3mm (thickness) with a constant rate of transverse of the moving grip of 40 mm /min was used in evaluating the tensile properties.

Flexural testing. 3 - point flexural test using tenstometer (Model: M500-25KN, OL11 1NR, England) was carried out at Foundary Department, Federal Institute of Industrial Research, Osodi, Lagos in accordance with BS EN ISO 903: 1998 on a rectangular shape of CDF-HDPE composites having dimensions of 80 mm (span) × 25mm (width) × 3mm (thickness) with a constant rate of 40 mm/min.

Impact testing. Unnotched Izod impact test using cantilevered beam configuration with tenstometer (Model: M500-25KN, OL11 1NR, England) was carried out at Foundary Department, Federal Institute of Industrial Research, Oshodi, Lagos in accordance with BS EN ISO 903: 1998 on a rectangular shape of CDF-HDPE laminates with dimensions of 80mm (span) × 25mm (width) × 3mm (thickness) for a constant rate of 40 mm /min.

Hardness testing. A standard Rockwell tester (model Testor HT 1a, Otto Wolpert-Werke, Germany) was used with steel indenter to measure the hardness of the test specimen. The hardness test was carried out at Material

and Metallurgical Department, Federal University of Technology, Owerri, Nigeria. A load of 150kgf was applied for each measurement on the specimen with parallel flat surfaces of the avail of the apparatus and minor load (15kg$_f$) was applied by lowering the steel ball onto the surface of the specimen. The dial was adjusted to zero on the scale under minor load and the major load was immediately applied by releasing the trip lever. After 15sec, the major load was removed and Rockwell hardness was recorded.

Scanning electron microscope (SEM). The SEM micrograph of tensile strength fractured surface of CDF - HDPE composites were taken using Scanning Electron Microscope (Model Phenom-Prox of Eindloven Netherlands) at Ahmadu Bello University, Zaria, Nigeria. The samples were sputter coated with gold within 24 h in a SEM coating unit. The fractured surfaces of gold coated samples were stored in desiccators till SEM observation was made.

Results and Discussion

Tensile properties. Figure 1(a) shows the effect of fibre loading on the tensile strength behaviour of untreated and treated *C. dolichopetalum* fibre - HDPE composites. The tensile strength of the composite of both untreated and treated *C. dolichopetalum* fibre - HDPE composites varies with increased fibre loading. The ultimate tensile strengths of uCDF, mCDF and aCDF - HDPE composites were obtained at fibre weight fraction of 2.5, 3.75 and 5.0% percent, respectively. This shows that the ultimate tensile strength of mCDF and aCDF - HDPE composite increased by 7.64 and 18.78% of the uCDF - HDPE composite, respectively. This may be attributed to increased interfacial adhesion between the fibre and matrix, hydrophilic nature of the fibres and the presence of strong hydrogen bonding as well as improved stress transfer between the matrix and fibre, thereby, maximizes utilization of the fibre in the composite as also reported by many researchers (Arfin *et al*., 2012; Ramanaiah *et al*., 2012; Zhong *et al*., 2007; Yang *et al*., 2004). Figure 1(b) shows the tensile modulus of untreated and treated *C. dolichopetalum* fibre - HDPE composites with varying fibre loading. The ultimate tensile modulus for untreated, mercerized and acetic anhydride treated HDPE composites was obtained at fibre loading of 2.5, 3.75 and 2.5 %, respectively. The mercerized and acetylated fibre loading increased the tensile modulus by 4.83 and 129.84%, respectively, as compared to that of untreated composite. This indicated

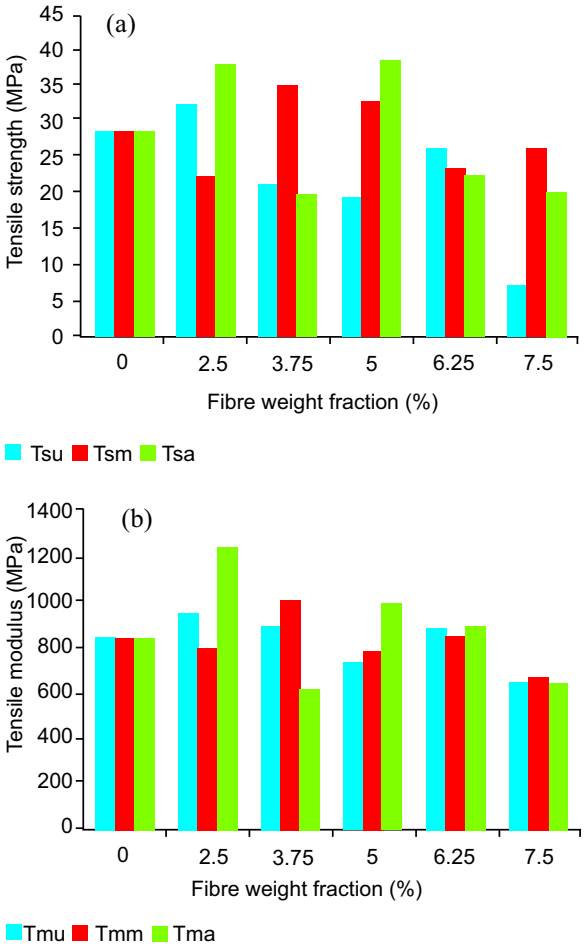

Fig. 1. Chemical surface modification of CDF - HDPE composite on (a) tensile strength (b) tensile modulus.
Tsu, Tsm and Tsa, represent the tensile strength of untreated, mercerized and acetic anhydride treated fibre-HDPE composites, respectively. Tmu, Tmm and Tma means tensile modulus of untreated, mercerized and acetic anhydride treated fibre-HDPE composites, respectively.

that mercerization and acetylation of fibres increases the fibre distribution which increases the stiffness of the CDF - HDPE composites. This is in agreement with the report of Arfin *et al.* (2012).

Flexural properties. Flexural strength of CDF - HDPE composites as illustrated in Fig. 2(a). It was observed that the flexural strength of uCDF and mCDF - HDPE composites initially decreases which may be attributed to non- uniform distribution of the fibre in the matrix and then, increases which may be due to good

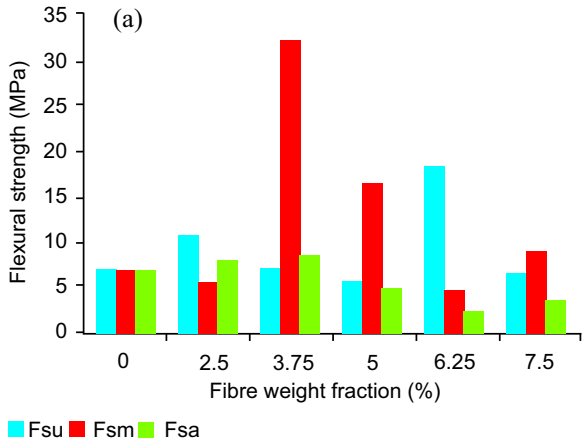

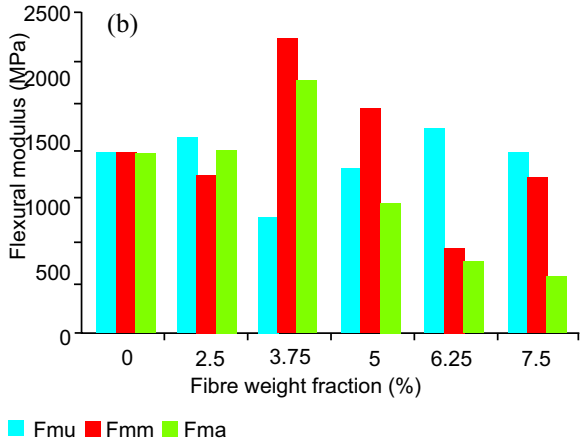

Fig. 2. Chemical surface modification of CDF - HDPE composite on (a) flexural strength (b) flexural modulus Fmu. Fsu, Fsm and Fsa means flexural strength of untreated, mercerized and acetic anhydride treated fibre - HDPE composites, respectivily. Fmm and Fma means Flexural modulus of untreated, mercerized and acetic anhydride treated fibre-HDPE composites, respectively.

compatibility between the fibre and matrix with increased fibre loading. This shows that the ultimate flexural strength of mCDF - HDPE composite increased by 76.19% and that of an acetylated one reduces by 53.24% of the uCDF - HDPE composite at fibre loading of 3.75%. However, the ultimate flexural modulus of mCDF and aCDF - HDPE composites increased by 45.22 and 23.99%, respectively, at fibre loading of 3.75% compared with uCDF - HDPE composite at 6.25% of the fibre loading as shown in Fig. 2(b). This may be attributed to the increased interfacial adhesion,

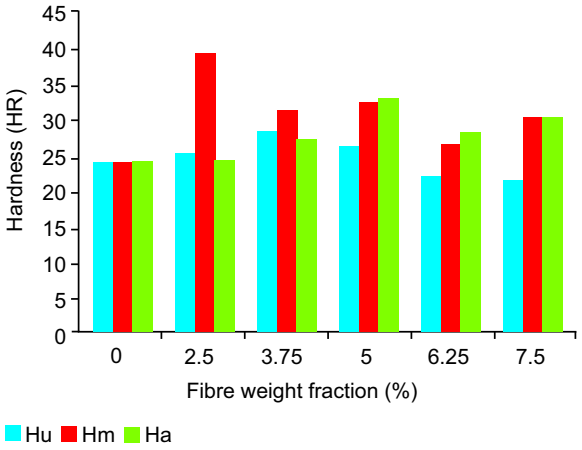

Fig. 3. Chemical surface modification of CDF - HDPE composite on hardness property. Hu, Hm and Ha means Hardness of untreated, mercerized and acetic anhydride treated fibre-HDPE composites, respectively.

dispersion of fibre in the matrix and stabilization of molecular orientation of fibre (Chandramohan and Marimuthu, 2011).

Hardness. The hardness of untreated and treated of *C. dolichopetalum* fibre - HDPE composites were initially increased with increasing fibre loading and later declined as shown in Fig. 3. The ultimate hardness of mCDF and aCDF - HDPE composites increased by 39.29 and

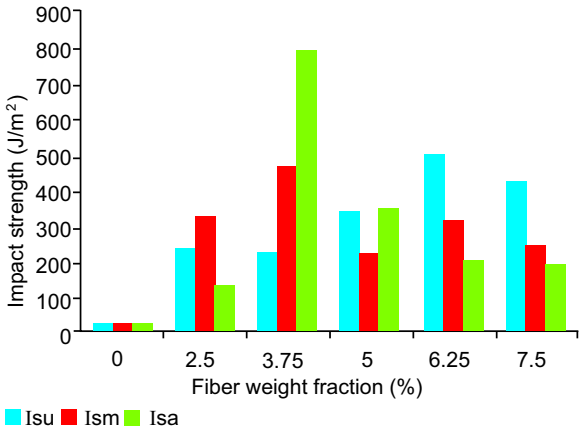

Fig. 4. Chemical surface modification of CDF-HDPE composite on impact strength. Isu, Ism and Isa means Impact strength of untreated, mercerized and acetic anhydride treated fibre-HDPE composites, respectively.

17.85% at fibre loadings of 2.5 and 5.0%, respectively, compared with that of uCDF - HDPE composite at fibre loading of 3.75%. This indicated that mercerization and acetylation of *C. dolichopetalum* fibre improved the hardness of the HDPE composite which is in agreement with the report of researchers (Aldousiri *et al*., 2011; Ishidi *et al*., 2011).

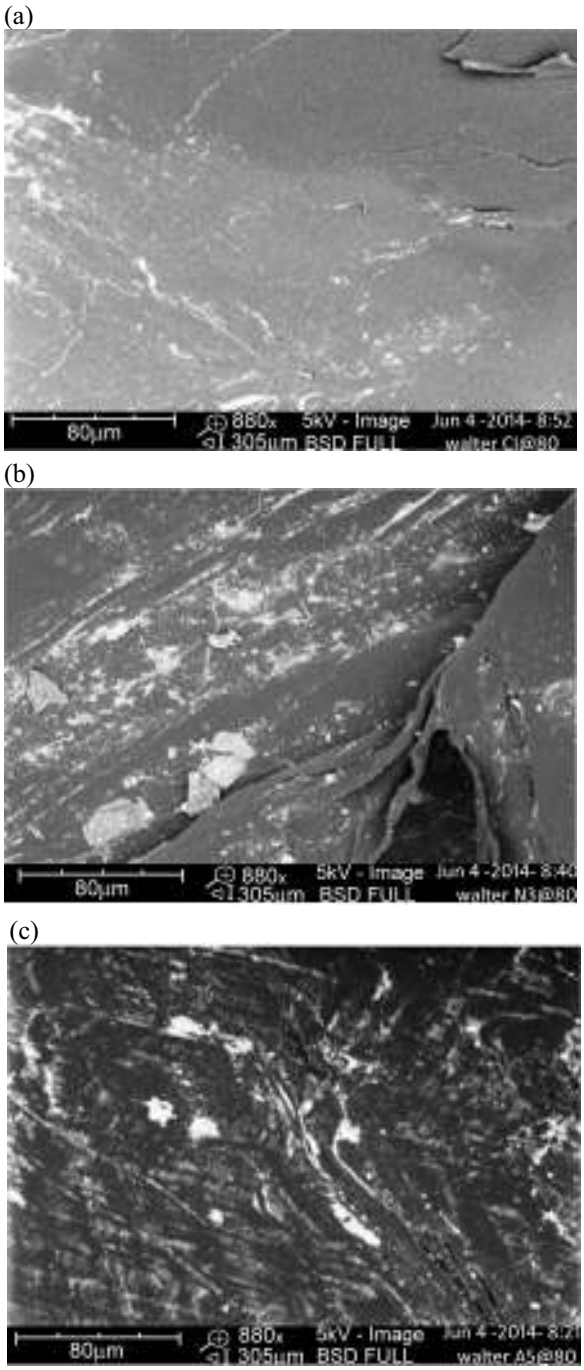

Fig. 5. SEM micrographs of CDF - HDPE composites (2.50% v/v) with magnifications of x 880 for (a) untreated (b) mercerized and (c) acetylated.

Impact strength. Figure 4 shows that the impact strength of the uCDF, mCDF and aCDF - HDPE composites increases with increasing fibre loading for up to 3.75%. Ultimate impact strength was obtained at 3.75% for mCDF and aCDF - HDPE composites while that of uCDF - HDPE composite reaches at fibre loading of 6.25%. It can be deduced that the ultimate impact strength of mCDF - HDPE composite reduced by 5.33% while that of aCDF - HDPE composite increased by 58.73% of uCDF - HDPE composite.

Scanning electron microscope analysis. The changes in the topography and morphology of *C. dolichopetalum* fibre - HDPE composites were studied by SEM. It can be observed that *C. dolichopetalum* fibre distribution into the HDPE matrix is reasonably good with minimal voids found in the composites. It seems that the uCDF were not evenly distributed in HDPE matrix as observed in Fig. 5a compared with mCDF and aCDF as shown in Fig. 5b and 5c, respectively. However, acetylated *C. dolichopetalum* fibres are more evenly distributed than mercerized fibres. This indicates mercerization and acetylation treatments of *C. dolichopetalum* fibres in the HDPE composite has a profound effect in creating a reasonably good dispersion and better interfacial adhesion between the components, which have been confirmed with the mechanical studies. Though, acetylated fibre shows superiority when compared with mercerized fibre in reinforcement of HDPE composites. This is similar to the report of Muhammed *et al.* (2015) and Favaro *et al.* (2010).

Conclusion

The influence of chemical surface modifications on the mechanical properties of *C. dolichopetalum* fibre reinforced HDPE composites was studied for fibre process conditions of 12% NaOH and 6% acetic anhydride solutions for 30 min, respectively, at room temperature. HDPE composites with acetylated *C. dolichopetalum* fibres showed superior improvement in tensile strength, tensile modulus and impact strength compared to untreated and mercerized composites due to improved fibre distribution, fibre - matrix interaction and mechanical interlocking facilitated by fibre surface

modification. Mercerized *C. dolichopetalum* fibre proved to have the best improvement in flexural properties and hardness of HDPE composites.

Acknowledgement

We appreciate the support of personnel at the Laboratory of Material and Metallurgical Department, Federal University of Technology, Owerri, Nigeria and Federal Institute of Industrial Research Oshodi, Lagos for assistance in Mechanical analysis.

References

Aldousiri, B., Alajmi, M., Shalwan, A. 2013. Mechanical properties of palm fiber reinforced recycled HDPE. *Advances in Material Science and Engineering Journal*, **10:** 1-7.

Arsene, M.A., Bilba, K., Soboyeyo, A.B.O., Soboyejo, W.O. 2005. Influence of chemical and thermal treatments on tensile strength of fibers from sugar cane bagasse and banana tree trunk. Inter-American Conference on Non-Conventional Materials and Technologies in Ecological and Sustainable Construction (IAC-NOCMAT, 2005), Rio de Janerio -Brazil, Brazil.

Arfin, J., Rahman, M.M., Md. Humayan, K., Farid, A., Md. Adbul, H., Md. Abdul, G. 2012. Comparative study of physical and glass fiber reinforced LDPE Composites. *International Journal of Science and Technology Research*, **1:** 68-72.

Ashik, K.P., Sharma, R.S. 2015. A review on mechanical properties of natural fibre reinforced hybrid polymer composites. *Journal of Minerals and Materials Characterization and Engineering*, **3:** 420 - 426.

Azeez, T.O., Onukwuli, D.O. 2017. Effect of chemically modified *Cissus populnea* fibres on mechanical, microstructural and physical properties of *Cissus populnea*/high density polyethylene composites. *Engineering Journal,* **21:** 25-42.

Beckermann, G.W., Pickering, K.L. 2008. Engineering and evaluation of hemp fibre reinforced polypropylene composites: Fibre treatment and matrix modification. *Composites Part A: Applied Science and Manufacturing,* **39:** 979-988.

Chandramohan, D., Marimuthu, K. 2011. Tensile and hardness tests on natural fiber reinforced polymer composite materials. *International Journal of Advanced Engineering Science and Technologies*, **6:** 97-104.

Fávaro, S.L., Ganzerli, T.A., de Carvalho Neto, A.G.V., da Silva, O.R.R.F., Radovanovic, E. 2010. Chemical, morphological and mechanical analysis of sisal fibre-reinforced recycled high-density polyethylene composites. *Express Polymer Letters,* **4:** 465-473.

Hussain, S.A., Pandurangadu, V., Palanikuamr, K. 2011. Mechanical properties of green coconut fibre reinforced HDPE polymer composite. *International Journal of Engineering Science and Technology*, **3:** 7942-7952.

Hossain, S.I., Hassan, M., Md. Hassan, N., Hassan, A. 2014. Effect of chemical treatment on physical, mechanical and thermal properties of ladies finger natural fiber. *Advances in Material Science and Engineering*, **10:** 1-6.

Hashim, M.Y., Roslan, M.N., Amin, A.M., Zaidi, A.M.A., Ariffin, S. 2012. Mercerization treatment parameter effect on natural fibre reinforced polymer matrix composite: A brief review. *World Academy of Science, Engineering and Technology*, **68:** 1638-1644.

Ishidi, E.Y., Kolawale, E.G., Sunmonu, K.O., Yakubu, M.K., Adamu, I.K. Obele, C.M. 2011. Study of physiomechanical properties of high density polyethylene (HDPE) - palm kernel nut shell (Elaeis Guineasis) composites. *Journal of Emerging Trends in Engineering and Applied Sciences*, **2:** 1073-1078.

Ishak, M.R., Leman, Z., Sapaun, S.M., Edeerozey, A. M.M., Othman, I.S. 2009. Comparative study of tensile properties of kenaf bast and core fibre reinforced unsaturated polyester composites. *Proceedings of the 9th National Symposium on Polymeric Materials 2009 (NSPM 2009)*, Universiti Putra Malaysia, Malaysia.

Li, X., Tabil, L.G., Panigrahi, S. 2007. Chemical treatments of natural fibre use in natural fibre-reinforced composites: A review. *Journal of Polymer and Environment*, **15:** 25-33.

Muhamed, H.E., Yehia, M.S.E., Ashraf, A.M., Muhamed, H.Z. 2015. Composites from rice straw and high density polyethylene: Thermal and mechanical properties. *International Journal of Engineering Science,* **4:** 57-64.

Noranizan, I.A., Ahmad, I. 2012. Effect of fibre loading and compatibilizer on rheological, mechanical and morphological behaviors. *Open Journal of Polymer Chemistry*, **2:** 31-41.

Noorunnisa, K.P., Abdul, K.H.P.S., Ramachandra, R.G., Venkata, N.S. 2011. Tensile, flexural and chemical resistance properties of sisal fibre reinforced

polymer composites: effect of fibre surface treatment. *Journal of Polymers and the Environment*, **19:** 115-119.

Nguyen, T.P., Toru, F., Bui, C., Takashi, M., Kazuya, O. 2012. Study on how to effectively extract bamboo fibres from raw bamboo and wastewater treatment. *Journal of Material Science and Research*, **1:** 144-155.

Osorio, M.C.J., Baracaldo, R.R., Florez, O.J.J. 2012. The influence of alkali treatment on banana fiber's mechanical properties. *Ingenieria e Investigacion*, **32:** 83-87.

Punyamurthy, R., Sampathkumar, D., Bennehalli, B., Badyanki, P.V. 2014. Study of the effect of chemical treatments on the tensile behavior of abaca fibre reinforced polypropylene composites. *Journal of Advances in Chemistry*, **10:** 2814-2822.

Raj, G., Balnoiso, E., Baley, C., Grohens, Y. 2011. Role of polysaccharides on mechanical and adhesion properties of flax fibres in flax/PLA biocomposite. *International Journal of Polymer Science,* **2011:** 1-11.

Ramanaiah, K., Ratna, A.V., Reddy, K.H.C. 2012. Effect of fiber loading on mechanical properties of borassus seed shoot fibre reinforced polyester composites. *Journal of Material and Environmental Science*, **3:** 374-378.

Sakthivei, M., Romesh, S. 2013. Mechanical properties of natural fibre (banana, coir and sisal) polymer composites. *Science Park*, **1:** 1-6.

Sampathkumar, D.R., Punyamurth, R., Venkateshappa, S.C., Bennehalli, B. 2012. Effect of chemical treatment on water absorption of Areca fibre. *Journal of Applied Research,* **8:** 5298-5305.

Saira, T., Munawar, A., Khan, S. 2007. Natural fibre-reinforced polymer composites. *Journal of Polymer Science,* **44:** 129-144.

Sanjay, M.R., Arpitha, G.R., Naik, L.L., Gopalakrishna, K., Yogesha, B. 2016. Applications of natural fibres and its composites: An overview. *Natural Resources*, **7:** 108-114.

Shah, H., Srinivasulu, B., Shit, S. 2010. The effect of surface treatment on the properties of woven banana fabric based unsaturated polymer resin composites. *International Journal of Scientific Engineering and Technology*, **1:** 86-90.

Singha, S. A., Thakur, K.V. 2014. Fabrication and study of lignocellulosic Hibiscus *sabdariffa* fibre reinforced polymer composites. *Bioresources*, **3:** 1173-1186.

Sinha, E., Rout, S.K. 2009. Influence of fibre-surface treatment on structural, thermal and mechanical properties of jute fibre and its composites. *Bulletin of Material Science*, **32:** 65 - 76.

Siregar, J.P., Sapuan, S.M., Rahman, M.Z.A., Zaman, H.M.D. 2010. The effect of alkali treatment on the mechanical properties of short pineapple leaf fibre (PALF) reinforced high impact polystyrene (HIPS) composites. *Journal of Food, Agriculture and Environment*, **8:** 1103-1108.

Srinivasa, C.V., Bharath, K.N. 2011. Impact and hardness properties of areca fibre-epoxy reinforced composites. *Journal of Materials and Environmental Science*, **2:** 351-356.

Thomson, R. 2013. Effect of fibre loading on the mechanical properties of kenaf and flax fibre reinforced phenol-formaldehyde composites. *Journal of Material Science Composites*, **44:** 2265-2288.

Tlijania, M., Gouadriab, A., Benyounesc, R., Durastantid, J.F., Mazioude, A. 2014. Study and optimization of palm wood mechanical properties by alkalization of the natural fiber. *Global Journal of Science Frontier Research: C. Biological Science*, **14:** 29-35.

Walter P.E., Azeez, T.O., Onukwuli O.D., Atuanya, C.U. 2016. Effects of chemical surface modifications on *Combretum dolichopetalum* fiber for sustainable applications. *International Journal of Engineering and Scientific Research*, **4:** 81-96.

Yang, H.S., Kim, H.J., Son, J., Park, H.J., Lee, B.J. Hwong, T.S. 2014. Rice-husk flour filled polypropylene composites, mechanical and morphological study. *Journal of Composite Structures*, **63:** 305-312.

Zhong, L., Fu, S., Li, F., Zhan, H. 2010. Chlorine dioxide treatment of sisal fiber: surface lignin and its influences on fiber surface characteristics and interfacial behaviour of sisal fibre/phenolic resin composites. *Bioresources Journal*, **5:** 2431-2446.

Zhong, L.B., Wei, C., Lv, J. 2007. Mechanical properties of sisal fibre reinforced urea-formaldehyde resin composites. *Express Polymer Letters*, **1:** 681-687.

Pak. j. sci. ind. res. Ser. A: phys. sci. 2018 **61A**(1) 35-42

Enhanced Storage Capacity and Quality of Haleji and Hadero Lakes Connecting with Indus River for their Sustainable Revival

Zia uddin Abro[a]*, Abdul Latif Qureshi[a], Shafi Muhammad Kori[b] and Ali Asghar Mahessar[c]

[a]US-Pakistan Centers for Advanced Studies-Water, Mehran University of Engineering &Technology, Sindh, Pakistan

[b]Department of Civil Engineering, Mehran University of Engineering &Technology, Sindh, Pakistan

[c]Sindh Barrages Rehabilitation Project, Sindh Irrigation Department, Karachi, Pakistan

(received September 7, 2017; revised December 29, 2017; accepted December 29, 2017)

Abstract. Over 50% of wetlands in the world have been lost in the past century, and the remaining wetlands have been degraded to different degrees because of the adverse influences of human activities and climate change impacts. Though protected under Ramser convention, the situation of Haleji wetland complex and Hadero wildlife sanctuary is not very promising. The current paper is focusing to revitalize the abandoned and devastated Ramsar site "Haleji Wetland Complex" and a forgotten wetland "Hadero Wildlife Sanctuary", situated in Thatta district, Sindh province of Pakistan. Both these wetlands are of great importance for natural habitat and reducing risk of coastal disasters and floods. The study mainly employed Arc-Hydro tools using remotely sensed data of ASTER GDEM 2 to determine the topography of both wetlands and their possibilities to connect with freshwater sources, and leeway to increase their respective water holding capacity. The study reveals that all the three wetlands can be re-connected with Indus River to turn them into fresh water bodies for sustaining natural habitat and increasing water harvesting capacities to cater human drinking water needs

Keywords: wetlands, groundwater quality, natural habitat, remote sensing

Introduction

Current global population is around 7.2 billion and is still growing with increasing pace, while the earth's total resources are shrinking and scattered unevenly. The way we are living, we are already consuming two to three times more of the earth's natural resources than what is sustainable. The increasing population, depleting resources and changing climatic conditions have inverse impacts on the natural eco-system of earth.

Water is one among three main resources on Earth which are depleting at higher rate. Only 2.5% of the world's total water is fresh, out of which 70% is frozen in the shape of glaciers and icebergs. The remaining is in the form of ground water, rivers and wetlands. Wetlands are considered as the kidneys which serve to filter runoff water which sustain life in many ways. Wetlands too need to be refreshed by periodic supply of river water, precipitation and healthy biological activities. They settle pollutants such as phosphorus and heavy metals in their soils, transform dissolved nitrogen into nitrogen gas, and break down suspended solids to neutralize harmful bacteria (Seminara *et al*., 2011).

*Author for correspondence; E-mail: Ziadinabro@yahoo.com

The destruction of wetlands is a concern because they are some of the most productive habitats on the planet. They often support high concentrations of animals-including mammals, birds, fish and invertebrates. Wetlands serve as nurseries for many of these species (WWF, 2017). Apart from the serving as nurseries for fish and birds species, wetlands also serve as flood protection facilities for communities living around the wetlands (Marsooli *et al*., 2016). Thus they provide a range of ecosystem services that benefit humanity, including water filtration, disaster risk reduction, flood control and recreation (Greb *et al*., 2006).

Despite the general arid climate of country, Pakistan has more than 225 significant wetland sites, estimating on area about 7,800 km^2 which covers 9.7% of the total surface area of the country (Kazmi *et al*., 2006) which was once home of biodiversity and heaven for migratory birds. Later due to shortage of river flows, over-exploitation of groundwater, and construction of dams, the wetlands became polluted and reduced in size. The other studies on the devastation of wetlands included extensive surveys made by Fraser and Keddy (2005); Koning and Walmsley (1972), Savage and Isakov (1970). Savage (1967); also indicated the depleting situation of wetlands.

In year 1971 Ramsar convention was held in Ramsar, Iran and declared 19 sites in Pakistan as protected and recognized as Ramser sites along with hundreds other sites all over the world. The other endangered locations were listed by Government of Pakistan and declared them as protected sites, wildlife sanctuary and gem sanctuary. Indus delta, Haleji wetland, and Keenjhar wetland are among the Ramser protected sites while Hadero Lake is protected by Government of Pakistan Laws of Wildlife Sanctuary.

The current situation of Indus delta and both Haleji and Hadero wetlands is not very promising. The continuous environmental degradation, and pollution, scarcity of rainfall and shortage of inflow of river water, increasing human induced activities and atrocities with natural atmosphere like deposition of industrial drainage effluent (Qureshi *et al*., 2015) tend to deteriorate the wetland eco-system with a steady and alarming pace (Zhao *et al*., 2016). The increasing population of cosmopolitan city Karachi demands new strategies to cater the needs of water for drinking, industrial, agricultural and more importantly for environment sustainability. The current paper focuses to interconnect (Golden *et al*., 2014) the adjacent wetlands with each other and with source of fresh water.

Research study area. The study area falls under the administrative boundaries of district Thatta of Sindh, Pakistan, along the right bank of River Indus. The area masked for study purpose comprising of Haleji wetland complex, Hadero and Keenjhar Lakes, is about 1,123 km^2.

The western side is rocky mountaineous area; south-west is Arabian Sea approximate 50 kms away, while on eastern side River Indus is flowing with fertile flat plateau towards Indus Delta (Fig. 1).

Hadero Lake. Lake Hadero is situated at 67 52'E and 24° 49'N. It lies about 85 km to the east of Karachi. Hadero is set on the edge of stony desert. It is a natural lake in a shallow depression. Hadero Lake is situated within the radius of 5 km of Haleji lake wildlife sanctuary and about 16 km to the south-west of Keenjhar Lake wildlife sanctuary. Hadero Lake was declared wildlife sanctuary with objects to conserve and protect the natural environment in and around the Lake for different migratory and resident birds. It was initially protected for shooting purpose in year 1971 keeping in view its adjacent larger wetlands only appear/filled in heavy monsoon/rainfall season.

Fig. 1. Satellite image highlighting the study area

Haleji Lake. Haleji is an earth-filled artificial lake, spread over an area of 6.58 km^2 (1,704 ha) with water level of about 1-1.5m and maximum depth of about 5-6 m. It is located at 067° 46'E and 24° 47'N with 60 m elevation from mean sea level. The area is silty, muddy and sandy. The lake is situated at a distance of 21 km from Thatta and 88 km from Karachi. It is a perennial freshwater lake with associated marshes and adjacent brackish seepage lagoons, set in stony desert of limestone and sandstone bedrocks. This lake was a saline lagoon and in late 1930s it was converted into reservoir to feed 28 MGD to Karachi as the first water supply source for thousands of American and British troops stationed in Karachi during World War II. Haleji Lake is also considered Asia's largest bird sanctuary. Since it attracts thousands of migratory birds between November to February. It can be termed a paradise for bird lovers. Halej Lake used to supply water to Karachi before year 2006. Water used to be supplied to Haleji Lake from Kalri Baghar feeder and then it was supplied to Karachi. After the construction of a direct supply line to Karachi from Keenjhar, the water of the lake has become stagnant which has resulted in the deterioration of water quality. Due to passage of time, local inhabitants dug out illegal water courses (small channels) from the Jamwah branch (which was feeding river water to Haleji Lake) and cut off the supply of fresh water to Haleji Lake.

Figure. 2 shows the detailed locations of Keenjhar, Haleji and Hadero Lakes along with adjacent small lakes and their respective connecting canals.

Materials and Methods

Field survey. Field survey has been conducted to check the actual ground situation, ground truthing and collection of water samples for physicochemical analysis.

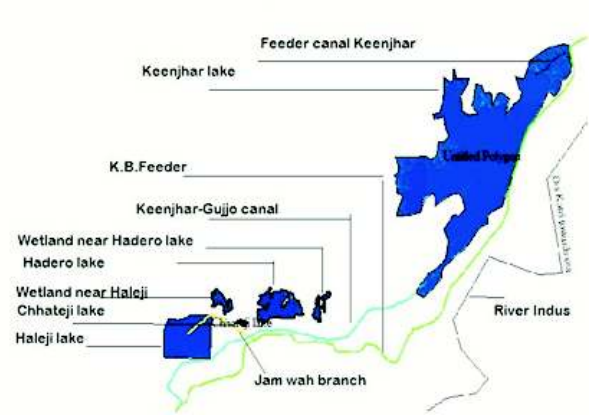

Fig. 2. Wetlands in study area with feeder canals

The field survey also included the interviews of key informants, and two focus group discussions (FGDs) on close ended questionnaires designed for the purpose of identifying the KAP (knowledge, attitude and practices), and solutions based on the local knowledge and folk wisdom. Transect walks have been conducted with FGDs participants along wetlands to understand ground situations and confirming the remotely sensed data acquired through satellites. The main elevation points which were remotely sensed through Google Earth pro were physically recorded through GARMIN 64s handheld GPS device.

Physiochemical analysis. Water samples for water quality analysis have been collected from different locations of both wetlands and water sources. However, previous research studies conducted by various researchers have been referred to determine the physicochemical situation of water quality. The main physicochemical parameters which have been studied were pH, dissolved oxygen (DO), electric conductivity (EC), total dissolved solids (TDS), chloride (Cl), sulphates (SO_4), sodium (Na), magnesium (Mg), potassium (K) and hardness.

Remotely sensed revival plan. Google Earth and Global mapper have been used on ASTER GDEM V002 data to quantify the amount of water to be stored and possibilities to connect all reservoirs with river through Keenjhar Lake or directly with river Indus through Kalri Baghar (KB) Feeder. The elevation profiles are constructed using Google Earth pro, whereas volumes of reservoirs have been calculated using global-mapper cut and fill volume calculator method.

Results and Discussion

Field survey. Key informants interviews (KII) have been conducted with the curator of Haleji wetland and an official of Sindh Irrigation and Drainage Authority. They disclose that the fresh water supply to Haleji is not regular and only the additional available water is diverted to lake during rainfall season. They also confirmed that a revival plan of Haleji is under consideration with government of Sindh to increase its capacity for providing drinking water to cosmopolitan Karachi. The officials were also discussed about possibilities of connecting all wetlands with fresh water source to increase the water harvesting and improving the quality of lakes. The officials were of the view that a thorough physical survey will be required to chalk out the possibilities of connecting surrounding wetlands with fresh water source.

Two FGDs were also conducted, one in the village Usman Hallo situated in the vicinity of Haleji Lake and other in village Jumo Mallah on the bank of Hadero Lake. The participants of FGDs were of the opinion to refresh the wetlands through river water, and control hunting of migratory birds in the lakes. The transect walk along Haleji Lake identifies one water course which was illegally drawn from the Jam Wah branch (which feeds water to Haleji Lake) before it reaches the inlet of Haleji Lake. The FGD participants told that some influentials have cultivating government land in wetland areas under the supervision of concerned officials.

The KAP analysis revealed that however people were of the opinion to revive the wetlands but they were not willing to contribute by not polluting the lakes or stop taking water illegally from the feeding canals. Despite the fact that the water quality of Hadero was much beyond the permissible limits for drinking purpose, the local people claims that they use water for drinking as well as household purposes.

Physicochemical analysis. Khan *et al*. (2012) conducted a research on environmental pollution effects on natural habitat of Heleji and Keenjhar Lakes. The data was collected from year 2006 to year 2009. Four-years study discovered that pesticide contamination of organophosphate (OP) and organochlorine (OC) were above the maximum acceptable concentration (MAC) in Haleji Lake, while it was below MAC in Keenjhar Lake.

Further investigations revealed that the KB feeder canal was the major source of pollution. KB feeder canal off-

takes from GM barrage, and feed water to Keenjhar Lake. While passing through Kotri Industrial area, the hazardous effluent from different industrial units is dumped into KB feeder canal without any environmental treatment. That hazardous chemical waste is dumped round the year. The researchers' analysis of Haleji Lake during the study period identified the issue of depleting dissolved oxygen in lake water which imposes threat to natural habitat.

Another study was conducted by Mahessar *et al*. (2015) (Table 1) on environmental impacts and threats to Haleji Lake, which reveals that the dissolved oxygen level of the lake water was around 3 mg/L, which was less than the permissible limits defined by National Environmental Quality Standards (NEQS). The other parameters were found within permissible range defined by NEQS except at few locations with higher concentrations.

The above study was not limited to physicochemical analysis but a physical survey was also conducted to record the facts behind deterioration of the lake. On the basis of physicochemical analysis, it revealed that the depleting oxygen level in lake water poses a great threat to habitat. Similar findings revealed from physical survey recorded that migratory birds and natural habitat of lake is reducing day by day (Khan *et al*., 2014; Aziz *et al*., 2013; Fisher *et al*., 2008). The research concludes to divert fresh river water to increase the oxygen level of the lake.

The current study however, is not directly involved with detailed physicochemical analysis of lake waters but selected water quality parameters were analysed to determine the quality of water of both lakes to be inter-connected for extending and enhancing water harvesting during heavy monsoon and flooding years. Figure 3 indicates the points from where water samples were collected for current study. The results of the water samples collected from Haleji wetland complex and Hadero Lake are given in Table 2. The chemical analysis of sample "S6" (Hadero Lake) shows a very higher concentration of minerals and dissolved salts. The rest of the samples from inlets and outlets of Haleji Lake, were found within the permissible limits of WHO for drinking purpose and in association with the findings of Mahessar *et al*. (2015) and Khan *et al*. (2012). Sample S5 was collected from the drain (RBOD) which is under construction on the right side of river Indus passing along with Hadero and Haleji Lakes.

Remotely sensed revival plan. The remotely sensed data ground truthed by field verification were used to analyse the possibilities of interconnecting wetlands on right side of river Indus and quantifying their water holding capacities using different remote sensing tools and applications. Google image of August 2016 was analysed for elevation difference of Keenjhar Lake and Haleji Lake. The elevation profile of Keenjhar-Gujjo

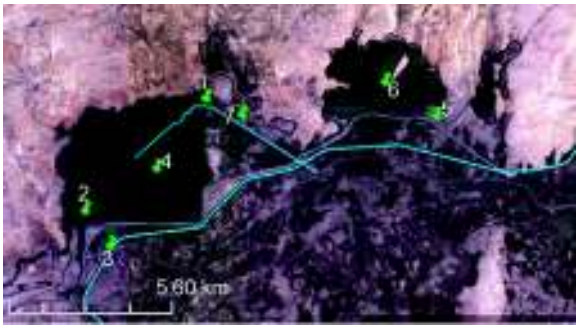

Fig. 3. Water sample collection points

Table 1. Physicochemical analysis (Mehassar *et al*., 2015)

Parameter	Available range	Permissible limits(NEQS)
pH	6-8	6.2 -8.5
DO	3 - 4	>8
EC(µS/cm)	400 - 1180	680
TDS (mg/L)	250 - 800	1000
CC(mg/L)	50 - 175	250
Sulphate(mg/L)	45 - 75	250
Sodium(mg/L)	50 - 150	200
Magnesium(mg/L)	20 - 40	150
Potassium(mg/L)	8 - 18	12
Hardness	190 - 180	500

Table 2. Water quality analysis for current study

Water quality parameter	Electrical Conductivity (µ-S/cm)	Hardness $CaCO_3$ (mg/L)	pH (30.50C)	TDS (mg/L)
Permissible Limits results	NGVS	500 (WHO)	6.5- 8.5 (WHO)	100 (WHO)
S1	619	220	7.3	396
S2	1,073	270	7.3	686
S3	1,161	290	7.2	743
S4	1,273	320	7.0	814
S5	1,785	510	7.3	1,142
S6	1,9,280	3,190	7.7	12,339
S7	954	260	7.6	610

Canal off taking at Chilia passing nearby (0.8 km) from Hadero Lake and 1.2 kms from Chhateji Lake (dried lake revealed by temporal detection of landsat imageries) shows a drop 14.6 m over 17.7 kms (at siphon near Jam wah branch). Similar trend of elevation difference was recorded in KB Feeder from adjacent locations from Keenjhar -Gujjo channel. However de-silting of Keenjhar-Gujjo channel will be required from 5.6 kms to 10.78 kms from off-taking point to feed required quantity of water to proposed lakes. The designed inlet to feed Haleji Lake was Jam Wah branch off-taking from KB feeder at 67°50'22.14″ E and 24°48′6.41″ N. Jam Wah branch is passing under Keenjhar -Gujjo canal at 67°50'3.35"E and 24 °48'16.56"N. The FGDs also resulted in the knowledge base of availability of three lakes adjacent to Hadero and Haleji Lakes. The name of Chhateji Lake was identified as separate Lake while other two lakes identified in the Fig. 2 revealed as the extension of Hadero and Haleji Lakes, respectively. These water bodies were also recognized through historical Google images during wet years, later they were verified through transect walk and FGDs. The outline polygons of wetted perimeters were developed in Google map and exported as layer to Global mapper v 18 for further analysis. The imported layers of wetlands in Global mapper were imposed on the ASTER GDEM V2 worldwide elevation data (1 Arc second resolution) to get three-dimensional measurements of the water bodies. Similarly possible sources connecting all wetlands were also marked through polylines and imported in Global mapper as KML files.

Figure 4 shows the drawn elevation profiles of water channel feeding Keenjhar Lake from KB Feeder (189 RD) shows a drop of 5 m, over the length of 4.62 kms, but due to silt and vegetation the channel is silted 2/3rd of its total length, thus limiting the intake of water from KB feeder. Same elevation points were re-confirmed through GARMIN GPS handheld device and confirmed the elevation difference and obstacles in channel bed. The situation was discussed with the officials of irrigation department and they confirmed that de-siltation was not done from last few years.

Figure 5 shows the elevation profile of Jamwah canal feeding Haleji Lake from KB Feeder. A drop of 6 m was recorded over the total length of 7.9 kms starting from Jamwah off-taking point from KB feeder to the location having maximum depth in Haleji Lake. Again some de-silting and excavation will increase the water intake to fill the reservoir at its maximum level. Apart from the original design there is also a possibility to connect Jamwah branch with Keenjhar–Gujjo canal at 67°50′3.18″E and 24°48′16.58″ N as Keenjhar-Gujjo canal is siphoning over the Jamwah branch on mentioned location. The elevation differences were re-confirmed through GARMIN GPS handheld device during ground truthing process.

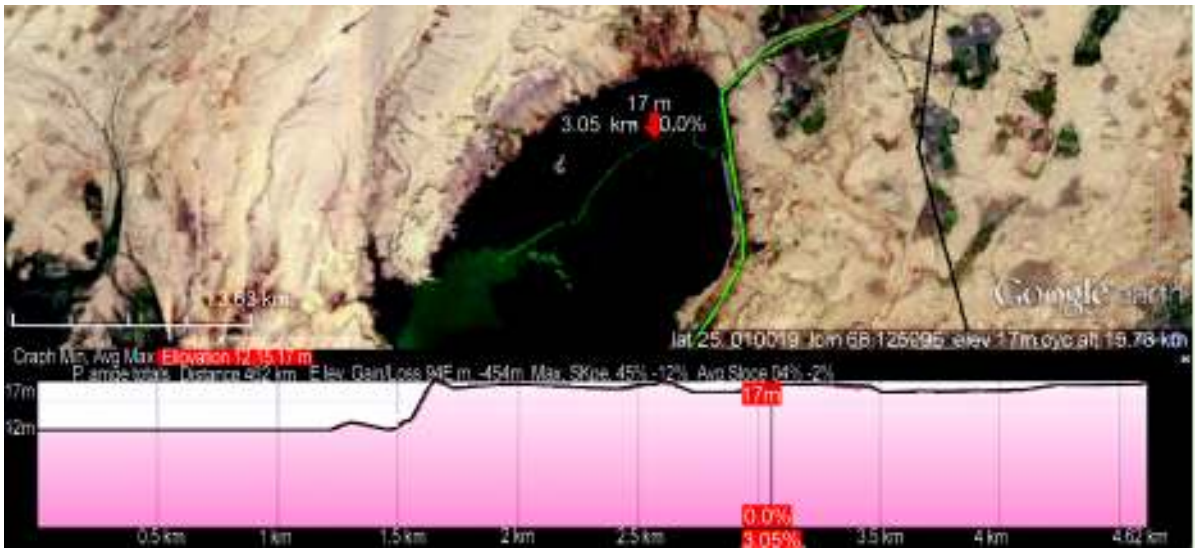

Fig. 4. Elevation profile canal feeding Keenjhar

Fig. 5. Elevation profile of Jamwah Canal feeding Haleji Lake.

The inter-connectivity of all wetlands (Keenjhar wetland complex and Haleji wetland complex) is feasible as mentioned in Fig. 6. The Hadero Lake and suggested point at KB feeder as well as Keenjhar-Gujjo Canal had a drop of 5 m to feed the Hadero Lake as well as a wetland near Hadero lake. Hadero Lake can be washed to reduce the salt concentration as RBOD drain is passing beside the Hadero Lake which can be used to remove the excess salt water.

Similarly the Jamwah branch can be connected with Chhateji Lake and the wetland near Haleji to revive the Haleji wetland complex through natural water ways which are now either occupied by land grabbers or washed due to weathering process. Natural depressions can be revived not only to increase the water conservation capacity but can be effective to re-vitalize the depleting environment and natural habitat of coastal wetlands.

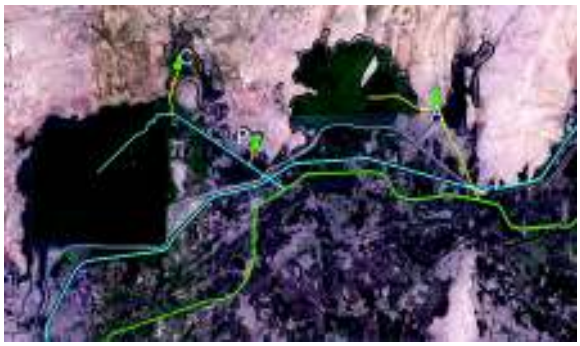

Fig. 6. Inter-connecting possibilities of adjacent wetlands

The storage capacities of different wetlands were calculated in Table 3 using cut and fill volume process in Global mapper v 18. The wetted perimeter polygons were prepared in Google map and exported as KML files to Global mapper.

The KML files of wetlands were imposed on ASTER GDEM V2 to get the Z axis values of depressions. The cut and fill volume option in Global mapper divide the entire polygon of each wetland in meshes of different default sizes as per wetted perimeter area of particular polygon. The volumes are then calculated using cut and fill method in cubic meters.

Table 3. Area and volumetric capacities of wetlands

Wetland	Area (Km^2)	Volume (BCM)
Keenjhar Lake	133.61	21.75
Hadero Lake	9.14	0.142
Lake near Hadero	1.92	0.031
Haleji Lake	17.46	0.066
Chhateji Lake	0.33	0.003
Lake near Haleji	2.16	0.028
Total	164.62	21.96

Total amplified wetland areas will be increased upto 164.62 km^2, while the storage capacity can be increased from 21.75 BCM to 21.96 BCM. This will provide additional supply of water to cosmopolitan Karachi.

Conclusion

The detailed field survey and remotely sensed analysis of the study area confirms the possibility of connecting Keenjhar Lake as well as KB Feeder with Hadero, Haleji and adjoining dried wetlands, not only for their revival but to increase the water holding capacities of main wetlands (Haleji and Hadero). The water can be stored in the identified three adjoining wetlands during flooding/ monsoon periods.

The study confirms the interconnecting possibilities of KB Feeder and Keenjhar-Gujjo canal with all wetlands to increase the storage capacity of drinking water to cosmopolitan Karachi.

The connectivity of Hadero Lake with Keenjhar Lake and/or KB Feeder which will improve the water quality in the Hadero Lake and turn it into the fresh water Lake.

Keeping in view the environmental degradation, loss of aquatic habitat, and destruction of wetlands, it is suggested to allocate separate water budget for revival of wetlands for future harvesting of water and ground water recharge.

Illegal water courses and water lifting for irrigation purpose should be strictly discouraged by local administration to give due share of water to wetlands.

Further studies should be conducted on socio-economic impacts of wetlands and KAP survey of villages around wetlands/ water bodies for increasing awareness and behavioral change.

Acknowledgement

The authors are grateful to the communities around Keenjhar, Haleji and Hadero Lakes for their warm welcome and consuming time with team. Thanks to the curator of Haleji Lake and his staff during walk-thru survey. Thanks are also due to support of PCRWR, Islamabad, for water sample analysis at DRIP, TandoJam, Pakistan.

References

Aziz,F., Azmat,R., Jabeen, F., Bilal, B. 2013. A comparative study of physico-chemical parameters of Keenjhar Lake, Thatta, Sindh, Pakistan. *International Journal of Advanced Research*, **1:** 482-488.

Fisher, B., Turner, K., Zylstra, M., Brouwer, R., Groot, R.D., Farber, S., Balmford, A. 2008. Ecosystem services and economic theory: integration for policy-relevant research. *Ecological Applications*, **18:** 2050-2067.

Fraser, L.H., Keddy, P.A. 2005. *The World's Largest Wetlands: Ecology and Conservation*. 446p. Cambridge University Press, Cambridge. ISBN: 9780511113864.

Golden, H.E., Lane, C.R., Amatya, D.M., Bandilla, K.W., Kiperwas, H.R., Knightes, C.D. 2014. Hydrologic connectivity between geographically isolated wetlands and surface water system: A review of select modeling methods. *Environmental Modeling & Software*, **53:** 190-206.

Greb, S.F., DiMichele, W.A., Gastaldo, R.A. 2006. Evolution and importance of wetlands in earth history. In: *Wetlands Through Time*, G. F Greb and W. A. Michele (eds.), Geological Society of America Special Papers. **399**, pp. 1-40.

Kazmi, J., Qureshi, S., Siddiqui, M.U. 2006. Depleting Wetlands of Lower Sindh, Pakistan: A Spatio-Temporal Study through Satellite Remote Sensing. 1 - 5. 10.1109/ICAST.2006.313786.

Khan, M. Z., Jabeen, T., Ghalib, S. A., Siddiqui, S., Alvi, M. S., Khan, I. S., Yasmeen, G., Zehra, A., Tabbassum, F., Hussain, B., Sharmeen, R. 2014. Effect of right bank outfall drain (RBOD) on biodiversity of the wetlands of Haleji wetland complex, Sindh. *Canadian Journal of Pure and Applied Sciences*, **8:** 2871-2900.

Khan, M. Z., Abbas, D., Ghalib, S. A., Yasmeen, R., Siddiqui, S., Mehmood, N., Zehra, A., Begum, A., Jabeen, T., Yasmeen, G., Latif, T. A. 2012. Effects of environmental pollution on aquatic vertebrates and inventories of Haleji and Keenjhar lakes: Ramsar sites. *Canadian Journal of Pure and Applied Sciences*, **6:** 1759-1783.

Koning, F. J., Walmsley, J. G. 1972, IWRB mission to West Pakistan. *IWRB Bulletin,*. **33**, pp. 42-51.

Mahessar, A. A., Qureshi, A. L., Mukwana, K. C., Jakhrani, A. Q. 2015. Study of environmental impacts and threats to the Ramsar Haleji Lake, Sindh, Pakistan. *International Journal of Applied Environmental Sciences*, **10:**1577-1590.

Marsooli, R., Orton, P.M., Georgas ,N., Blumberg ,A.F. 2016. Three-dimensional hydrodynamic modeling of coastal flood mitigation by wetlands. *Journal*

of Coastal Engineering, **111:** 83-94.

Qureshi, A. L., Mahessar, A. A., Leghari, M. E. H., Lashari, B. K., Marri, F. M. 2015. Impact of releasing wastewater of sugar industries into drainage system of LBOD, Sindh, Pakistan. *International Journal of Environmental Science and Development*, **6:** 381-386.

Savage, C.D.W., Isakov J.A. 1970. International cooperation in management of waterfowl and wetlands in Asia, Project Marine Pakistan. *Journal of Forestry*, **20:** 387-391.

Savage, C.D.W. 1967. The Wildfowl and wetland situation in West Pakistan. Proceedings Technical Meeting on Wetland Conservation, Ankara-Bursa-Istanbul, 9-16 Oct,1967. *IUCN Publication New Series* No.**12:** 122-128.

Seminara, G., Lanzoni, S., Cecconi, G. 2011. Coastal wetlands at risk: learning from Venice and New Orleans. *Journal of Ecohydrology and Hydrobiology,* **11:** 183-202.

Walters, K.M., Sebens, M.B. 2016. Using climate change scenarios to evaluate future effectiveness of potential wetlands in mitigating high flows in a Midwestern U.S. *Journal of Ecological Engineering*, **89:** 80-102.

WWF, 2017. Threats to wetlands. http://wwf.panda.org/about_our_earth/about_freshwater/intro/threats/ **21:** 11.2017.

Zhao, Q., Bai, J., Gu, B., Lu, Q., Gao, Z. 2016. A review of methodologies and success indicators for coastal wetland restoration. *Ecological Indicators*, **60:** 442-452.

Pak. j. sci. ind. res. Ser. A: phys. sci. 2018 **61A**(1) 43-50

Monthly Monitoring of Physicochemical and Radiation Properties of Kufa River, Iraq

Sadiq Kadhum Lafta Alzurfi, Ali Abid Abojassim* and Hussien Abid Ali Mraity
Faculty of Science, University of Kufa, Al-Najaf Box 21, Najaf, Iraq

(received September 8, 2017; revised December 14, 2017; accepted January 19, 2018)

Abstract. Increasing anthropogenic activities can lead to a dramatic effect on the quality of the planet surface water such as river, lake and wetland among others (i.e. groundwater and atmospheric water). Water samples were collected from Kufa river during six months (i.e. started from November, 2015 to April, 2016). Six stations were selected alongside the river flow. The samples were analysed for physico-chemical and radiation properties (air temperature, water temperature, pH, total hardness, Ca^{+2}, Mg^{+2}, total dissolved solids, dissolved oxygen, biological oxygen demand, turbidity, total alkalinity, electrical conductivity and radon concentration). The resulted data of various physicochemical parameters indicate that in some water samples, the EC, total hardness, BOD, turbidity, and total dissolved solids were found to be high when compared with the limits of WHO standards. Regarding the radon concentration, the results reveal that the radon level of all studied areas were lower than those published in literature. Finally, the findings the river's water could be unsafe for drinking when the physicochemical analysis taken into account.

Keyword: physicochemical properties, radon concentrations, Kufa river

Introduction

Kufa river extends from Al-Kifl city via Al-Najaf governorate to Al- Diwaniyah city; the total length of this river is around 36 km long with an approximate flow rate of 552 m^3/ sec. The water level in this river undergoes large fluctuations. To illustrate, the highest level occurs during the high rainy season (end of March to early of April), whereas the lowest water level occurs in summer (MWR, 2007). Increasing urbanization of Kufa city had negative implications on water quality where the domestic effluents are directly disposed into the river without any consideration for the environmental consequences. Nevertheless, transported radioactive matters (e.g. radon gas) should also be considered as they may have their own impact too. Radon is a colourless, odourless and radioactive noble gas that is resulted from uranium decay series, which exists elsewhere on the earth. Furthermore, radon is an alpha particle emitter that decays into a chain of progenies of gamma and alpha emitters. This means that the radon atoms in the air can decay and produce other new atoms. The resulting atoms called radon progeny. These atoms can attach themselves to a tiny dust particle in an indoor air. As a result, the dust particles could easily be entered into the respiratory system and increase the chance of developing lung cancer over long period of time. In this context, certain types of radon based lung cancer have been recognized in literature especially those caused by smoking (BEIR, 1999). Overall, the US Environmental Protection Agency (USEPA, 1991) has identified pollutants relying on quality standards as follows:

- The concentration of chemical compounds and elements, i.e organic, chlorine, nitrates, ammonia, phosphorus, sulphates, and others.
- Pollutants that have an effect on the physical and chemical properties such as temperature, alkalinity conductivity, pH, DO, hardness and TDS.
- Biological contaminants include pathogenic bacteria, viruses, protozoa, helminthes, and phytoplankton.
- Radionuclides also includes natural radioactive families such as ^{238}U and ^{232}Th and their decay chain includes the production of radon-222; 220; 219 progenies. The latter are all emitting alpha particles. Some other radioactive elements emit beta and gamma rays.

It should be noted that the destination of industrial pollutants when entering the water surface either remain unchanged and immobile in primary station or move via transportation, volatilization, leaching, adsorption, and sedimentation processes. Finally, it might also move under the influence of gravity and diffusion where in some cases transmitted *via* biological and chemical

*Author for correspondence;
E-mail: ali.alhameedawi@uokufa.edu.iq

processes (e.g. aerobic and anaerobic decomposition) and bioaccumulation *via* some weathering processes (Weiner, 2000).

This study is aimed to monitor the physical, chemical and radiation properties of the six stations along side of the Kufa river's water using different techniques and comparing the findings with published standards for water. These stations were identified as sampling sites using a geographical positioning system (GPS)

Study area. Euphrates river in the Kifl city is divided into two branches namely, Abbasid and Kufa rivers. It runs from the Kifl city to the Diwaniyah city with a total length of about 36 kilometers and a flow rate of 375 [m^3/s], and an actual capacity of 552 [m^3/s]. The depth of water in this river changes and has a marked high level during the flooding seasons at the end of March to beginning of April and has a low water level in the summer's months (Al-Haidarey, 2009).

Many villages, farm lands and cities (e.g.Najaf and Kufa) lie alongside the river, where the waste of human and industrial fluid (industrial district area, Kufa cement plants and leather factory and others), together with rainy water and hospitals waste drain into the river directly without treatment.

The geographical positionging system (GPS) use in (Fig. 1) as follows:

- First station (St.1): Located north of Imam Ali Bridge about 1 km; this characterized by there was no industrial activity or human except agricultural activities.
- Second station (St.2): Located near Al-Barrakhia treatment plant for domestic wastes of the Kufa city.
- Third station (St. 3): located at 1 km away from the second station.
- Fourth station (St. 4): Located at 1.3 km away from the third station.
- Fifth station (St. 5): Located at 1.7 km away from the fourth station under the cement plant bridge.
- Sixth station (St. 6): Located 3 km away from the fifth station.

Materials and Methods

Samples of water were collected during day from the selected stations of Kufa river for the period starting from November, 2015 to April, 2016. Six stations were chosen for monitoring the physical, chemical and radiation properties of water in Kufa river. Analysis of the samples was achieved in the laboratory of Ecology Department/Faculty of Science/Kufa University. The samples were collected from a depth of 20 cm in each station (using polyethylene container). Air and water temperature was measured using mercury thermometer (0-100°C, UK), while the electrical conductivity, TDS, salinity, and pH were measured using multi meter (WTW, Germany). A modified method of Winkler (APHA,1995) was adapted to determine DO after fixing in field, the turbidity was measured using portable Turbid meter (Lovibond, Germany) after calibration of the meter using different solutions (0.01,10,1000). Total alkalinity was measured according to Lind (1979), whereas, total hardness, Ca^{+2} and magnesium hardness were measured according to APHA (1995). Radon concentration (Bq/m^3) was measured using RAD-7 detector. The RAD-7 is a radon-in-air monitor containing an inside vacuum pump associated with an alpha semiconductor detector that employs energy discrimination to count the daughters of radon 222 and thoron (radon-220).This tool has widely been used in the recent water studies; (Abojassim *et al*., 2017; Al-Hamidawi, 2015). The RAD-7 can be considered as an absolutely machine controlled and moveable element detector, capable of running endlessly for days. An important demand of this method is that the air stream provided to the unit remains dry (humidity < 10%).

Statistical analysis. Two-way ANOVA test was used for further statistical analyses together with correlation analysis. The value $P<0.05$ was considered statistically significant. All statistics were performed using Microsoft Excel 2007.

Results and Discussion

The study area is known to be affected by the local weather of middle part of Iraq which is variable from cold in winter to dry hot in summer; this associated with a moderate temperature during spring and autumn. Figure 2 illustrates monthly variations of air temperature in the research area. The highest values of the temperature were recorded in April at the sixth stations (34 °C), while the lowest value was seen in January at the first station (10.4 °C). Figure 3 shows the monthly variations of water temperature in the studied area. The highest value was recorded in April at the sixth station (28.5 °C) and the lowest value in January was seen at the first station (9.8 °C). The temperature during the present study was recorded at measurement time and does not represent the variation during the whole day.

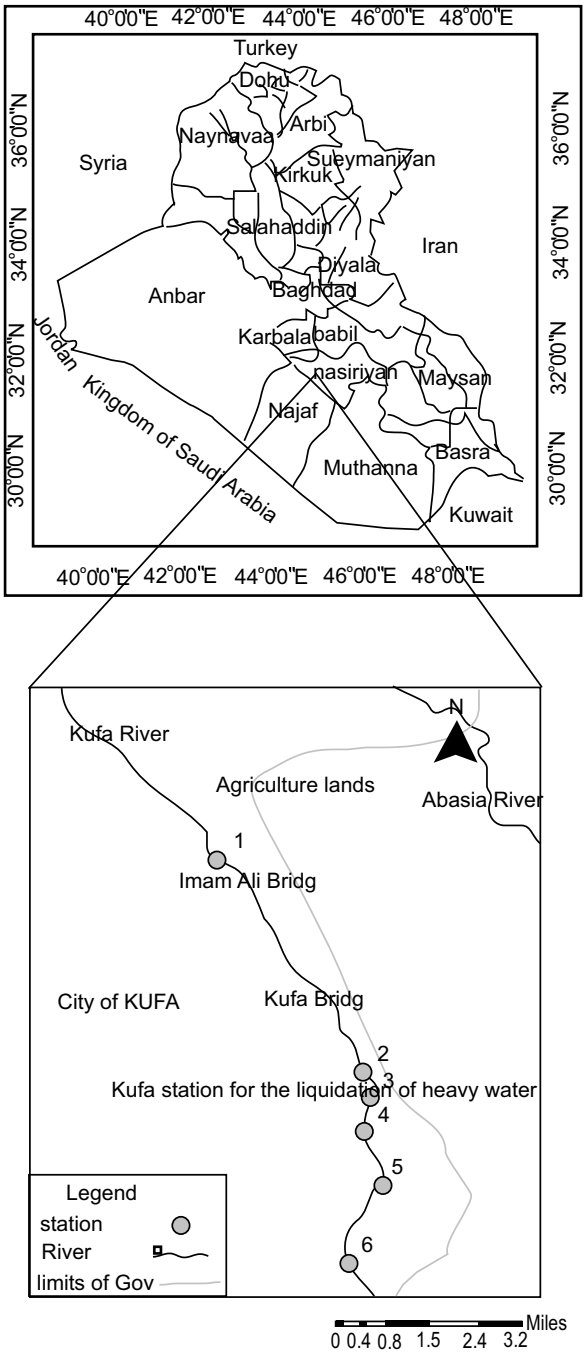

Fig. 1. Base map of the study stations.

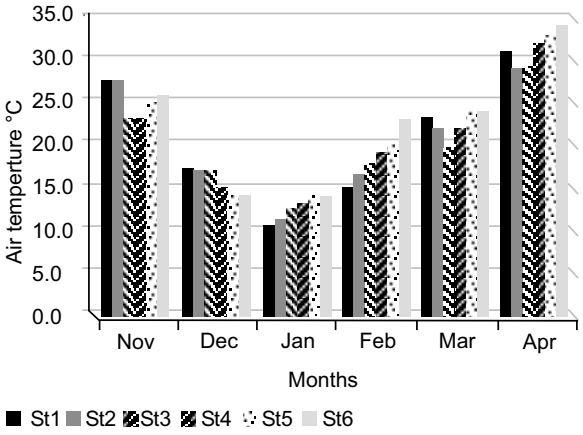

Fig. 2. Monthly variations of air temperature (mean) in study stations.

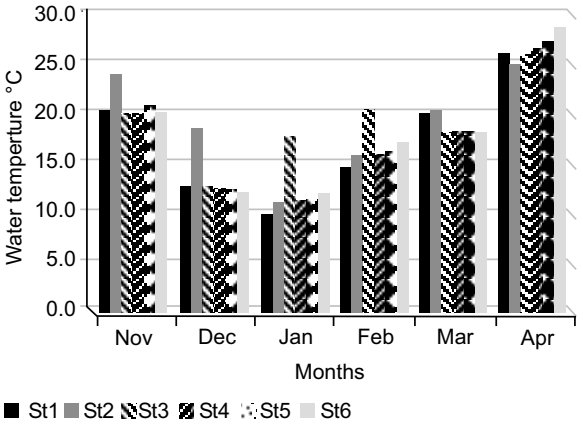

Fig. 3. Monthly variations of water temperature (mean) in study station.

Air and water temperature were clearly variable in relation to the weather conditions during measurement time.

The monthly variations of pH were found to be between 5 and 8.5 for stations 1 and 2 during November and February, respectively. The pH findings demonstrate a narrow range in the selected stations due to its high ability to be regulated in hardness water and rich alkalinity with bicarbonates (i.e. buffer system) (Goldman and Horne,1983) and showed in Fig. 4. The value of pH decreased in station 2 during November due to the drainage of the domestic wastes from Barrakhia treatment plant across the river that contains a large amount of wastes which would be expected to affect the pH levels. High proportions of electrical conductivity, salinity and total dissolved solid values were recorded in station 2 as (2963 µs/cm, 1.9 ppt. and 1491 mg/L), respectively during February in Fig. 5-7. The electrical conductivity is an important factor through which estimation of the total salts in water can be obtained (Table 1). Water in station 1 was fresh but in station 2 was brackish which would indicate that the domestic wastes have a marked impact in increasing

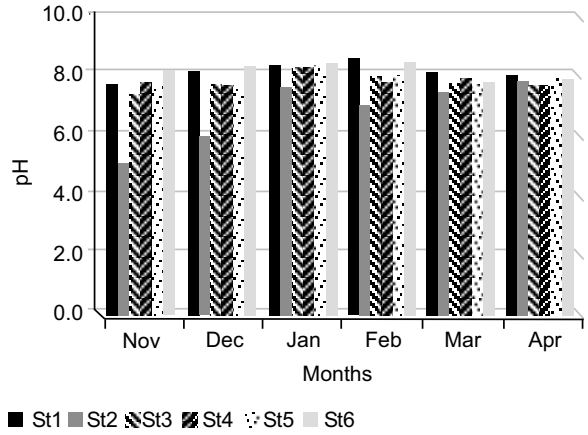

Fig. 4. Monthly variations of pH (mean) in study station.

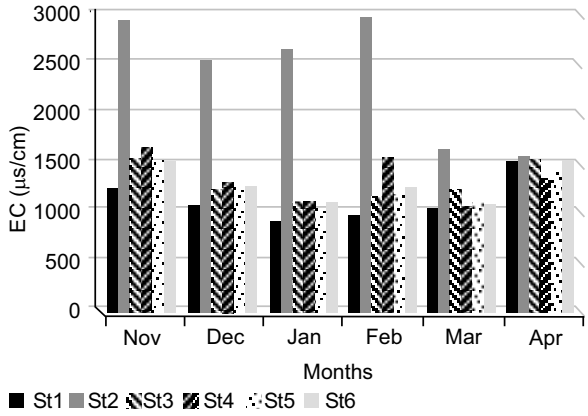

Fig. 5. Monthly variations of electrical conductivity (mean) in study station.

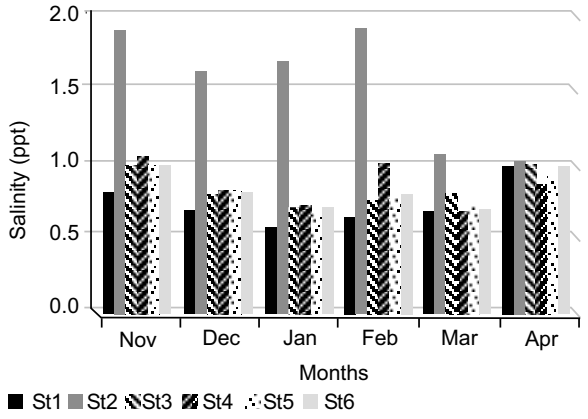

Fig. 6. Monthly variations of salinity (ppt) (mean) in study station.

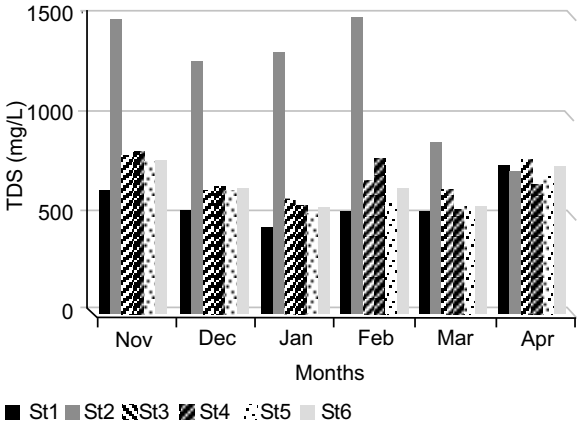

Fig. 7. Monthly variations of total dissolved solid (mean) in study station.

the electrical conductivity, salinity and total dissolved solid values of the river (Al-Zurfi *et al*., 2010). Figure 8 demonstrates the monthly recorded variations of turbidity where a high rate can be seen in station 2; this can be attributed to the amount of drainage of domestic wastes plant to the river and the growth of high numbers of microorganisms which has a positive relation to the turbidity. In this regard, Wetzel (2001) referred to the DO in water that has essential role in the metabolic processes of all aquatic organisms. The oxygen is added to water from atmosphere or due to photosynthesis processes of phytoplankton and aquatic plants (Wetzel and Linkens, 2000). It is well known that the DO is a limiting factor to the growth of much of aquatic organisms (Douabul *et al*., 2013). Variation in the levels of the DO can be attributed to the variation in temperature

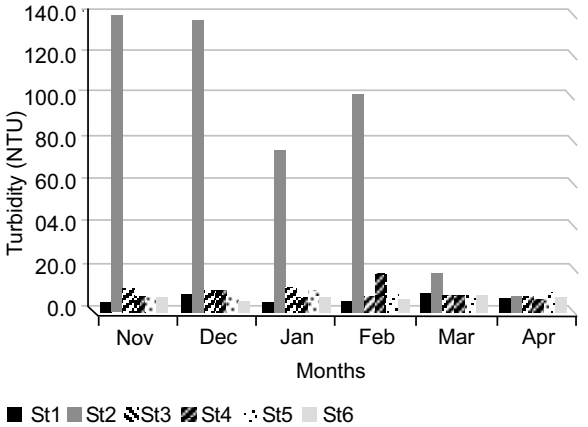

Fig. 8. Monthly variations of turbidity (mean) in study station.

(Haward, 1998), pressure and different ions concentration in water (Wetzel and Linkens, 2000). This study reveals that there is a clear depletion in the DO values at station 2 which is below the detection limit (DL) during November (Fig. 9), this is owing to the decrease in water level and decay processes of organic material which may be caused by the drainage of domestic wastes in this station (Al-Saadi *et al*., 1999). However, DO increase in other stations during February could be attributed to good aeration, continuous mixing, high water level and decrease of temperature during this month (Hassan, 2004) as seen in Table 1. The biological oxygen demand (BOD_5) refers to consumptive amount of oxygen of the added organic material to water that are destroyed by microorganisms. This has a negative effect on the quality of water (Wiener, 2000). The results demonstrate that the rise in the BOD values in station 2 during March was 6 mg/L than in (Fig.10) which is exceeding the acceptable international limit of 5 mg/L (WHO, 1996). This can be attributed to the direct addition of domestic wastes from Barkyia plant to the river. This finding agrees with (Al-Zurfi *et al*., 2010; Al-Mousawi *et al*.,1995). The recorded BOD values in the present study was found to be high compared with results of the Euphrates river at Simawah city (Mushkor, 2002) and lower than the values obtained by Salman (2006) in Euphrates river at Hindhia city. Total hardness values were found in the range between (160 and 1347) mg/L in station 6 and 2 during March and December in Fig.11, respectively. The results demonstrate that the total hardness during the study period was higher than the total alkalinity concentration which may be attributed to the amount of Ca^{+2} and Mg^{+2} ions that affected the total hardness (Lind, 1979), where the rise in the Ca^{+2}, Mg^{+2} ions and bicarbonates in the north area of Iraq is owing to the soil nature, rise of sodium, chloride, sulphates and carbonate ions compared with the south. This change is concurrent with groundwater nature that has a level in medium and southern areas (Al-Lami *et al*., 1999; Talling, 1980). The findings of this study are well agreed with many previous studies that were concerned with rise of total hardness in Iraqi water (Al-Zurfi *et al*., 2010; Salman, 2006).

This study mostly shows that the Ca^{+2} concentration is higher than that of Mg^{+2} as in Fig. 12. This is because the reaction of CO_2 with Ca^{+2} is higher and stronger than the reaction with Mg^{+2} ions, and large amount of Ca^{+2} is converted into dissolve bicarbonates, which

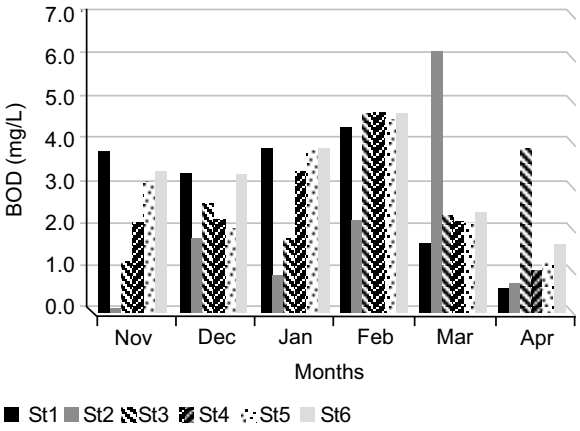

Fig. 10. Monthly variations of biological oxygen demand (mean) in study station.

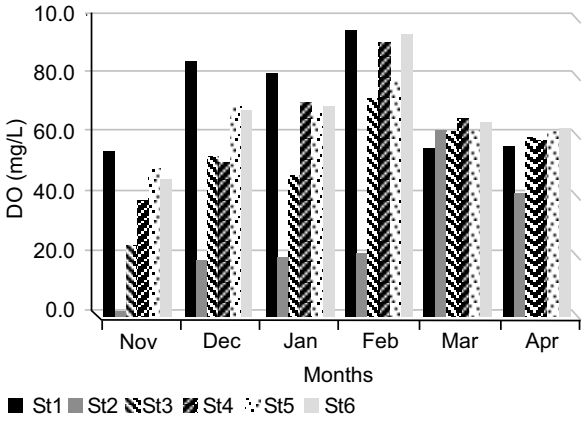

Fig. 9. Monthly variations of DO (mean) in study station.

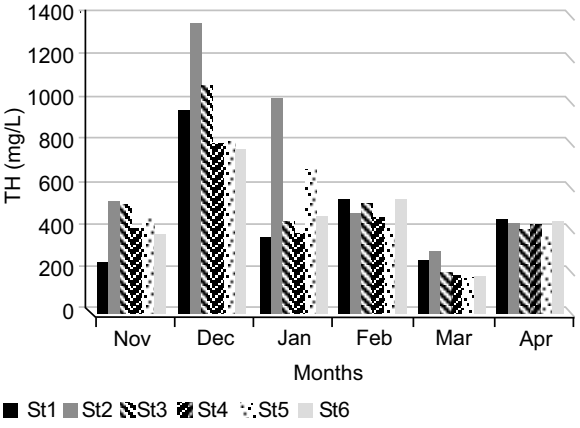

Fig. 11. Monthly variations of total hardness (mean) in study station.

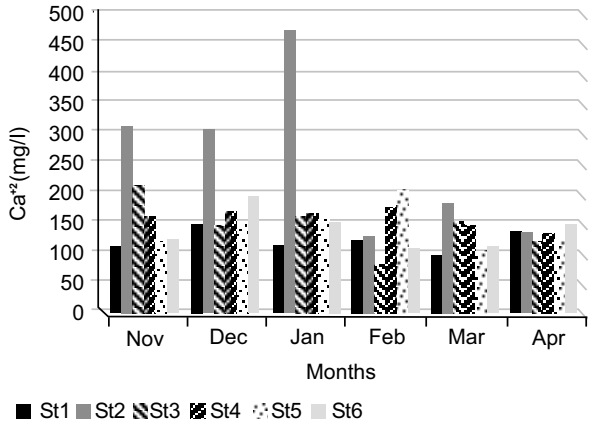

Fig. 12. Monthly variations of Ca^{+2} hardness (mean) in study station.

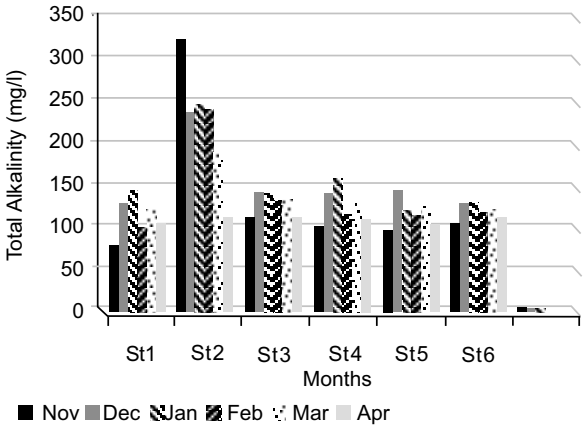

Fig. 14. Monthly variations mean of total alkalinity in study station.

affects on the hardness level as reported by Kassim (1986). The high concentration of Ca^{+2} shows in some stations of Mg^{+2} ions in Fig. 13. This is due to driftage processes from adjacent soil or flowage caused by the domestic and industrial wastes (Al-Lami *et al*.,1999) or may be due to the presence of huge numbers of phytoplankton (Maulood and Al-Mousawi, 1989). In the present study, no carbonate is reported, whereas the hydroxide alkalinity of the river is high due to high bicarbonates which was high in station 2 during November at 323 mg/L and low in station 1 during February at 99 mg/L as showed in Fig. 14.

The high value of alkalinity of the river can be attributed to the rise of temperature and increasing decay rates of organic material which would increase the conversion of insolvent Ca^{+2} carbonate to bicarbonate (Hassan *et al*., 2004). The expectant rate of total alkalinity in natural water is ranged from 20 to 200 mg/L (APHA, 1985). It was observed in the present study that the results are within this range and slightly higher; similar findings were also observed with the bicarbonates alkalinity level. The latter findings were agreed with that of previous studies when alkalinity in Iraqi water was taken into account which could be explained by presence of bicarbonate salts in water and adjacent soil recorded (Al-Lami *et al.*, 1999; Al-Saadi *et al*.,1996; Maulood *et al.*,1994; Sabri *et al*., 1989; Al-Nimma,1982). In term of radon investigation, a positive correlation was found between the Ca^{+2}, Mg^{+2} and radon concentrations at 0.88 and 0.67, respectively as showed in Fig. 15. The investigation also revealed that the maximum radon

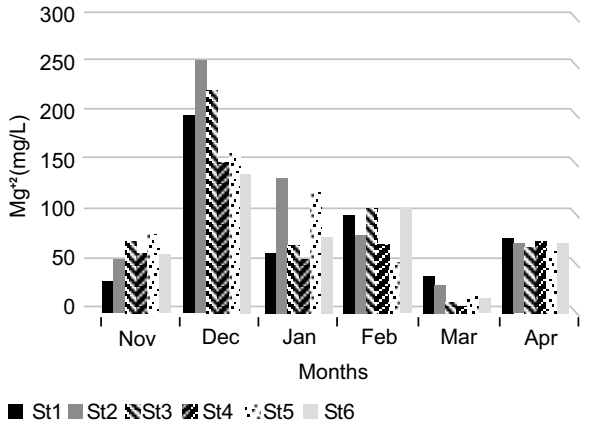

Fig. 13. Monthly variations of Mg^{+2} hardness (mean) in study station.

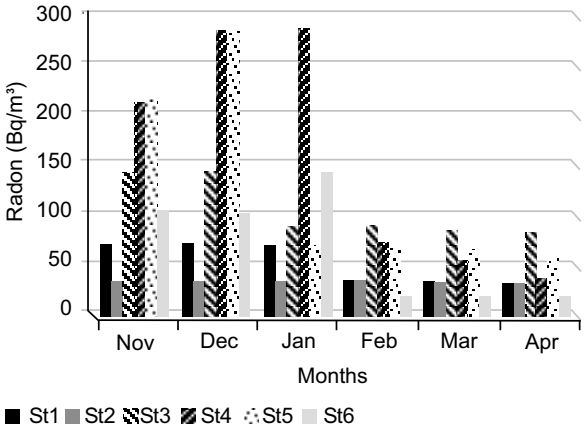

Fig. 15. Monthly variations of radon (mean) in study station.

Table 1. Correlation beteen physical and radiation properties during study period.

	W.temp	A.temp.	pH	EC	Salinity	TDS	Turbidity	DO	BOD	T.H	Ca^{+2}	Mg^{+2}	T. Alk.	Radon
W.temp	1.00	0.99	-0.37	0.34	0.34	0.28	-0.53	-0.3	-0.59	-0.46	-0.69	-0.49	-0.97	-0.56
A.temp.	0.99	1.00	-0.46	0.36	0.36	0.30	-0.49	-0.36	-0.61	-0.53	-0.68	-0.47	-0.94	-0.50
pH	-0.37	-0.46	1.00	-0.68	-0.68	-0.67	-0.45	0.73	0.41	-0.01	0.03	-0.11	0.19	-0.40
EC	0.34	0.36	-0.68	1.00	1.00	0.99	0.57	-0.54	-0.14	0.16	0.06	0.16	-0.27	0.31
Salinity	0.34	0.36	-0.68	1.00	1.00	0.99	0.57	-0.54	-0.14	0.16	0.06	0.16	-0.27	0.34
DO	-0.30	-0.36	0.73	-0.54	-0.54	-0.50	-0.27	100	0.66	0.04	-0.36	0.09	0.07	-0.52
BOD	-0.59	-0.61	0.42	-0.14	-0.14	-0.04	0.34	0.66	1.00	0.01	-0.04	0.02	0.45	-0.13
T.H	-0.46	-0.53	-0.01	0.16	0.16	0.15	0.63	0.04	0.01	1.00	0.62	0.99	0.53	0.73
Ca	-069	-0.68	0.03	0.06	0.06	0.07	0.58	-0.36	-0.04	0.62	1.00	0.53	0.78	0.88
Mg	-0.49	-0.47	-0.11	0.16	0.16	0.15	0.60	0.09	0.02	0.99	0.53	1.00	0.46	0.67
T.Alk.	-0.97	-0.94	0.19	-0.27	-0.27	-0.20	0.60	0.07	0.45	0.53	0.78	0.46	1.00	0.69
Radon	-0.56	-0.50	0.40	0.31	0.31	0.32	0.79	-0.52	-0.13	0.73	0.88	0.67	0.69	1.00

W.temp= water temperature; A.temp= Air temperature; T. Alk= Total alkaline; T. H= Total hydroxide alkalinity

concentration was in December, 2015 at station 4 was 284 Bq/m^3 which is within acceptable limit as indicated by WHO (1996).

Conclusion

In the present study the analytical data of various physicochemical properties indicate that some parameters such as EC, hardness, BOD, turbidity, and total dissolved solids found to be higher than the prescribed limit in some water samples as compared to WHO (1996). The Barrakhia treatment plant affected the water quality of the river during wastes drainage that sometimes occurs directly without treatment and this is incompetent with waste treatment process. However, the radon concentration in water can be considered as safe therefore no doubt can be raised due to radon.

References

Abojassim, A.A., Kadhim, S.H., Mraity, H.A.A., Munim, R.R. 2017. Radon levels in different types of bottled drinking water and carbonated drinks in Iraqi markets. *Water Science and Technology Water: Supply*, **17:** 206-211.

Al-Hamidawi, A.A.A. 2015. Monitoring of ^{220}Rn concentrations in buildings of Kufa Technical Institute, Iraq. *Science and Technology of Nuclear Installations*, **2015:** 1-5.

Al-Haidarey, M.J. 2009. D*iurnal Variation of Heavy Metals in Al-Kufa River/Najaf, Iraq*, 10th Conference of Biogeochemistry of Trace Element, July, Maxico.

Al-Lami,A.A., Kassim, T.I., AL-Dylymei, A.A. 1999. A limnological study on Tigris river, Iraq. *The Scientific Journal of Iraqi Atomic Energy Commission*, **9:** 59-66.

Al-Mussawi, A.H.A., Hussien, N.A., Al-Aarajy 1995. The influence of sewage discharge on the physico-chemical properties of some ecosystem at Basrah city, Iraq. *Basrah Journal of Agriclture Science*, **13:** 135-148.

Al-Nimma, B.A.B. 1982. A Study on the Limnology of the Tigris and Euphrates Rivers, *M.Sc. Thesis* Salahaddin University, Erbil, Iraq, 72pp.

Al-Saadi, H.A., Al-Edany, T.Y., Neama, J.D. 1999.On the distribution and ecology of aquatic plants in the Shatt Al-Arab river, Iraq. *Marina. Mesopotamica*, **11:** 49-62.

Al-Saadi, H.A., Al-Lami, A.A., Kassim, T.I., Al-Jaberi, H.H. 1996. Heavy metals in Qadisia lake and its aquatic plants. *Journal of the College of Education For Women*, **10:** 281-292.

Al-Zurfi, S.K., Mohammed, A.K., Shaheed, A.I. 2010. Study of some physical and chemical of Kufa River. *Journal of Babylon University/Pure and Applied Sciences*, **18:** 1399-1411.

APHA, 1995. *Standard Methods for the Examination for Water and Wastewater.* 19th edition. American Public Health Association, Byrd Prepress Springfield, Washington, USA

APHA, 1985. *Standard Methods for the Examination of Water and Wastewater*. 1268pp, 16th edition. American Public Health Association, Washington, D.C. USA.

BEIR, 1999, Biological Effect On Ionizing Radiation Report VI, *Health Effects of Exposure to Radon*, pp 516, The National Academics Press, Washington, USA.

Douabul, A.A.Z., Al-SAAD, H.T., Abdullah, D.S., Salman, N.A. 2013. Designated protected Marsh within Mesopotamia: water quality. *American Journal of Water Resources*, **1:** 39-44.

Goldman, C.R., Horne, A.J. 1983. *Limnology*, 464pp, McGraw Hill, New Yark, USA.

Hassan, F.M. 2004. Limnological features of Diwaniyah river, Iraq. *Baghdad Science Journal*, **1:** 119-124.

Howard, A.G. 1998. *Aquatic Environment Chemistry*. 96pp. Oxford Science Publications, November, UK.

Kassim, T.A. 1986. Environmental Study on Benthic Algae of Some Marsh Regions in Southern of Basra. *MSc. Thesis*. University of Basra, Iraq.

Lind, G.T. 1979. *Handbook of Common Methods in Limnology*, 2nd edition., 199pp., London, UK

Maulood, B.K., Al-Azzawi, M.N.A., Saadalla, A.A. 1994. An ecology study of the Tigris river pre and after crossing Baghdad. *Journal of College of Education for Women*, **5:** 43-50

Maulood, B.K., Al-Mousawi, A.H. 1989. Limnological investigation on Sawa lake, Iraq. *Basrah Journal of Agriculture Sciences*, **21:** 113-122.

Mushkor,S.K. 2002. Sewage wastewater and industrial effect for Smwia city in Euphrates river pollution. *Journal of Al-Qadisiyah for Pure Sciences*, **7:** 29-40. (Arabic)

MWR, 2007. *General Properties of Al-Kufa River*, Ministry of Water Resources / Najaf Annual Report, June 2007.

Sabri, A.W., Maulood, B.K., Sulaiman, N.E. 1989. Limnological studies on river Tigris: Some physical and chemical characters. *Journal of Biological Sciences, Research*, **20:** 565-579.

Salman, J.M. 2006. Environmental Study of Potential Pollution in Euphrates River Between Hindyhia Dam and Kufa City, Iraq. *PhD Thesis*, Babylon University. 192 pp.

Talling, J.F. 1980. Phytoplankton. In: *Euphrates and Tigris, Mnnogr. Biol*. J., Rzoska, and W Junnk (eds.) Junk, W. 122 pp., The Hague-Boston, London, UK.

USEPA, 1991. Methods for aquatic toxicity identification evaluations: Phase I, toxicity characterization procedures. T. Norberg-King, D.I. Mount, E. Durhan, G. Ankley, L. Burkhard, J. Amato, M. Lukasewycz, M. Schubauer Berigan, and L. Anderson-Carnahan (eds). *Environmental Research Laboratory, U.S. Environmental Protection Agency*, Duluth, Minnesota, 2nd edition, USA.

Weiner, E.R. 2000. *Application of Environmental Chemistry*. 276 pp. Lewis Publisers, London, New York, USA.

Wetzel, R. G. 2001. *Limnology, Lake and River Ecosystems*, 3rd edition, 1006pp. Academic Press, An Elsevier Science, Imprint,

Wetzel, R.G., Linkens, G.E. 2000. *Limnological Analysis.* 3rd edition, pp. 429. Springer Science: Business Media.

WHO 1996. *Guideline for Drinking Water Quality*, 2nd eddition, 94pp., World Health Organization, Switzerland.

Pak. j. sci. ind. res. Ser. A: phys. sci. 2018 **61A**(1) 51-55

Evaluation of Metals and Organic Contents in Locally Available Eye Shadow Products in Lahore, Pakistan

Amina Abrar*, Sofia Nosheen, Faiza Perveen and Moneeza Abbas
Department of Environmental Science, Lahore College for Women University, Lahore, Pakistan

(received February 7, 2017; revised June 2, 2017; accepted August 16, 2017)

Abstract. This study was conducted to evaluate the concentration of some heavy metals (lead, cadmium, chromium and zinc) and synthetic organic contents in non branded eye shadows locally available in Lahore, Pakistan. Twenty five samples of five eye shadow colours (red, golden, orange, white and pink) were purchased from local market in Lahore. Samples were pre-treated and atomic absorption spectrometer was used to determine the concentration of lead (Pb), cadmium (Cd), chromium (Cr) and zinc (Zn). Total organic content in these samples was determined by wet oxidation technique. Maximum concentration of Pb in eye shadow samples was detected to be 15.33 μg/g. Concentration of Pb in 80% of samples was found to be higher as compared to the permissible limit (10 μg/g) of Pb in cosmetics provided by Health Canada. 26% samples showed Cd concentration higher than permissible limit (3 μg/g). Although there are no available internationally acceptable maximum limits for Cr and Zn, but these metals were found to be present in detectable limits ranging from 5.5-8.23 μg/g and 7.9-11.84 μg/g, respectively. Total organic content (TOC) in the samples was found to be ranging from 2.15-2.92 mg/g.

Keywords: eye shadows, heavy metals, permissible limit, organic contents

Introduction

Cosmetics are applied directly to human skin, hair and nail therefore, these should be safe for health. Heavy metals in cosmetics are considered toxic to human body (Bocca *et al*., 2014). These are considered a part of routine body care in all strata of society. An average adult uses nine cosmetics daily and more than 25% women use 15 or more (Chauhan *et al*., 2010). Eye shadows are a typical example of pigmented make-up products used by women all over the world. Among the hazardous substances contained in cosmetics, heavy metals are widely diffused in coloured make-up products.

As the issues of heavy metals have been addressed, attention is turned to the presence of these substances as impurities. The deliberate use of metals as active ingredients in cosmetic products is prohibited by legislation in most countries, but metal impurities do exist in such products due to their persistence and ubiquitous nature. Metals such as Cd, Pb, Ni, Cr and Co are retained as impurities in the pigments of eye shadows or released by the metallic devices used during the manufacturing of these products. The continuous use of these cosmetic products could lead to the absorption of metals through skin. Cd and Zn exist in pigments and all other raw materials in all industries including the cosmetics industry (Nnorom, 2011).

There is a connection between use of makeup at young age and skin allergies by heavy metal contaminants in makeup. It has been found that young girls do react to these metals especially if they are prone to skin allergies or have damaged skin, such as from scrapes or cuts (Corazza *et al*., 2009). In an American survey consisting of 30,000 consumers, 700 reactions occurred during one year period and was estimated that 1-3% of the populations were allergic to a cosmetic or cosmetic ingredients (Mehta and Reddy, 2003). Use of cosmetic products is increasing rapidly all over the world and various toxic chemicals including heavy metals are used in the production of cosmetics which can cause health risks to consumer especially low cost products. Heavy metal toxicity takes place in the form of various diseases when inhaled or absorbed through skin (Saeed *et al*., 2011).

Skin absorption of heavy metals salts varies greatly with different physical parameters (Ullah *et al*., 2017). Heavy metal ions when come in contact with human body, they get absorbed and form complexes with carboxylic acid (–COOH), amine ($–NH_2$), and thiol (–SH) of proteins resulting in dis-functioning or death of the cells and consequently lead to a variety of diseases (Flora and Pachauri, 2010). Some cosmetics are benign,

*Author for correspondence;
E-mail: amina.abrar@outlook.com

others can cause harmful effects such as cancer, allergies, mutations, respiratory diseases as well as reproductive problems (CDC, 2003).

Heavy metal exposure leads to metal toxicity. Characteristic features of lead toxicity include anemia, neuropathy, nephropathy and coma. Exposure of human body to low-levels of lead has also been linked with abnormalities in human behaviour, learning impairment, and decreased hearing in humans and in experimental animals (Chauhan *et al*., 2010). Zinc and lead develop same signs of illness and can easily be diagnosed as lead poisoning (Theresa *et al*., 2011). An increase level of cadmium is a cause of inhibition of DNA mismatches. Inhaling large amount of cadmium can cause stomach, kidney and liver problems, nose redness, irritation, nosebleed, runny nose and even death. When skin comes in contact with chromium compounds, it results in skin ulcers (Gondal *et al*., 2010).

Hexavalent chromium (Cr^{+6}) cause allergies of the skin. Cr^{+6} compounds are classified as carcinogens by the International Agency for Research on Cancer (IARC). Toxic effects of the Cr^{+6} on the skin may result in ulcerations, dermatitis, and skin allergies. Inhalation of Cr^{+6} compounds can result in ulceration and pores in the mucous membranes of the nasal septum, discomfort of the pharynx and larynx and asthmatic bronchitis. Respiratory symptoms may include coughing, shortness of breath, and nasal itch (Sahu *et al*., 2014). It can cause increased blood leukocytes, wounds of eye and skin ulcers by inhalation, ingestion, and by skin and eye contact (CDCP, 2014).

Pakistan has no technologically developed cosmetic industry. There are certain rules and safety limits for regulating the use of chemicals (both organic as well as inorganic) but these rules are not followed in small scale, local and cheap industries, so there is a need to focus on this area of investigation. A major proportion of Pakistani population has low income status and low literacy rate so they use mostly locally available cosmetics. The present study was therefore, taken to give attention to a very critical issue.

Materials and Methods

The study was carried out to detect heavy metals contents (lead, cadmium, chromium and zinc) and total organic content in eye shadows purchased from local market in Lahore. Different eye shadows (red, golden, orange, white and pink), the most commonly used colours were selected and total 25 samples were analysed.

Determination of heavy metals. Glasswares were washed thoroughly with detergent and dilute nitric acid and rinsed with distilled water before use. Each sample kit was dealt separately to avoid any cross contamination. All pellets of each colour in eye shadow kit were taken out and weighed accurately for further processing. One gram of each sample was placed into a 100 mL glass beaker. Weighed sample was digested with 5 mL of concentrated nitric acid on a hot plate at 80 °C until the sample was dried. Once the sample was dried, the process was repeated again by adding 5 mL of concentrated nitric acid and dried on a hot plate at 80 °C. Then 1mL of concentrated hydrogen peroxide (H_2O_2) was added in order to oxidise the organic matter of residues completely. The residual material was diluted by using de-ionized water to the final volume of 50 mL. The solution was then filtered by Whatman filter paper. Same procedure was repeated for all samples. Samples prepared for determination of the metal ions in the solution were kept in test tubes, covered by aluminum foil and stored in cool incubator until analysed (Nourmoradi *et al*., 2013). Atomic absorption spectrophotometer (AAS Thermo Scientific M series GF95Z Zeeman, Furnace) was used for metal analysis. A standard stock solution of 1000 mg/L was diluted into series of standard solutions (2, 4 and 6 ppm) up to the level of distilled water. The standard stock solution was further diluted into series of standard solution (1, 2 and 3 ppm) up to the mark with distilled water. Concentrations of lead, cadmium, chromium and zinc was determined in eye shadow samples by AAS. Mean concentration of each heavy metal was calculated and the results were compared with the permissible limits of these metals in cosmetics provided by Health Canada.

Determination of total organic content. Organic content was determined in terms of total organic carbon in eye shadows. For determination of organic content the wet oxidation method was employed using exothermic heating. It involved oxidation of carbon content with potassium dichromate (1N) as oxidizing agent along with concentrated sulphuric acid. In the second step excess dichromate (leftover) was titrated with 0.5 N ferrous ammonium sulphate solution till end point was achieved. Diphenylamine was added as indicator. The solution was back titrated with 0.5 N ferrous solution (Avramidisa *et al.*, 2015; Gaudette *et al*., 1974).

Results and Discussion

The analysis of eye shadow samples of different brands showed detectable amount of heavy metals impurities but with varying concentrations. Health Canada has recommended that the maximum Pb concentration in cosmetics to be lesser than 10 µg/g while Cd permissible limit in cosmetics is 3 µg/g (Hazard, 2011). Results of present study showed mean concentration of Pb ranging from 7.56-15.33 µg/g in selected eye shadow colours (Fig. 1). 80% of samples were having Pb content higher than the permissible limit of 10 µg/g. Lead is considered a very dangerous heavy metal in cosmetics, but is largely used in the make-up items. Lead impairs the renal, homopoietic and nervous system. Reports of various surveys suggest that Pb is casually related to deficiency in cognitive functioning. Mean concentration of Cd in different colours was found to be ranging from 0.41-2.23 µg/g (Fig. 1). Although mean concentration of Cd in different colours was found to be within the permissible limit of 3 µg/g but 26% of individual samples had higher Cd content as compared to the permissible limit established by Health Canada.

Mousavi *et al*. (2013) also reported high content of Pb and Cd in eye shadows purchased from local market in Tehran, Iran. They also reported that the type of pigment used in eye shadows contributes to its heavy metal content, brown and golden colours in all brands have the highest concentrations of lead, while blue and green colours have the lowest lead content and the golden and blue colour have the highest and lowest concentration of cadmium, respectively. The present study showed higher concentration of Pb in pink and white colours than in other colours while pink and white colours were also having higher concentrations of Cd as well. Another research study conducted by Nourmoradi *et al*. (2013) to assess lead and cadmium levels in frequently used cosmetic products in Iran, showed higher concentration of Pb and Cd in eye shadows ranging from 0.85-6.90 µg/g and 1.54-55.59 µg/g, respectively.

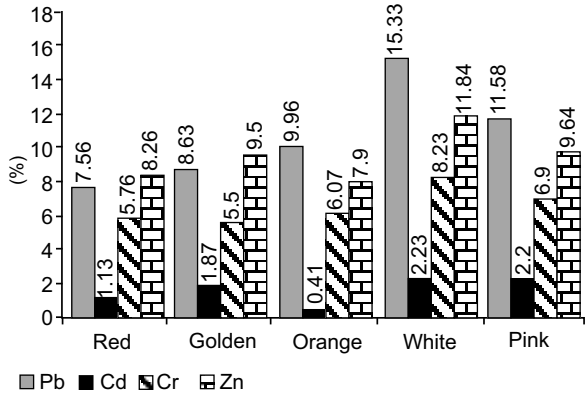

Fig. 1. Mean concentrations in µg/g of Pb, Cd, Cr and Zn in (red, golden, orange, white and pink) eye shadows randomly purchased from local market in Lahore, Pakistan.

The present study showed mean concentration of Zn in different eye shadow colours to be ranging from 7.9-11.84 µg/g and mean concentration of Cr to be ranging from 5.5-8.23 µg/g (Fig. 1). There are no permissible limits of Cr and Zn found in cosmetics but the present study showed detectably high amount of these metals in different eye shadow colours. A study on determination of chromium in cosmetics conducted by Zhou *et al*. (2011) showed high concentration of Cr in majority of the cosmetics available in the market of China. High concentration of Zn and Cr in eye shadows can lead to systemic contact dermatitis (SCD). Contact dermatitis is produced by external skin exposure to metals like chromium, zinc, cobalt and arsenic. A review study conducted by Yoshihisa and Shimizu (2012) reported that when exposed to skin, chromium salts can induce cutaneous irritation, which may progress to SCD in cases of chromium hypersensitivity. Zinc is an essential trace element involved in many physiological functions, including catalytic and structural roles in metallo-enzymes, as well as regulatory roles in diverse cellular processes, such as synaptic signaling and gene expression. Compared to several other metal ions with similar chemical properties, zinc is relatively harmless. Only exposure to high doses has toxic effects, making acute zinc intoxication, a rare event. In addition to acute intoxication, long-term, high-dose zinc supplementation interferes with the uptake of copper. Hence, many of its toxic effects are in fact due to copper deficiency. Skin exposure to zinc can also lead to zinc allergies and SCD as reported in many studies (Plum *et al*., 2010).

High metal content in cosmetics applied on skin can be absorbed in blood and accumulate in various organs to produce toxic and allergic effects. Skin allergies and contact dermatitis are topical effects due to exposure to heavy metals in various cosmetics (Boroska and Brzoska, 2015).

Sainio *et al*. (2000) conducted a research study to detect the metal content in eye shadows. The results indicated

that 66 out of 88 (75%) of the colours contained more than 5 ppm of at least one of the elements, and all 49 products contained more than one ppm of at least 1 of the elements. They also determined the systemic and topical effects of metals in eye shadows and found that eye shadows generally have no systemic toxicity but can pose a great risk of allergies. Another study conducted by Oh *et al*. (2016) investigated the contact allergens in eye shadow products. They found heavy metals to be one of the major contact allergens in eye shadows responsible for eyelid dermatitis. They found eye shadow products having significant amount of nickel, cobalt or chromium to elicit allergic reactions.

In current study organic content was also detected in samples. As products were not labeled as organic product so it was assumed that it should show no detectable contents of organic carbon. But a reasonably high level was determined in eye shadows ranging from 2.15-2.92 mg/g (Fig. 2). Synthetic organic contents have the ability to affect the skin in a variety of unpleasant ways for a long time regular use like coal tar and di-ethanol amine. Presence of organic contents along with heavy metals potencies the alarming condition of these cheap local cosmetic products. Quality assurance with health significance should be practiced before market availability of the cosmetic products.

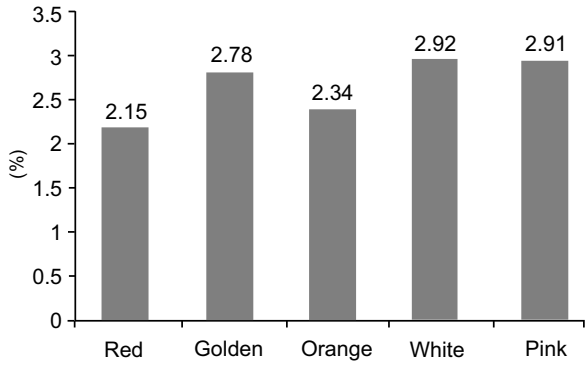

Fig. 2. Mean concentrations in mg/g of organic content in (red, golden, orange, white and pink) eye shadows randomly purchased from local market in Lahore, Pakistan.

Conclusion

The present study showed that the quality of eye shadow purchased from local markets of Lahore was found unsatisfactory. 80% samples showed high Pb contents while 26% samples showed Cd contents above the permissible limits. Detectable amounts of Cr and Zn impurities were also present in the eye shadows along with high organic content. Higher concentration of these metals and organic content in eye shadows can cause allergies, dermatitis, skin irritation or eczemas on eyelid skin. They can also accumulate in body and cause systematic effects. There is no proper safety standards in Pakistan related to heavy metal contamination in eye shadows or in other cosmetics products. Therefore, it is difficult to ascertain if the values of metals obtained in this study are very high or low. Further studies can be conducted on exposure assessment of these cosmetics.

References

Avramidis, P., Nikolaou, K., Bekiari, V. 2015. Total organic carbon and total nitrogen in sediments and soils: a comparison of the wet oxidation–titration method with the combustion-infrared method. *Agriculture and Agricultural Science Procedia*, **4:** 425-430.

Bocca, B., Pino, A., Alimonti, A., Forte, G. 2014. Toxic metals contained in cosmetics: a status report. *Regulatory Toxicology and Pharmacology*, **68:** 447-467.

Borowska, S., Brzóska, M.M. 2015. Metals in cosmetics: implications for human health. *Journal of Applied Toxicology*, **35:** 551-572.

CDCP, 2014. NOISH *Pocket Guide to Chemical Hazards: Chromic Acid and Chromates*. Centers for Disease Control and Prevention. Online:

CDCP, 2003. *Second National Report on Human Exposure to Environmental Chemicals*. Centers for Disease Control and Prevention. Online: .

Chauhan, A.S., Bhadauria, R., Singh, A.K., Lodhi, S.S., Chaturvedi, D.K., Tomar, V.S. 2010. Determination of lead and cadmium in cosmetic products. *Journal of Chemical and Pharmaceutical Research*, **2:** 92-97.

Corazza, M., Baldo, F., Pagnoni, A., Miscioscia, R., Virgili, A. 2009. Measurement of nickel, cobalt and chromium in toy make-up by atomic absorption spectroscopy. *Acta Dermato-Venereologica*, **89:** 130-133.

Flora, S.J., Pachauri, V. 2010. Chelation in metal intoxication. *International Journal of Environmental Research and Public Health*, **7:** 2745-2788.

Gaudette, H.E., Flight, W.R., Toner, L., Folger, D.W.

1974. An inexpensive titration method for the determination of organic carbon in recent sediments. *Journal of Sedimentary Research*, **44:** 249-253.

Gondal, M.A., Seddigi, Z.S., Nasr, M.M., Gondal, B. 2010. Spectroscopic detection of health hazardous contaminants in lipstick using laser induced breakdown spectroscopy. *Journal of Hazardous Materials*, **175:** 726-732.

Hazard, H.M. 2011. *Report: The Heavy Metals Hazard: The Health Risks of Hidden Heavy Metals in Face Makeup*. Environmental Defence, Toronto, Canada.

Mehta, S.S., Reddy, B.S.N. 2003. Cosmetic dermatitis-current perspectives. *International Journal of Dermatology*, **42:** 533-542.

Mousavi, Z., Ziarati, P., Shariatdoost, A. 2013. Determination and safety assessment of lead and cadmium in eye shadows purchased in local market in Tehran. *Journal of Environmental and Analytical Toxicology*, **3:** 2161-0525.

Nnorom, I.C. 2011. Trace metals in cosmetic facial talcum powders marketed in Nigeria. *Toxicological & Environmental Chemistry*, **93:** 1135-1148.

Nourmoradi, H., Foroghi, M., Farhadkhani, M., Vahid Dastjerdi, M. 2013. Assessment of lead and cadmium levels in frequently used cosmetic products in Iran. *Journal of Environmental and Public Health*, http://dx.doi.org/10.1155/2013/962727.

Oh, J.E., Lee, H.J., Choi, Y.W., Choi, H.Y., Byun, J.Y. 2016. Metal allergy in eyelid dermatitis and the evaluation of metal contents in eye shadows. *Journal of the European Academy of Dermatology and Venereology*, **30:** 1518-1521.

Plum, L.M., Rink, L., Haase, H. 2010. The essential toxin: impact of zinc on human health. *International Journal of Environmental Research and Public Health*, **7:** 1342-1365.

Saeed, M., Muhammad, N., Khan, H. 2011. Assessment of heavy metal content of branded Pakistani herbal products. *Tropical Journal of Pharmaceutical Research*, **10:** 499-506.

Sahu, M.R., Saxena, M.P., Johnson, S., Mathur, H.B., Agarwal, H.C. 2014. *Heavy Metals in Cosmetics*. 28 pp., Pollution Monitoring Laboratory, Centre for Science and Environment, New Delhi, India.

Sainio, E.L., Jolanki, R., Hakala, E., Kanerva, L. 2000. Metals and arsenic in eye shadows. *Contact Dermatitis*, **42:** 5-10.

Theresa, O.C., Onebunne, O.C., Dorcas, W.A., Ajani, O.I. 2011. Potentially toxic metals exposure from body creams sold in Lagos, Nigeria. *Researcher*, **3:** 30-37.

Ullah, H., Noreen, S., Rehman, A., Waseem, A., Zubair, S., Adnan, M., Ahmad, I. 2017. Comparative study of heavy metals content in cosmetic products of different countries marketed in Khyber Pakhtunkhwa, Pakistan. *Arabian Journal of Chemistry*, **10:** 10-18.

Yoshihisa, Y., Shimizu, T. 2012. Metal allergy and systemic contact dermatitis: an overview. *Dermatology Research and Practice*, doi:10.1155/2012/749561.

Zhou, L.Y., Huang, J., Ning, Z.Y., Cai, L., Li, C.X. 2011. Determination of Cr (VI) in cosmetics by FAAS after cloud point extraction. *Guangzhou Chemical Industry*, **4:** 1-5.

Pak. j. sci. ind. res. Ser. A: phys. sci. 2018 **61A**(1) 56-58

Short Communication

Cleaning of Dalwal-Punjab Coal by Using Shaking Table

Muhammad Shahzad* and Zulfiqar Ali
Mining Engineering Department, University of Engineering & Technology, Lahore, Pakistan

(received August 2, 2016; revised October 9, 2017; accepted October 13, 2017)

Abstract. The aim of this research is to evaluate the cleaning amenability of Dalwal-Punjab coal by using tabling technique. Total eighteen tabling tests were performed on two size fractions; 3.327 × 1.168 and 1.168 × 0.295 mm. The effects of table tilt (0 to 10 mm/m) and water flow rate (14 to 36 l/min) on clean coal yield and ash were investigated. It was found that both clean coal yield and ash were increased with increasing table tilt and water flow rate.

Keywords: Dalwal coal, shaking table, coal cleaning, gravity concentration

Gravity separation methods being cheaper and simple in operation are commonly used worldwide for cleaning various size ranges of coal (Shahzad *et al*., 2015). Shaking table is one of the most versatile gravity concentration device and is found in most types of gravity concentration plants (Lee *et al*., 2012). Tables are characterised by low power consumption and low costs of operation, installation and maintenance but suffer with disadvantages of low capacity and occupying more floor space (Sivamohan and Forssberg, 1985). The probable error of shaking table is less as compared to spiral and water only cyclone, which makes it relatively more efficient separation technique (Gupta and Yan, 2006; Bethell and Moorhead, 2003). It is generally applicable on coal particles ranging in size from 0.075 to 15 mm (Wills and Napier-Munn, 2006; Gupta and Yan, 2006) but preferably employed on the size ranging from 0.5 to 5 mm (Anastassakis, 2004).

In this study, coal sample was collected from the coal mine of Iqbal Sons Coal Company situated in Dalwal Coalfield of Punjab, Pakistan. The gross sample amounting over 240 kg was collected from a coal pile according to the guidelines described in ASTM D-2234 and ASTM D-6883 then crushed to -38.00 mm and divided into four parts after mixing properly. One part was prepared according to ASTM D-2013 for proximate analysis. Sieve analysis was performed on the second part while the remaining portion was used for cleaning tests. Deister shaking table was used for coal cleaning. Total eighteen tests were performed on two different particle size ranges; 3.327 × 1.168 and 1.168 × 0.295 mm. Stroke frequency and stroke length were kept at 260 stroke/min and 15 mm, respectively. The values of diagonal tilt were kept at 0, 5 and 10 mm/m while water flowrate was maintained at 14, 24 and 36 l/min. Only two products were obtained; concentrate at the transverse end and tailings at the longitudinal end. The products were dried and analysed for ash content.

Proximate analysis showed that Dalwal coal was consisted of 2.9% moisture, 29.7% ash, 28.8% volatile matter and 38.6% fixed carbon. Table 1 shows the results of sieve analysis and ash determination tests performed on each size fraction. It was found that crushed coal was mostly consisted of coarse particles. The largest (-38.00+26.67 mm) and smallest fraction (-0.295 mm) contained the highest amount of ash contents while the fraction (-26.67+13.33 mm) containing the largest amount of material possessed the smallest amount of ash. It may be safely concluded that the mineral matter was attached with organic matrix at different size levels. The cumulative ash contents were become almost equal to that value found in proximate

Table 1. Results of sieve analysis and ash distribution in various size fractions

Fraction size	Individual		Cumulative	
	Weight	Ash content	Weight	Ash content
	(%)			
-38.00+26.67	19.53	34.4	19.53	34.4
-26.67+13.33	47.30	26.8	66.83	29.0
-13.33+6.67	17.09	28.9	83.92	29.0
-6.67+3.327	8.40	33.5	92.32	29.4
-3.327+1.168	4.44	33.1	96.76	29.6
-1.168+0.295	2.06	30.9	98.83	29.6
-0.295	1.17	36.2	100.00	29.7

*Author for correspondence; E-mail: m.shahzad87@uet.edu.pk

analysis when the size of the coal became smaller than 3.327 mm. Therefore, the coal size less than 3.327 mm was selected for performing tabling tests.

The effect of water flow rate on clean coal yield and ash content is shown in Fig. 1-3. At 0 mm/m tilt, both clean coal yield and ash content were increased by increasing water flow rate. The clean coal yield and ash content were found higher for coal size of -1.168+0.295 mm at low water flow rate but at higher values of water flow rate, the yield of -3.327+1.168 mm coal size became higher with lower amount of ash content. At low water flowrate, the density difference between coal and mineral matter becomes more apparent and light particles (coal) report to the concentrate launder. The role of stroke frequency and stroke length becomes significant at low water flow rate which causes large particles to move along the longitudinal axis and report to the tailing launder resulting in lower concentrate yield. At high water flow rate, the film of flowing water becomes thicker and the upper layers of water film having more velocity exert more force on upper part of larger particles which increases their rolling action and results into their movement to concentrate launder, thus increasing the yield.

Similar trend was found for table tilt of 5 mm/m for clean coal yield but clean coal ash of -3.327+1.168 mm was also increased at higher water flow rate. Tilting of table increases the movement of particles along the flowing water due to gravity effect which results in higher yield. At larger table tilt e.g. 10 mm/m, the effect of water flow rate was found very significant on clean coal yield and ash for the coal size of -3.327+1.168 mm but coal particles of size -1.168+0.295 mm were found to be little affected because the yield of these particles had already been reached at peak value e.g. more than 90%. At low water flow rate, the larger particles did not experience sufficient forces due to flowing film of water which resulted in their lower yield while larger flow rate with larger table tilt increased forces along the transverse direction which resulted in higher yield.

Maximum yield of 41.00 and 43.67% with 14.3 and 13.1% clean coal ash were achieved for the particle size range of -1.168+0.295 and -3.327+1.168 mm, respectively at 36 l/min water flowrate for 0 mm/m tilt. Although the yields were higher for both size ranges at table tilts of 5 and 10 mm/m with water flow rate of 36 l/min but the clean coal ash were not reduced enough to be considered for utilization of clean coal in cement industry. The cement industries in Pakistan usually require coal with less than 15% ash content. Therefore, the best cleaning practice would be to clean -3.327+1.68 and -1.168+0.295 mm size fractions at 36 l/min water flow rate with no table tilt. This would result in cumulative product yield of 42.34% and clean coal ash of 13.7%. The cumulative yield and ash contents of tailings at these conditions would be 57.66 % and 41.4%, respectively.

In Punjab coal mines, coals with more than 40% ash content are normally sold to brick kiln industry with reasonable price ranging from 5000 to 7000 rupees per ton while coals containing ash contents between 20 to 30% are normally sold at prices from 7000 to 9000 rupees per ton. Cement industries of Punjab are using more than 70% imported coal which costs more than 13000 rupees per ton at arrival to the factory. Dalwal coal mines are situated within the distance of 20 km from three major Cement industries of Punjab namely Pakistan Cement Industry, DG Cement Industry and Bestway Cement Industry. Since the costs for coal processing normally varies from 300 to 450 rupees per ton

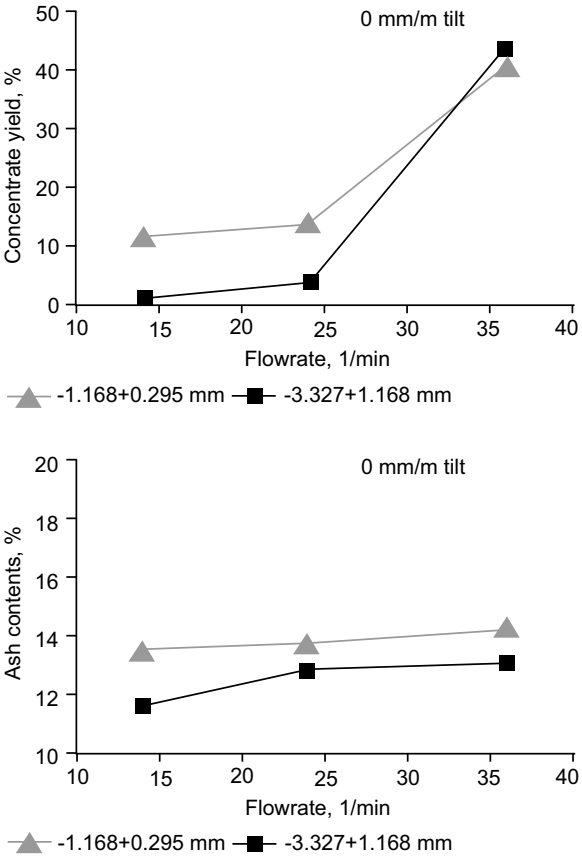

Fig. 1. Effect of water flowrate on concentrate yield and ash contents with 0 mm/m table tilt.

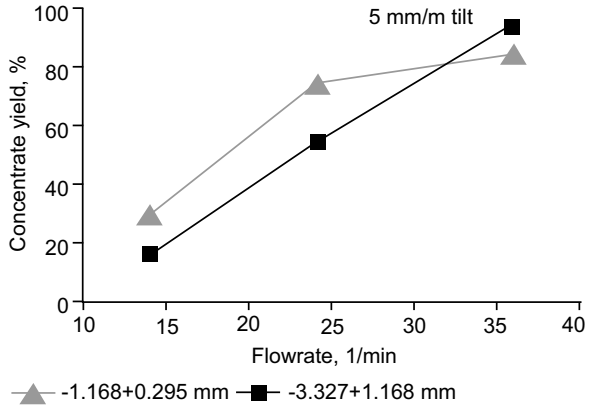

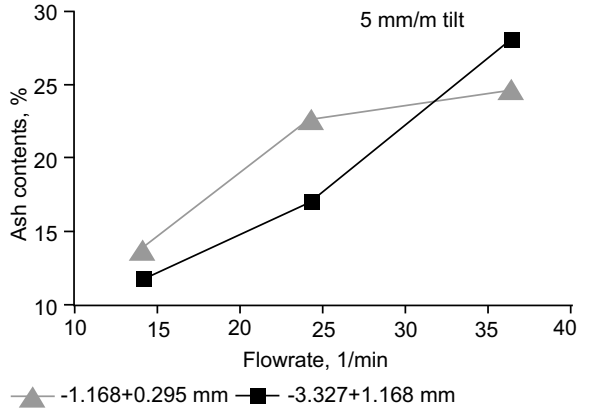

Fig. 2. Effect of water flowrate on concentrate yield and ash contents with 5 mm/m table tilt.

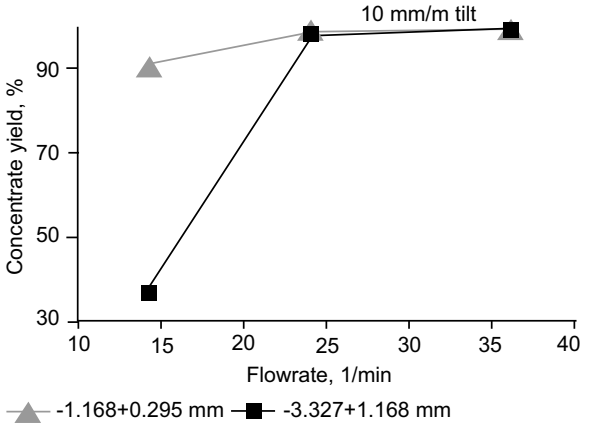

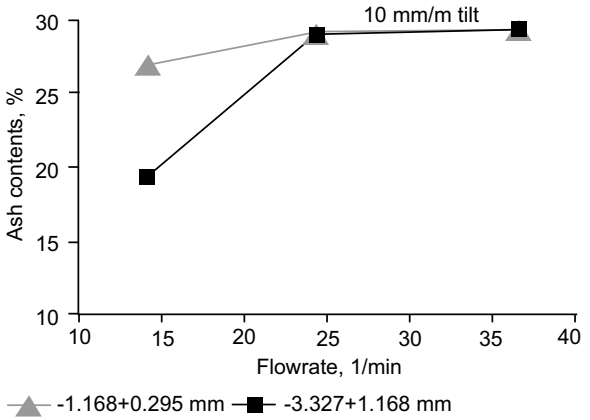

Fig. 3. Effect of water flowrate on concentrate yield and ash contents with 10 mm/m table tilt.

and transportation cost per ton would be minimal therefore, it is concluded that the selling of clean coal to the cement industry and tailings to the brick kiln industry could result in higher revenue for the coal mine owners.

References

Anastassakis, G.N. 2004. Beneficiation of Greek lignites. *Coal Preparation*, **24:** 19-34.

ASTM, 2004. *Annual Book of ASTM Standards*, vol. **05.06,** American Society for Testing and Materials, West Conshohocken, PA, Specifically:
· ASTM D-2013. Standard Practice for Preparing Coal Samples for Analysis.
· ASTM D-2234. Standard Practice for Collection of a Gross Sample of Coal
· ASTM D-6883. Standard Practice for Manual Sampling of Stationary Coal from Railroad Cars, Barges, Trucks and Piles.

Bethell, P., Moorhead, R.G. 2003. Operating characteristics of water-only cyclone/spiral circuits cleaning fine coal. In: *Advances in Gravity Concentration*, R. Q. Honaker and W. R. Forrest (eds.). Society for Mining, Metallurgy, and Exploration, Inc. (SME) 8307 Shaffer Parkway Littleton, Colorado, USA.

Gupta, A., Yan, D.S. 2006. *Mineral Processing Design and Operation*. 1st edition, Elsevier Radarweg 29, Amsterdam, The Netherlands.

Lee, S.J., Cho, H.C., Kwon, J.H. 2012. Beneficiation of coal pond ash by physical separation techniques. *Journal of Environmental Management*, **104:** 77-84.

Shahzad, M., Tariq, S.M., Iqbal, M.M., Arshad, S.M., Saqib, S. 2015. An assessment of cleaning amenability of salt range coal through physical cleaning methods. *Pakistan Journal of Scientific and Industrial Research. Series A: Physical Sciences*, **58:** 74-78.

Sivamohan, R., Forssberg, E. 1985. Principles of tabling. *International Journal of Mineral Processing*, **15:** 281-295.

Wills, B.A., Napier-Munn, T. 2006. *Mineral Processing Technology*, pp. 16, 7th edition, Elsevier Science & Technology Books, Amsterdam, The Netherlands.

INSTRUCTIONS TO AUTHOR

Pakistan Journal of Scientific and Industrial Research, Series A: Physical Sciences and ***Series B: Biological Sciences publish original researches as full research papers, short communications and reviews papers. The manuscript written in clear, concise English will be accepted for review. Authors who are not native English speakers should note that the manuscript must be edited for linguistic errors by some professional experts.***

The manuscripts will be entertained covering the following subjects of Physical and Biological Sciences: Agriculture, Agronomy, Biochemistry, Biotechnology, Botany, Chemistry, Ecology, Environmental Sciences, Epidemiology, Food Sciences, Genetics, Geography, Geology, Microbiology, Nanotechnology, Natural Products, Pharmaceutical Sciences, Physics, Proteomics, Radiation, Soil Sciences, Spectroscopy and Applied Sciences, Toxicology, Veterinary Sciences and Zoology. However, we do not entertain articles of pure Mathematics, Computer Sciences, pure Engineering and Medical Sciences.

All manuscripts are evaluated by subject experts of advanced countries. However, authenticity of the contents remains the sole responsibility of the author/s. The Journal reserves the rights to edit, wherever considered necessary to make contribution harmonized with the format of the journal.

Manuscripts should be submitted online *via* PJSIR website:

- Simply log on to our website and follow the onscreen instructions for all submissions (you will need to register before your first submission to PJSIR).
- If you have any technical problems or questions related to the electronic submission process or uploading your files, please contact to our Editorial Office.

Types of Manuscript:

The journal publishes **(1) Regular manuscripts, (2) Short communication and (3) Reviews.**

(1) Regular Manuscripts:

The manuscript being submitted must consist of original research performed by the authors and the research must include new information that is significant.

(2) Short Communications:

Short communication should contain description of findings in a concised form that would be of interest to readers of the journal. The material should be formatted as per PJSIR style and should not exceed 1500 words/3 printed pages.

(3) Reviews:

Regular Reviews: Reviewing scientific discoveries including the recent results of author(s) and articles must having total length of the paper along with references approximately 10 printed pages.

Invited Reviews: Submitted by invitation from the Editorial Board and encompass recent important scientific discoveries of approximately 10 printed pages (including tables, figures and references).

Prerequisites for Publication:

- **Certificate:** A certificate must be submitted that the paper has neither been submitted nor will be sent to any other journal after submitting to PJSIR.
- **Co-authors verification:** Author should certify that the co-author(s) has / have been informed about the submission of the paper to the journal.
- **Reviewers' names:** The author should submit at least four experts and their e-mail for review of the paper out of their country.
- **Illustrations/photographs:** It should be prepared for reproduction as halftones or line drawings. All illustrations are to be submitted in complete and finished form, with adequate labeling.

Photographs in JPEG/TIFF format preferably direct from original with minimum reduction and clear resolution. Symbols and lines should be chosen to remain legible after the degree of reduction that will be used (single column 7.5:double column 16 cm) for better results.

- **Copyright:** PJSIR owns all copyright to any work published in the Journal. Any material submitted, whether appearing in the journal or not, may not be used, reproduced, or transmitted without the written consent of PJSIR.
- **Plagiarism Report:** PJSIR observes/follows HEC guidelines/Criteria for plagiarism. It is the author's responsibility to apprise themselves of plagiarism in any form. All the papers submitted to PJSIR should be accompanied by Turnitin Plagiarism Report up to 19% similarity index. If plagiarism report has been taken earlier, submit a certificate for the same.
- **Conflict of interest/Financial disclosure statement:** At the time of submission declaration must be submitted that the authors have no conflict of interest. Authors should disclose in the online submission system any commercial affiliation or consultancy that could be construed as a conflict of interest with respect to the submitted data.
- **Authors' contribution:** All papers submitted to PJSIR should be accompanied with statement describing contributions of each author of the paper.

Manuscript preparation:

- Manuscripts should be submitted with double spaced with proper margin on left and right side preferably in MS-Word (version 2003 and upwards) in 12-point size font on A4 size sheet with pages numbers from 1st to last in the bottom of the paper .Author/s may submit electronic copies in Ms Word via e-mail or through our website.
- **Cover letter:** Manuscript should be submitted with a covering letter at every time of submission.
- **Title of the paper:** The manuscript should contain title of the paper and unabbreviated names of all authors with their complete postal addresses e-mail and phone numbers. An asterisk (*) should be added to the right of the corresponding author's name.
- **Abstract:** The manuscript should contain abstract (not more than 300 words for research paper and 150 words for short communication).
- **Key words:** Up to six keywords identifying the nature of the subject matter may be used to alert readers. Key words should be listed below the summary of the paper.
- **Introduction:** The section should contain a clear statement of the purpose of work, the reasons for undertaking the research and pertinent background of the study that allows readers outside the field to understand the purpose and significance of the work.
- **Materials and Methods:** Description of methods should be brief, but with sufficient details to enable the experiments to be repeated by the readers. The design of the study or experiments, any specific procedures used, and statistical analyses must be described clearly and carefully. References to other papers describing the techniques may be given. The name and location (city and state/country) of commercial suppliers of uncommon chemicals, reagents, or instruments should be mentioned.
- **Results and Discussion:** The results and discussion should be presented concisely. Tables and figures should be used only if they are essential for the comprehension of the data. The purpose of the discussion is to interpret the results and to relate them to existing knowledge in the field.
- **Conclusion:** Conclusion should be provided under separate heading and highlight new aspects arising from the study. It should be in accordance with the objectives.
- **Tables:** Tables should be numbered (Arabic numerals) in the order in which they are referred to in the text. Each Table should have brief title, be on a separate page, and be double-spaced throughout. Non-standard abbreviations should be used sparingly and must be defined in a legend at the bottom of the Table. For Table title, use lower case letters with only the first letter capitalized.
- **Figures:** All illustrations (line drawings and photographs) are classified as figures. Digital photograph files should have a resolution of at least 300 dpi. Figures should be cited in consecutive order in the text. The abbreviation "Fig." should be used (e.g., (Fig. 1), If a figure

consists of multiple parts, letters (a, b, c, etc.) should be used to label them (e.g**,** Fig. 1a). Legends for the figures should be double-spaced, in numerical order, and on a separate page. Non-standard abbreviations should be defined in legends. For figure title, use lower case letters with only the first letter capitalized.

- **Units:** IUPAC rules for units and their abbreviations should be used, i-e length (m, cm, mm, µm, nm, Å), mass (kg, g, mg, µg, ng pg, mol, mmol, µmol), volume (L, mL, µL), time (s, min, h, d), temperature (°C, ^{o}K), radiation (Bq, dpm, Gy, Sv), and concentration (M, mM) mol/L, mmol/L, mg/mL, (v/v), (w/v), ppm, ppb).
- **Spectral and elemental analysis data:** Please report spectral and elemental analysis data in the following format. ^{1}H-NMR ($CDC1_3$) δ : 1.25 (3H, D, J=7.0Hz) 3.55 (1H, q, J=7.0Hz), 6.70 (1H, m) ^{13}C-NMR ($CDC1_3$) δ:20.9 (q) 71.5 (d), 169.9 (s). IR (KBr) cm^{-1}: 1720, 1050, 910 UV λmax (EtOH) nm (ε) : 241 (1086), 288 (9380). UVλ_{max} (H_2O)nm(log ε): 280 (3.25). FAB-MS m/z: 332.1258 (Calcd for $C_{18}H_{20}O_6$: 332.1259). MS *m/z*:332 (M^+) 180, 168, $[\alpha]^{23}_{D}$ – 74.5 (c=1.0 MeOH). Anal. Calcd for $C_{19}H_{21}NO_3$:C, 73.29; H, 6.80; N, 4.50 Found: C, 73.30; H, 6.88: N, 4.65.
- **References formation:** All references should be as per PJSIR format, and cited in the text by the last name of the author and year into a chronological descending order. All references in the bibliography should be listed in alphabetical order of the authors' last names followed by date of publication and other complete details with full names of Journals as given below:

In "Text" References :

Park (2005), Aksu and Kabasakal (2004) and Evans *et al.* (2000)

(Park, 2005; Aksu and Kabasakal, 2004; Evans *et al.,* 2000)

In "List" References :

Evans, W.J., Johnson, M.A., Fujimoto, Cy. H., Greaves, J. 2000. Utility of electrospray mass spectrometry for the characterization of air-sensitive organolan-thanides and related species. *Organometallics,* **19:** 4258-4265.

For Standards :

ASTM, 2007. Standard Test Method for the Determination of Iron Ion Ores and Related Materials (E247-OD) P.O. Box C700, West Conshohocken, USA, *Annual Book of ASTM Standards*, vol, 30.5 pp.163-165.
PCRWR, 2007. *Water Quality Monitoring, Fifth Monitoring Report* 2005-6 . ISBM 978-969-8469-184, Pakistan Council of Research in Water Resources. Pakistan

Books:

Cinar, A., Parulekar, S.J., Undey, C., Birol, G. 2003. *Batch Fermentation: Modeling, Monitoring, and Control,* 250 pp.Marcel Dekker Inc., New York, USA.

Chapters in Edited Books:

Newby, P.J., Johnson, B. 2003. Overview of alternative rapid microbiological techniques. In: *Rapid Microbiological Methods in the Pharmaceutical Industry,* M.C. Easter (ed.), vol. **1**, pp. 41-59, 1st edition, Interpharm / CRC, Boca Raton, Florida, USA.

Papers in Proceedings:

Marceau, J. 2000. Innovation systems in building and construction and the housing industry in Australia. In: *Proceedings of Asia-Pacific Science and Technology Management Seminar on National Innovation Systems,* pp. 129-156,Japan Int. Sci. Technol. Exchange Centre, Saitama, Japan.

Reports:

*SIC, 2016. Annual Report, 2014-15,*Scientific Information Centre, Pakistan Council of Scientific and Industrial Research, PCSIR Laboratories Campus, Shahrah-e-Dr. Salimuzzaman Siddiqui, Karachi, Pakistan.

Thesis:

Saeed, A. 2005. Comparative Studies on the Biosorption of Heavy Metals by Immobilized Microalgal Cultures, Suspended Biomass and Agrowastes. *Ph.D. Thesis*, 248 pp., University of the Punjab, Lahore, Pakistan.

Patents:

Young, D.M. 2000. Thermostable Proteolysis Enzymes and Uses Thereof in Peptide and Protein Synthesis, US Patent No. 6,143,517, 7th November, 2000.

Data Set from a Database: (information should be retrievable through the input)

Deming, D; Dynarski, S. 2008. The lengthening of childhood (NBER Paper 14124) Cambridge, MA: National Bureau of Economic Research, Retrieved July 21, 2008 from http:// www.nber.org/papers/w14124) DOI No.....

Other Important Points :

1. In general, after submission of a paper, no authors may be added deleted or replaced with other names from the paper, and the order of the names of the authors cannot be changed at any stage i.e. modification, revision and galley proof.
2. The authors are given an opportunity to proofread the galley of an accepted manuscript. No additions and revisions are allowed other than the correction of typographical errors.
3. No reprints will be sent. Single hard copy will be sent to the corresponding author and co-authors may subscribe it. Full-text will be available on our website.
4. Any change in postal address or e-mail of the corresponding author should be communicated immediately to the Editorial Office.

- **Publication fees:** At the time of submission of an article, the author has to submit Publication fees of the paper PKR. 2000/= (through Cross Cheque in favour of **PCSIR NIDA 16-3, NBP** and send at the address given below).

The manuscripts should be addressed to:

The Executive Editor, Pakistan Journal of Scientific and Industrial Research, Scientific Information Centre, PCSIR Laboratories Campus, Sharah-e-Dr. Salimuzzaman Siddiqui, Karachi-75280, Pakistan.

Phone: (92-21)-99261914,16,17,99261949 **Fax:** (92-21) 99261913

Web: http://www.pjsir.org; **E-mail:** info@pjsir.org